MASARYKOVA UNIVERZITA
Přírodovědecká fakulta
Ústav fyzikální elektroniky

Výboje za atmosférického tlaku - diagnostika a aplikace

Habilitační práce

Vědní obor: Fyzika plazmatu

Brno 2010 **Mgr. Pavel Slavíček, Ph.D.**

Abstrakt

Předložená habilitační práce s názvem -"Výboje za atmosférického tlaku - diagnostika a aplikace"shrnuje a komentuje články, které jsou věnovány čtyřem typům barierových výbojů za atmosférického tlaku - vysokofrekvenční tryskový výboj v argonu - plazmová tužka, barierový excimerní výboj, diafragmový výboj v kapalině a difuzní koplanární povrchový barierový výboj - DCSBD. Komentář je věnován konstrukčnímu řešení jednotlivých výbojů, diagnostickým metodám a možným aplikacím těchto výbojů. V příloze jsou uvedený články z různých časopisů, které se těmto výbojům věnují.

Abstract

The present habilitation work titled - "Discharge at atmospheric pressure - diagnostics and applications", summarizes and comments articles that focus on four types of barrier discharges at atmospheric pressure - high-frequency jet discharge in argon - Plasma pencil, excimerní barrier discharge, the diaphragm discharge in the liquid and diffuse coplanar surface barrier discharge - DCSBD. Comment is dedicated to design solutions of each discharges, diagnostic methods and potential applications of these discharges. The attached file contains the articles from various magazines that are devoted to these discharges.

Obsah

1 Úvod

Předložená habilitační práce s názvem "Výboje za atmosférického tlaku - diagnostika a aplikace"shrnuje a komentuje hlavní výsledky mého působení na Ústavu fyzikální elektroniky na Masarykově univerzitě. Jednotlivé kapitoly se věnují různým typům výbojů za atmosférického tlaku, jejich diagnostice, zejména optické emisní spektroskopii a jejich možným aplikacím pro průmysl.

Plazmové výboje můžeme dělit podle různých kriterií, například podle použité budící frekvence na stejnosměrné, nízkofrekvenční, vysokofrekvenční a mikrovlnné, nebo podle tlaku při kterém výboj probíhá na výboje za sníženého tlaku, za atmosférického tlaku a na vysokotlaké výboje.

Výhodou výbojů za nízkého tlaku je, že probíhají v čistém a definovaném prostředí, bez nežádoucích příměsí, které mohou ovlivnit výboj a plazmochemické reakce, které v něm probíhají. Nízkotlaké výboje mají dobrou homogenitu a snadno se generují. Velkou nevýhodou nízkotlakých výbojů je nutnost rozměrné a nákladné vakuové aparatury, složitější manipulace se substráty, které jsou modifikovány v plazmatu a tím nákladný provoz celého systému.

Výboje za atmosférického tlaku jsou velmi zajímavé pro řadu aplikací a v současné době se velmi intenzivně zkoumají. Mají řadu výhod, není potřeba nákladný vakuový systém, je možné použít plyny s nižší čistotou, je snadná implementace do výrobních linek.

Předložená práce se zabývá jen nízkoteplotními neizotermickými výboji za atmosférického tlaku. První kapitola komentuje tryskový výboj, který byl vyvinut na našem pracovišti, tzv. "plazmovou tužku". Druhá kapitola se věnuje barierovým výbojům v excimerních směsích plynů, jako zdrojům UV záření. Třetí kapitola komentuje výsledky dosažené na nízkofrekvenčním diafragmovém výboji v kapalině. Poslední kapitola se věnuje koplanárnímu výboji - DCSBD(Diffuse Coplanar Surface Barrier Discharge), který navrhl prof. M.Černák.

Seznam použité literatury obsahuje odkazy jen na ty práce, které jsou součástí přílohy.

2 Tryskový výboj - "plazmová tužka"

2.1 Úvod

Tato kapitola shrnuje výsledky, kterých bylo dosaženo při výzkumu tryskového výboje - tzv. plazmové tužky [1]. Studium plazmových trysek má na našem ústavu dlouhou tradici [2], začínalo se s kovovými tryskami za nízkého tlaku a postupným vývojem a konstrukčními modifikacemi se vyvinula vysokofrekvenční barierová plazmová tryska, která jako pracovní plyn používá argon. Kromě měření základních fyzikálních parametrů se zabýváme i možnými aplikacemi tohoto typu výboje. Teplota těžkých částic (atomů, molekul) v plazmatu se dá měnit v širokém rozsahu, je možné získat nízké teploty výboje, kdy je možné opracovávat a modifikovat tepelně citlivé materiály, jako různé druhy plastů, nebo papír, nebo naopak vysoké teploty potřebné pro tavení tenkých drátků, svařování platinových drátků, výrobu termočlánků, nebo tavení keramických materiálů. Speciální varianta plazmové trysky může pracovat i pod hladinou různých kapalin, výboj hoří v bublinách pracovního plynu, který je do pracovní kapaliny vyfukován.

2.2 Konstrukční řešení

Plazmová tužka je z konstrukčního hlediska dutá válcová elektroda, kterou protéká pracovní plyn. První varianta byla kovová elektroda s vnitřním průměrem 0.5-5 mm, nejčastěji byla používaná tryska s průměrem 1 mm. Testovaly se trysky z různých materiálů - nerez, měď a mosaz. Nerezová ocel se neosvědčila, vlivem špatné tepelné vodivosti docházelo k přehřívání a tavení konce trysky. Přes trysku proudí pracovní plyn typicky argon s čistotou 99.996%, nebo argon s příměsí nějakého plynu - N_2, O_2, He, H_2.

Jako zdroj byl používán vysokofrekvenční generátor s frekvencí 13.56 MHz, který dodával maximální výkon 500 W. Výboj hoří uvnitř kovové trysky a je vyfukován z trysky do okolního prostředí proti uzemněné elektrodě. Výboj může pracovat ve dvou režimech, jako "dvoupólový výboj"- plazmový kanál se dotýká uzemněné elektrody, nebo jako "jednopólový výboj"- plazmový kanál se nedotýká uzemněné elektrody, výboj je kapacitně vázán vůči okolí.

Mezi vysokofrekvenčním generátorem a vlastní kovovou tryskou je přizpůsobovací impedanční člen, který zajišťuje, aby se do generátory vracel minimální odražený výkon. Plazmová tryska může být připojena přímo k přizpůsobovacímu členu, výhodou je minimalizování ztrát výkonu, nebo může být mezi tryskou a přizpůsobovacím členem koaxiální kabel, v tom případě část dodávaného vf výkonu ztrácíme v tomto kabelu, ale s plazmovou tryskou můžeme snadno manipulovat, např. pohybovat s ní nad substrátem, což je výhodné pro řadu aplikace.

Jednou z vlastností kovové plazmové trysky je, že plazmový kanál je v přímém kontaktu s materiálem elektrody a dochází k pomalému rozprašování materiálu elektrody. Tato vlastnost je výhodná pro diagnostické účely, v emisním spektru výboje můžeme identifikovat atomové čáry materiálu elektrody a můžeme je využít pro určení parametrů plazmatu, nebo tento jev můžeme využít pro depozici tenkých vrstev, ale pro řadu aplikací je nevýhodná, protože dochází ke kontaminaci materiálem elektrody a k změně geometrických rozměrů trysky a tím i ke změně

parametrů plazmatu. Proto byla vyvinuta nová varianta, kdy je plazma od kovové elektrody odděleno dielektrickou trubičkou a výboj hoří pouze v této trubičce a je z ní vyfukován do okolní atmosféry.

Tato nová varianta patří do kategorie barierových výbojů (DBD - dielectric barrier discharge) za atmosférického tlaku. Jako dielektrická trubička se používá křemenné sklo, nebo korundová keramika. Byly testovány vnitřní průměry trysek 0.3-5 mm, nejčastěji je používaná tryska z křemenného skla s vnitřním průměrem 2 mm a s vnějším průměrem 4 mm. Tato křemenná kapilára je zasunuta do kovové válcové elektrody, kovová elektroda je přes přizpůsobovací člen připojena k vysokofrekvenčnímu generátoru. Ostatní parametry jsou stejné, jako v případě kovové trysky. Výhodou, ve srovnání s kovovou tryskou, je podstatně prodloužená životnost trysky - nedochází k rozprašování elektrody, konstantní parametry - nedochází ke změně geometrie trysky a podstatně stabilnější jednopólový režim výboje - v případě připojení k přizpůsobovacímu členu pomocí koaxiálního kabelu snadná manipulace s tryskou.

2.3 Diagnostika

Jako základní diagnostická metoda byla použita optická emisní spektrometrie ve vlnové oblasti 200-1000 nm. Výhodou této metody je že nedochází k ovlivnění zkoumaného výboje, k měření a k výpočtům parametrů využíváme jen světlo vyzářené plazmatem. Z emisních spekter bylo určováno složení plazmatu a z poměru relativních intenzit emisních čar a molekulových pásů byly určeny teploty v plazmatu - rotační, vibrační a elektronová a z rozšíření atomových čar vodíku a argonu byla odhadnuta koncentrace elektronů ve výboji. Byl studován vliv změny jednotlivých parametrů, jako dodávaný vf výkon, průtok a složení pracovního plynu a geometrické rozměry trysky, elektrody a vzdálenost ústí trysky od substrátu, na jednotlivé parametry výboje.

V emisních spektrech, kromě atomových čar pracovního plynu argonu, byla naměřena řada dalších atomových čar a molekulových pásů např. O, H_α, H_β, OH, NH, N_2, NO, ..., které mají původ v nečistotách v pracovním plynu, v nečistotách v plynovém rozvodu a zejména v difuzi z okolní atmosféry.

Byly rovněž měřeny elektrické parametry výboje. Dodávaný vf výkon byl měřen přímo na generátoru, amplituda napětí byla měřena pomocí vysokonapěťové sondy s dělícím poměrem 1:1000 a amplituda vf proudu byla měřena pomocí proudové sondy a osciloskopu.

Pomocí bezkontaktních infračervených teploměrů, infračervené kamery a pomocí termočlánků typu K, byla měřena povrchová teplota trysky a teplota opracovávaného substrátu.

Typické parametry plazmové trysky: dodávaný vf výkon 80 - 200 W, rotační teplota 400 - 1000 K, vibrační teplota 2000 - 2500 K, elektronová teplota 3500 - 5000 K, koncentrace elektronů $2\times10^{20} - 3\times10^{21}\ m^{-3}$. Jedná se tedy o silně neizotermické plazma. Bylo experimentálně ověřeno, že je možné pulzní nízkofrekvenční modulací vf generátoru rotační teplotu ještě snížit. To může mít velký význam při opracování materiálů citlivých na teplotu.

2.4 Aplikace

Byla testována řada možných aplikací. Všechny uvedené aplikace jsou pro variantu DBD tryskového výboje. Jednou z nich je změna povrchové energie povrchu opracovaného substrátu. Byly testovány různé typy substrátů např. sklo, plasty, kovy, po krátké expoziční jednotky sekund se povrch stává podstatně hydrofilnější, ve srovnání s neopracovaným povrchem. Tato změna povrchových vlastností není trvalá a podle druhu substrátu mizí v řadu řádu jednotek hodin pro kovy až dnů pro plasty. Další zajímavou aplikací je depozice tenkých vrstev za atmosférického tlaku [3] . Do proudu pracovního plynu argonu se přidávají páry HMDSO - Hexamethyldisiloxanu a vytváří se tenká vrstva, která zatím nemá příliš dobré mechanické vlastnosti, ale za určitých parametrů výboje a geometrického uspořádání je možné připravit vrstvu, která je ultrahydrofobní [4]. Efekt dopadu kapky vody na ultrahydrofobní vrstvu byl naměřen pomocí rychlé optické kamery zapůjčené z VUT v Brně.

Ve spolupráci s analytickou chemií je testována možnost využití tohoto typu výboje pro chemické analýzy. Do proudu pracovního plynu argonu se definovaným způsobem přidává aerosol roztoku s různou koncentrací nějakého prvku a pomocí optického spektrometru se sleduje stabilita a změna relativní intenzity vybraných analytických spektrálních čar. Dosažené výsledky zatím nebyly publikovány.

V současné době se intenzivně zkoumají možnosti využití plazmatu v biomedicínských aplikacích [5]. Ve spolupráci s mikrobiology byla studována možnost sterilizace teplotně citlivých materiálů pomocí plazmové trysky. Bylo testováno několik druhů mikroorganizmů a vliv výkonu a expoziční doby na jejich přežití, bylo ověřeno, že dominantním sterilizačním efektem není UV záření generované výbojem, ale přímé působení výboje na mikroorganismy. Ve spolupráci s plastickou chirurgií byla testována možnost využití plazmové tužka jako chirurgického nástroje, jako plazmový skalpel. Dosažené výsledky ukazují možnost řezání i koagulace pomocí plazmové tužky, ale při porovnání se stávajícími plazmovými systémy, které se v chirurgii již využívají a mají všechny potřebné atesty, není tento aplikační směr pro plazmovou tužku příliš perspektivní.

Jednou z nevýhod plazmové trysky je malá plocha substrátu, kterou je možné opracovat jednou tryskou. Řešením je pohybovat tryskou, nebo substrátem například pomocí nějakého manipulátoru, nebo sestavení zařízení z několika trysek.

3 Barierové výboje, jako zdroje UV - záření

3.1 Úvod

Intenzivní a levné zdroje UV záření jsou velmi zajímavé pro řadu aplikací, např. modifikace povrchů, fotokatalytické reakce, sterilizace povrchů a kapalin, nebo jako primární zdroj pro buzení luminoforů v osvětlovací technice. Nejrozšířenějším zdrojem UV záření je v současné době nízkotlaký výboj v parách rtuti, kde dominantní spektrální čára v UV oblasti má vlnovou délku 253.65 nm. Probíhá intenzivní výzkum UV zdrojů záření založených na barierových výbojích v excimerních směsích plynů na bázi halogenních prvků Cl, F, I. Cílem je získat levný a intenzivní zdroj UV záření s velkou životnosti a dobrou účinností přeměny elektrické energie na UV záření.

3.2 Experimentální uspořádání

Existují dvě základní konfigurace excimerních barierových výbojů. První je uspořádání s objemovým barierovým výbojem, kde jedna, nebo dvě oddělené elektrody jsou pokryty dielektrickou vrstvou např. dvě rovnoběžné desky, nebo válcové - koaxiální uspořádání. Druhou variantu představuje povrchový barierový výboj, kdy je destička dielektrika pokryta na jedné straně systémem vodivých pásků a na druhé straně je dielektrikum pokoveno. Na našem pracovišti jsme zkoumali obě varianty, komentované články jsou zaměřeny pouze na povrchový barierový výboj [6], [7]. Jako pracovní plyny byly použity excimerní směsy plynu He-Kr-Xe-Cl_2 a He-Kr-Xe-I s různým poměrem jednotlivých složek a celkovým tlakem 100-1000 hPa. Jako dielektrikum byla použitá korundová destička Al_2O_3 s rozměry 100x100 mm, s tloušťkou 0.5 mm. Jako napájecí zdroj byl použit nízkofrekvenční generátor s frekvencí 1-100 kHz a maximální amplitudou napětí 11 kV.

3.3 Diagnostika a aplikace

Jako základní diagnostická metoda byla použita optická emisní spektrometrie v oblasti vlnových délek 200-1000 nm. V UV oblasti byly naměřeny následující excimerní molekulové pásy pro směs Kr-Xe-Cl_2 [6]: 222 nm - KrCl, 236 nm XeCl, 258 nm - Cl_2, 308 nm - XeCl, 345 nm - XeCl a pro směs Kr-Xe-I [7]: 253 nm - XeI, 320 nm - XeI, 342 nm - I_2. Pro směs Kr-Xe-Cl_2 měl největší intenzitu pás 308 nm - XeCl, pro směs Kr-Xe-I měl největší intenzitu pás 253 nm - XeI.

Kromě optické emisní spektrometrie byly monitorovány elektrické parametry barierových výbojů pomocí osciloskopu a napěťových a proudových sond. Pro odhad účinnosti přeměny elektrické energie na UV záření byl měřen celkový vyzářený světelný výkon v UV-VIS-NIR oblasti vlnových délek.

Ve směsi Kr-Xe-Cl_2 = 920-80-1 hPa byla dosažena hustota výkonu UV záření 6 $mWcm^{-2}$, zatímco maximální potlačení podílu viditelného a infračerveného (NIR) záření byla nalezena při celkovém tlaku 500 hPa(Kr-Xe-Cl_2 = 460-40-1 hPa).

Z možných aplikací barierových výbojů v excimerních směsích byla na našem pracovišti zkoumána možnost buzení luminoforů v osvětlovací technice [7].

4 Diafragmový výboj v kapalině

4.1 Úvod

Plazmová úprava povrchových vlastností materiálu se v poslední době velmi intenzivně studuje. Jedou ze zkoumaných variant je využití diafragmových výbojů v kapalinách. Článek [8] se zabývá diagnostikou a aplikací diafragmového výboje na opracování polyesterových vláken a článek [9] na opracování polypropylénových netkaných textilií.

4.2 Experimentální uspořádání

Základní konfigurace diafragmového výboje je nádoba s kapalinou rozdělená přepážkou s malým kruhovým otvorem na dvě části a v každé části je jedna kovová elektroda spojená s vysokonapěťovým generátorem. Výboj hoří v otvoru v přepážce. Tato varianta se hodí na opracování vláken, která jsou protahována tímto otvorem v přepážce. Další možná konfigurace je místo kruhového otvoru použít úzkou štěrbinu. Tato konfigurace je vhodná i pro opracování tenkých plošných materiálů. Při našich experimentech byl používán kruhový otvor s průměrem 1.2 mm v přepážce s tloušťkou 3 mm a štěrbina s šířkou 1 mm. Elektrody byly napájeny z vysokonapěťového pulzního generátoru postaveného na principu rotujícího jiskřiště s maximální amplitudou 60 kV a maximální opakovací frekvencí 60 Hz. Rychlost převíjení polyesterových vláken byla 5 cm/s.

4.3 Diagnostika a aplikace

Výboj vzniká vlivem velké proudové hustoty v místě, kde je otvor, nebo štěrbina v přepážce. Velký vliv na parametry výboji i opracování má použitá pracovní kapalina, zejména její elektrická vodivost. V případě opracování vláken, nebo netkaných textilií hraje roli i plyn sorbovaný na povrchu tohoto materiálu a plyn v pórech tohoto materiálu.

Pro určování základních parametrů diafragmových výbojů byla použita optické emisní spektroskopie. Dominantní ve spektrech byly vodíkové čáry H_α a H_β. Z rozšíření těchto čar byla určena koncentrace elektronů, která se pohybovala v rozsahu $1 \times 10^{22} - 2 \times 10^{24}\ m^{-3}$, podle toho jak se měnily parametry - druh kapaliny, vodivost kapaliny, rychlost pohybu vlákna, nebo textilie [8], [9].

Elektrické parametry diafragmových výbojů byly měřeny pomocí osciloskopu a vysokonapěťové sondy a kapacitního děliče a proudové sondy.

Diafragmové výboje poskytují unikátní systém, v kterém mohou vzájemně interagovat pevný substrát, kapalina a plazma. Tyto výboje mohou byt použity například k čištění odpadních vod, změně povrchových vlastností polymerních materiálů, k rozkladu, nebo syntéze chemických látek, nebo k nanášení nanočástic na různé materiály.

5 Koplanární povrchový výboj - DCSBD

5.1 Úvod

Pracovní skupinou prof. M.Černáka byl na Masarykově univerzitě v Brně a Komenského univerzitě v Bratislavě vyvinut plošný plazmový zdroj - difuzní koplanární povrchový barierový výboj (Diffuse Coplanar Surface Barrier Discharge - DCSBD). Tento výboj pracuje za atmosférického tlaku prakticky v libovolném plynu - vzduch, N_2, O_2, Ar, ...

Vývoj tohoto systému pokračuje dál a cílem je v rámci projektu CZ.1.05/2.1.00-/03.0086 - "Regionální VaV centrum pro nízkonákladové plazmové a nanotechnologické povrchové úpravy"a navazujících projektů, jeho využití v různých průmyslových aplikacích zejména k povrchové úpravě plošných substrátu.

5.2 Konstrukční řešení

Konstrukce DCSBD výbojky je tvořena systémem kovových elektrod ve tvaru pásků s délkou asi 150 mm a šířkou 0.5 mm v korundové (Al_2O_3) keramice. Plazma hoří na povrchu této korundové keramiky a elektrod se vůbec nedotýká, tím je zajištěna dlouhá životnost výbojky, protože nedochází k rozprašování elektrod vlivem výboje, ani k otěru elektrod vlivem pohybu substrátu ve výboji, plazma i substrát je v kontaktu pouze s korundovou keramikou. K napájení tohoto výboje se používá nízkofrekvenční vysokonapěťový generátor s pracovní frekvencí 1-20 kHz a amplitudou napětí asi 10 kV [10]. Díky účinnému olejovému chlazení dosahuje tato DCSBD výbojka plošné výkonové hustoty až 5 $\mathrm{Wcm^{-2}}$. Probíhá optimalizace geometrických rozměrů elektrod, tloušťky keramické destičky a frekvence a výkon vysokonapěťového generátoru s cílem zlepšit provozní vlastnosti výbojky, tepelnou odolnost prodloužit její životnost a zvětšit její účinnost.

5.3 Diagnostika

Elektrické parametry DCSBD výboje byly monitorovány pomocí osciloskopu, vysokonapěťové sondy s dělícím poměrem 1:1000, proudové sondy a měřiče výkonu nízkofrekvenčního vysokonapěťového generátoru. Typický výkon je 400 W a amplituda napětí 10 kV.

Další diagnostickou metodou byla optická emisní spektrometrie ve vlnové oblasti 200 - 1000 nm. Pro výboj ve vzduchu byly v emisním spektru naměřeny spektrální čáry kyslíku a molekulové pásy dusíku (druhý pozitivní systém) a v UV oblasti molekulový pás OH. Z poměru relativních intenzit rotačních čar OH byla určena rotační teplota asi 400 K a z poměru intenzit vibračních pásů druhého pozitivního systému dusíku vibrační teplota asi 2000 K, takže se jedná o nízkoteplotní neizotermické plazma.

Pro vyhodnocení účinku DCSBD výboje na opracovávané materiály se používají standardní metody pro analýzu povrchů, jako měřič kontaktního úhlu a povrchové energie, mikroskopy optické, SEM, AFM, nebo diagnostické metody MALDI-TOF, FTIR, XPS. Kromě těchto běžných univerzálních diagnostických metod se pro kon-

krétní aplikace používají speciální jednoúčelové metody, např. při úpravě živočišných vláken test zplsťování.

5.4 Aplikace

DCSBD výboj se zkoumá, nejen pro své zajímavé fyzikální vlastnosti, ale i pro konkrétní průmyslové aplikace. Je vhodný zejména pro povrchovou úpravu laciných plošných materiálů, jako papír, netkané textilie, kovové folie, sklo. K možným povrchovým úpravám patří zejména změna povrchové energie, čištění povrchu, nebo změna drsnosti povrchu. Výhodou DCSBD výbojek, díky jejich malým rozměrům a nenáročnému provozu, je možnost provádět testy přímo na výrobních linkách našich průmyslových partnerů. Jedním z nich je například firma Pegas a.s. významný výrobce netkaných textilií.

Jednou z posledních aplikací, která byla vyzkoušena ve spolupráci s firmou Tonak a.s.v Novém Jičíně, je úprava živočišných vláken za účelem zlepšení jejich plstících vlastností. V současné době se provádí úprava živočišných vláken před zplsťováním pomocí chemických metod založených na využití roztoků kyselin HCl, HNO_3, H_3PO_4 a H_2SO_4. Pokud se podaří nahradit tento chemický postup plazmovou úpravou, bude to mít významné ekologické i ekonomické výhody.

6 Seznam článků

Reference

[1] Janca J., Klima M., Slavicek P., Zajickova L., HF plasma pencil - new source for plasma surface processing, SURFACE & COATINGS TECHNOLOGY Volume: 116 Pages: 547-551 Published: SEP 1999

[2] Kapicka V., Sicha M., Klima M., Hubicka Z., Tous J., Brablec A., Slavicek P., Behnke JF., Tichy M., Vaculik R., The high pressure torch discharge plasma source, PLASMA SOURCES SCIENCE & TECHNOLOGY Volume: 8 Issue: 1 Pages: 15-21 Published: FEB 1999

[3] Slavicek P., Bursikova V., Brablec A., Kapicka V., Klima M., Deposition of polymer films by rf discharge at atmospheric pressure, CZECHOSLOVAK JOURNAL OF PHYSICS Volume: 54 Pages: C586-C591 Part: Part 4 Published: 2004

[4] Slavíček, P.,Klíma, M.,Skácelová, D.,Kedroňová, E.,Brablec, A.,Aubrecht, V. RF discharge at atmospheric pressure - diagnostics and applications. Chemické listy, 102, 16, od s. 1338-1340, 3 s. ISSN 1803-2389. 2008

[5] Cheruthazhekatt S., Cernak M., Slavicek P., Havel J., Gas plasmas and plasma modified materials in medicine, JOURNAL OF APPLIED BIOMEDICINE Volume: 8 Issue: 2 Pages: 55-66 Published: JUN 2010

[6] Guivan NN., Janca J., Brablec A., Stahel P., Slavicek P., Shimon LL., Planar UV excilamp excited by a surface barrier discharge, JOURNAL OF PHYSICS D-APPLIED PHYSICS Volume: 38 Issue: 17 Pages: 3188-3193 Published: SEP 7, 2005

[7] Guivan M. M., Malinin A. N., Brablec A., Janca J., Stahel P., Slavicek P.,Excitation of phosphors by UV XeI excimer radiatio, CZECHOSLOVAK JOURNAL OF PHYSICS Volume: 56 Pages: B659-B664 Part: Part 4 Suppl. B Supplement: Part 4 Suppl. B Published: 2006

[8] Brablec A., Slavicek P., Stahel P., Cizmar T., Trunec D., Simor M., Cernak M., Underwater pulse electrical diaphragm discharges for surface treatment of fibrous polymeric materials, CZECHOSLOVAK JOURNAL OF PHYSICS Volume: 52 Pages: 491-500 Supplement: Suppl. D Published: 2002

[9] Neagoe, G.,Brablec, A.,Ráheľ, J.,Slavíček, P.,Záhoran, M. Study of Polypropylene Nonwoven Fabrics Treatment in Underwater Electrical Diaphragm Discharge. Chemické listy, 2008, 102, od s. 1490-1493, 4 s. ISSN 0009-2770. 2008

[10] Cernak M., Rahel J., Kovacik D., Simor M., Brablec A., Slavicek P., Generation of thin surface plasma layers for atmospheric-pressure surface treatments, CONTRIBUTIONS TO PLASMA PHYSICS Volume: 44 Issue: 5-6 Pages: 492-495 Published: 2004

ELSEVIER

Surface and Coatings Technology 116–119 (1999) 547–551

SURFACE & COATINGS TECHNOLOGY

www.elsevier.nl/locate/surfcoat

HF plasma pencil — new source for plasma surface processing

J. Janča*, M. Klíma, P. Slavíček, L. Zajíčková

Department of Physical Electronics, Faculty of Science, Masaryk University, Kotlaoska 2, 61137 Brno, Czech Republic

Abstract

The high-frequency plasma pencil is a source of a highly active environment (electrons, ions, reactive radicals, excited atoms and molecules), which can be generated at atmospheric, reduced or increased pressure, preserving a broad control of performance. As an active medium flowing through the plasma jet a gas, a liquid as well as a mixture of dispersed particles (powders) can be used. The plasma jet can be controlled like hand-operated tools. Several technological applications have already been used (restoration of archeological glass artifacts, fullerene production, fragmentation of molecules for microelectrophoresis, plasma polymerization in liquids, various plasma surface treatments, etc.).

Keywords: High-frequency plasma; Hollow electrode; Plasma jet; Plasma pencil; Plasma surface processing

1. Introduction

The unipolar high-frequency (hf) discharges have been used as a plasma source of a non-isothermal plasma that can be excited in a wide range of pressures. The degree of non-isothermicity depends on the supplied power output, the working gas, and the pressure at which the discharge is excited [1,2]. Recently, the unipolar hf discharges were combined with a hollow cathode, which acts simultaneously as a nozzle for a working gas inlet [3,4]. The hollow cathode represents a very effective source of the gas discharge plasma. Its geometry promotes oscillations of hot electrons inside the cathode, thereby enhancing ionization and ion bombardment of inner walls, and influencing other subsequent processes. At the same power, the hollow cathode exhibits a plasma density 1-2 orders higher than with conventional electrode systems [5]. Up to now, the unipolar hf plasma reactor systems with hollow cathode electrodes have been applied at low pressures only (up to 2 kPa). Dense chemically reactive plasmas produced by hollow cathode unipolar hf discharges can also be favourably used for different plasma-processing technologies.

Diagnostics of unipolar and bipolar hf discharges (without hollow electrode) excited at atmospheric and subatmospheric pressures were frequently carried out in the 1960s and 1970s using various spectral, microwave and calorimetric diagnostic methods [6,7]. The results of these measurements have produced a comparatively unified idea of the parameters of this kind of hf discharge plasma. The possibility of hf generation of the hollow cathode plasma jet at atmospheric pressure brings about an extension of technological abilities of high-pressure discharges.

2. Experimental

The core of our experiment was an extension piece made of a pencil-shaped dielectric with a built-in special hollow electrode. The powered electrode consists of a thin pipe with an inner diameter of 1–2 mm and a length of several centimetres. The hollow electrode was connected with a cable with the matching network of the 13.56 MHz power supply and adapted like a current hand-operated tool. The power absorbed in the plasma pencil was adjusted in such manner that the torch discharge was created at the electrode edge. As an active medium flowing through the hollow electrode of the plasma pencil gas, a liquid or a mixture of dispersed particles (powders) was used. If liquid is used as the working medium, the second (earthed) electrode must be used, and the discharge is excited as a hf torch arc. Schematic diagrams of two possible experimental arrangements employed in the present study are shown in Figs. 1 and 2. The supplied power ranged from 20 to 200 W, and the hf amplitude voltage ranged from 100 to 1000 V. In studying optical emission, we found that

* Corresponding author.

0257-8972/99/$ – see front matter
PII: S0257-8972(99)00256-X

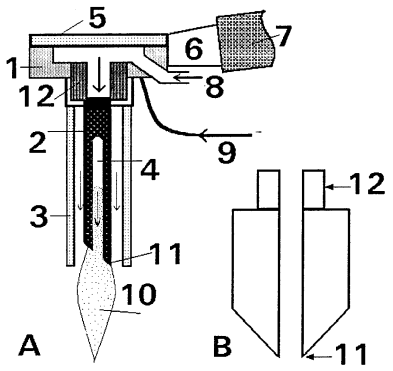

Fig. 1. Plasma pencil in two different experimental arrangements. (A) With a hollow needle and (B) with a hollow cylinder: 1, carrier electrode; 2, hollow electrode; 3, quartz capillary; 4, slit for spectral measurements; 5, glass window; 6, hinge; 7, grip; 8, gas inlet; 9, power supply; 10, plasma jet; 11, sharp edge of nozzle; 12, thread.

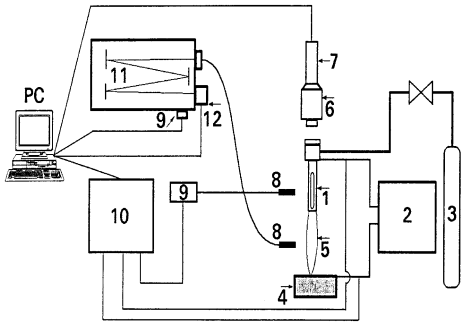

Fig. 2. Schematic drawing of the experimental arrangement: 1, hollow electrode; 2, power supply; 3, gas container; 4, counter electrode or the material treated; 5, plasma jet; 6, microscope; 7, video camera; 8, optical fibre; 9, photomultiplier; 10, oscilloscope; 11, monochromator; 12, optical multichannel analyser.

discharges were generated deep inside the hollow electrode but only in the monoatomic gases (Ar). The working gas that flows from the nozzle stabilizes the plasma jet, and a well-defined plasma channel is created downstream from the gas flow. Depending on the experimental conditions, the plasma flows at a subsonic or supersonic rate.

To obtain basic information on the discharge, optical emission spectroscopy has been used. Optical spectra have been recorded by means of the HR 640 (Jobin-Yvon) monochromator with a CCD optical multichannel analyser (OMA) and using a colour CCD camera Panasonic NV-MS5EG(S-VHS/VHS format).

Diagnostic and power measurements of the unipolar and bipolar hf discharges excited on sharp bulk electrodes at atmospheric pressure in monoatomic and molecular gases differ sharply from each other. The spectral diagnostic methods show that the neutral gas temperature is $(6–7)\times10^3$ K, the intensity of the electric field is $(11–16)\,\mathrm{V\,cm^{-1}}$, and the electron density is $2\times10^{13}\,\mathrm{cm^{-3}}$. In the discharge excited in air (N_2), the temperature of the neutral gas reaches a value of $(3–4)\times10^3$ K, and the electron temperature only slightly exceeds this value. The electric field strength in the discharge channel reaches $(300–500)\,\mathrm{V\,cm^{-1}}$ [6]. At an equal power output into the discharge excited either in argon or nitrogen, the thermionic output of the discharges differs remarkably. The hf discharge excited in pure argon at a higher output dissipates a great part of the supplied hf energy in the form of electromagnetic waves; for a summary of the results, see Fig. 3. On the contrary, the discharge excited in nitrogen and hydrogen at a higher output behaves like ohmic loading (i.e. almost all of the hf energy supplied to the discharges changes to a thermionic one). In molecular gases, the unipolar hf discharge has a torch form (shape); however, in argon, a very long and narrow channel, similar to a wire antenna, is formed. The thermal power output absorbed in the electrode reaches 30% of the total hf power input in molecular gases (air, nitrogen, hydrogen); however, in pure argon, it reaches only 15% (Fig. 4.).

At atmospheric pressure, the nozzle of the plasma pencil cannot act as a classic proper hollow cathode, and only the edge of the electrode is involved in the

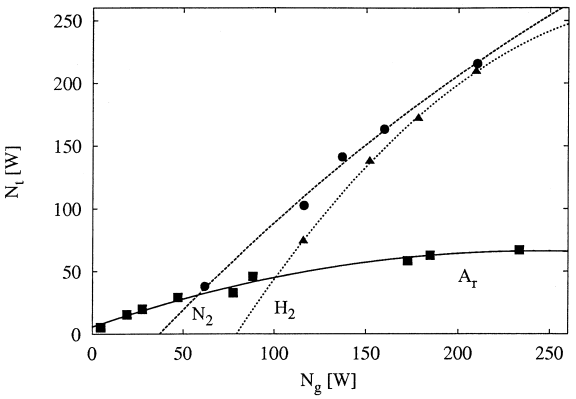

Fig. 3. Plot of thermal power output, N_t, versus the total hf input, N_g, of a unipolar hf discharge excited at atmospheric pressure in Ar, H_2, and N_2 ($f=27$ MHz, copper electrode).

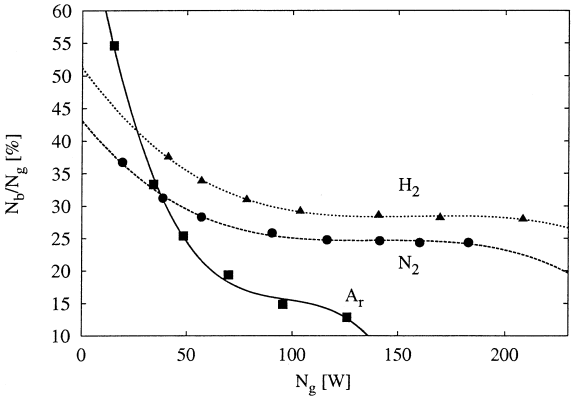

Fig. 4. Dependence of the thermal power output absorbed by the electrode (N_b) on the total power input, N_g (unipolar hf discharge excited in Ar, N_2,, and H_2).

discharge process. Our observations in Ar, by means of special arrangements of the CCD video camera, shows that the plasma column penetrated deep into the hollow electrode (Fig. 5). When the hf power, which is dissipated in the plasma jet, increases above a certain limit at which the temperature of the electrode is so high that the electrode material is evaporated, the plasma is formed in the mixture of working gas and vapours of the evaporated electrode material. Effective cooling of the electrode is necessary during the work at high hf power inputs. The actual arrangement of the hollow electrode depends on the required physical properties of the plasma streaming from the plasma pencil nozzle. Gradually, different types of electrode jet have been developed and technologies tried with both subsonic and supersonic jet plasma speeds.

3. Parameters of high-pressure hf discharge plasma generated in the plasma pencil

In the spectra of hf discharge generated in the plasma pencil, very intensive molecular bands of the N_2 (C $^3\Pi_u - B\ ^3\Pi_g$) system, molecular ions N_2^+ B $^2\Sigma_u^+ - X\ ^2\Sigma_g^+$) system and the OH radical (A $^2\Sigma - X - ^2\Pi$) system are observed. For measuring the rotational and vibrational temperatures, known methods were used [8,9]. The electron temperature is well approximated by the excitation temperature of Ar I or Cu I and Fe I atomic lines if the hf discharges are excited on the copper or iron electrode. The plasma generated in the plasma pencil at atmospheric pressure is a typical example of non-isothermal plasma where the electron temperature (T_e) > the vibrational temperature (T_v) > the rotational temperature (T_r) > the temperature of neutral gas (T_o), but these deviations from local thermodynamic equilibrium (LTE) depend on the total power input and gas flow rate.

The population of OH rotational states shows deviations from the Boltzmann distribution [10,11]. Two different groups of OH radicals were observed, the 'cold' group and the 'hot' group, characterized by two Boltzmann distributions with respect to rotation. The reason for the appearance of two groups is interpreted in terms of two excitation mechanisms. The 'cold' group (characterized by rotational quantum numbers $J<10$) arises upon simple excitation of the already existing diatomic OH radicals; the rotational temperature corresponds with the neutral gas temperature. Selected results of temperature measurements are presented in Figs. 6–9.

The vibrational temperature, T_v, was measured as a rule by means of excited electron states of the N_2 (C $^3\Pi_u - B\ ^3\Pi_g$) system, and the vibrational temperature did not correspond with the vibrational temperature of the N_2 ground electron state X $^1\Sigma_g^+$ (T_{vX}). The vibrational temperature, T_{vC}, was recalculated on T_{vX} using the method presented in Refs. [12,13].

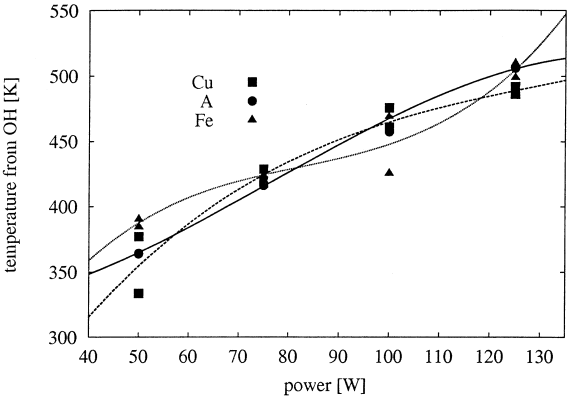

Fig. 6. Rotational temperature as a function of the hf power input for a fixed gas flow of 1100 sccm and different nozzle materials.

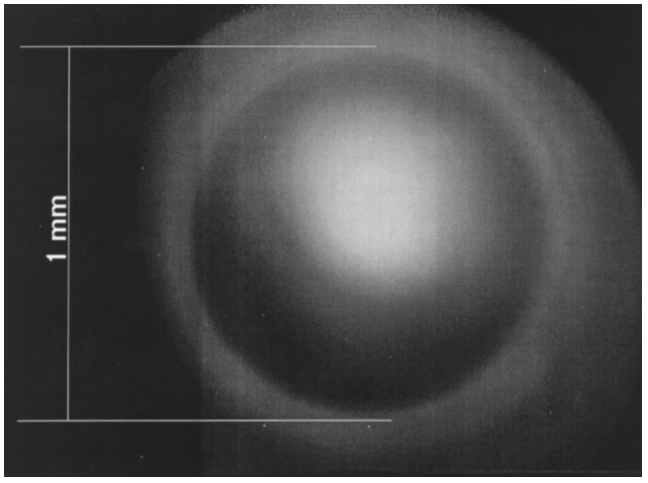

Fig. 5. Video snapshot of the plasma column inside the hollow electrode (i.d. 1 mm, 13.56 MHz, 25 W, Ar flow rate 900 sccm).

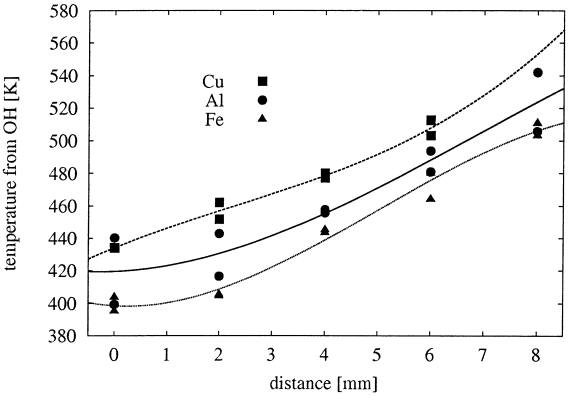

Fig. 7. Rotational temperature as a function of the distance from the nozzle for a fixed hf power input 75 W and a gas flow of 1100 sccm and different nozzle materials.

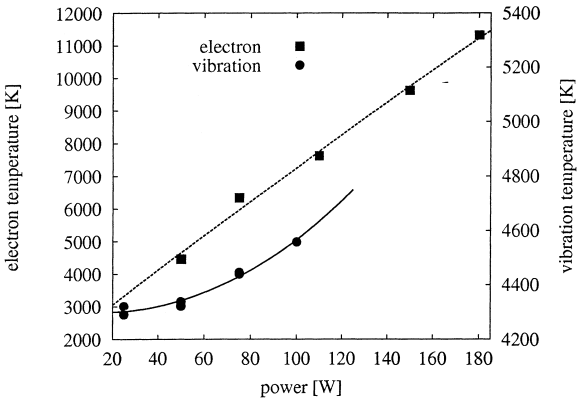

Fig. 8. Electron and vibrational temperatures as a function of the hf power input for a fixed gas flow of 900 sccm and the iron nozzle.

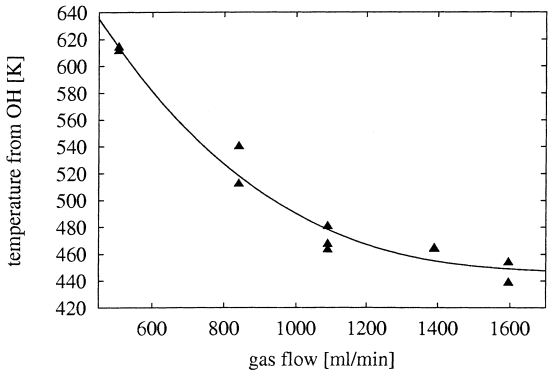

Fig. 9. Rotational temperature as a function of gas flow for the iron nozzle and a fixed hf power input of 75 W.

4. Applications of hf plasma pencil in surface coatings and technology

The plasma pencil jet has been used for a number of plasmachemical technologies with surprisingly good results. Most importantly, highly routed and selective plasma etching, very fine plasma ablation on the edges after laser and mechanical processing of different materials, locally initiated plasmachemical reactions and depositions on the surface of solid substrates are possible [17].

The low-pressure rf glow discharges have already been successfully applied to reduce the corrosion products on historical metal artefacts [14]. However, there is a huge amount of historical objects consisting of different inseparable materials that require special conservation technologies [15]. With the plasma pencil, each particular material can be treated individually without any vacuum demands. Moreover, when the object is immersed in a chemically reactive liquid, we can combine the high efficiency of the plasma treatment with the selectivity of chemical processes. A 10 mmol solution of Complexon III ($C_{10}H_{14}O_8N_2Na_2$) in distilled water was used as a liquid medium for archaeological applications. We studied the effects of the plasma pencil treatment in liquid for different archaeological and historical materials.

Especially for bronze artefacts immersed in Complexon III, the effects of the plasma pencil in a liquid environment were compared to (1) those of discharge between a metal rod electrode and the liquid surface and (2) those of pure electrochemical processes when the metal rod was placed in liquid. All bronze samples were first treated in low-pressure hydrogen hf plasma for 3 h. The details of the surface structure were examined using a scanning electron microscope (SEM). The discharge with the rod electrode showed several minor effects only when the object was placed close to the electrode. The hf plasma pencil destroyed the corroded layer very efficiently when the distance from the object surface was less than 2 mm. When the distance was 3–5 mm, visual changes on the surface were not observed, but SEM analyses showed that the plasma pencil affected the structure of corrosion inside the layer.

Archaeological glasses were treated by a hf (13.56 MHz) plasma pencil in a liquid environment. An argon flow of 200 sccm and a power of 100 W were used. The time of the treatment was several minutes. During the treatment, layers of precipitates of soil solutions were peeled off, but the important gelous degrading glass layer was treated moderately. The content of Ca, P, K, Fe and Mn in the upper corroded layer significantly decreased, and therefore, the glass transparency was restored [16].

Pilot experiments with the plasma pencil operating with an argon flow and carbon nozzle, immersed in liquid tetrachlormethane, produced a remarkable concentration of C_{60} fullerenes with respect to the hf power supplied. Measurements of fullerene concentrations were performed by NMR (nuclear magnetic resonance spectroscopy).

If the working gas (argon, helium) is enriched by a small concentration of monomer (siloxanes, cyclofluorbutane), then at low neutral gas temperatures, plasma polymers are deposited on the substrate immersed in liquid. The temperature of the neutral gas is near ambient, and plasma polymers are stable and cross-linked.

The plasma pencil can be utilized in chemistry to derive chemical compounds, *cis/trans* isomerization, substitution, elimination or cyclization. We have examined the possibility of discharge derivatization applicable for analytes that cannot be detected directly, e.g. for UV-VIS on-capillary detection of analytes without chromophores.

If a mixture of reactive gases is used (e.g. $Ar+O_2+CF_4$), very effective and selective plasma etching of different materials can be observed. The plasma pencil can be used also for the surface finishing of edges especially after laser drilling and milling.

5. Conclusions

The high-frequency plasma pencil and its broad range of applications are a unique instrument for interested workers which has not been expected and originally not planned. Gradually, six different types of the electrode jets have been developed and technologies tried with both subsonic and supersonic jet plasma speeds. The temperature of the neutral gas can be easily changed by the high-frequency power input and flow rate of the working media. So far, no source of plasma exists that would make literally 'watchmaker' work possible in the plasma processing of the sample details. Another advantage of the plasma pencil is the possibility of working in a free atmosphere, in a liquid, at a lowered or increased pressure. Some technologies have already been used in various applications (restoration of archaelogical glass artifacts, fullerene production, fragmentation of molecules for microelectrophoresis, plasma polymerization in liquids, plasma etching, etc.). The hf plasma pencil can be fastened in the dielectric holder and used as a hand-operated tool.

Acknowledgements

This work was supported by the Grant Agency of the Czech Republic, grant number 106/96/K245, and the Grant Agency of the Czech Ministry of Education VS96084.

References

[1] M. Moisan, J. Pelletier, Microwave Excited Plasmas, Elsevier, Amsterdam, 1992.
[2] V. Farský, J. Janča, Beitrage aus der Plasmaphysik 8 (1968) 129.
[3] L. Bárdoš, Proc. XXI. Int. Conf. Phenomena in Ionized Gases, Part III, Bochum (1993) 98.
[4] L. Soukup, V. Peřina, L. Jastrabík, M. Šícha, P. Pokorný, R.J. Soukup, M. Novák, J. Zemek, Surf. Coat. Technol. 78 (1996) 280.
[5] C.M. Horwitz, Appl. Phys. Lett. 43 (1983) 977.
[6] J. Janča, Czech J. Phys. B 17 (1967) 761.
[7] U. Jecht, W. Kessler, Z. Phys. 178 (1964) 133.
[8] W. Lochte-Holtgreven, Plasma Diagnostics, North-Holland, Amsterdam, 1968.
[9] R.H. Tourin, Spectroscopic Gas Temperature Measurement, Elsevier, Amsterdam, 1966.
[10] H. Meinel, L. Krauss, J. Quant. Spectr. Radiat. Transfer 9 (1969) 443.
[11] D.R. Crosley, R.K. Lengel, J. Quant. Spectr. Radiat. Transfer 15 (1975) 579.
[12] M.Z. Novgorodov, V.N. Ochkin, N.N. Sobolev, J. Tech. Phys. 40 (1970) 12678 in Russian.
[13] A.D. Kosoruchkina, E.S. Trekhov, J. Tech. Phys. 45 (1975) 1082 in Russian.
[14] S. Veprek, Ch. Eckmann, J.T. Elmer, Plasma Chem. Plasma Process. 8 (4) (1988) 455.
[15] M. Klima, L. Zajíčková, J. Jančva et al., Zeitschrift für Sweizerische Archeologie und Kunstgeschichte 54 (1997) 31–33.
[16] A. Brablec, P. Slavíček, M. Klíma, V. Kapička, Proc. ICPIG XXIII band I, Toulouse (1997) 128.
[17] M. Klíma, J. Janča, V. Kapička, P. Slavíček, P. Saul, Czech Patent PV 147698, 1998.

Plasma Sources Sci. Technol. **8** (1999) 15–21. Printed in the UK PII: S0963-0252(99)98877-1

The high pressure torch discharge plasma source

V Kapička†, M Šícha‡, M Klíma†, Z Hubička‡, J Touš‡, A Brablec†, P Slavíček†, J F Behnke§, M Tichý‡ and R Vaculík†

† Department of Physical Electronics, Faculty of Science, Masaryk University, Kotlářská 2, 611 37 Brno, Czech Republic
‡ Department of Electronics and Vacuum Physics, Faculty of Mathematics and Physics, Charles University, V Holešovičkách 2, 180 00 Prague 8, Czech Republic
§ Institute of Physics, Ernst-Moritz-Arndt University, Domstraße 10a, D-17487 Greifswald, Germany

Received 5 May 1997, in final form 3 August 1998

Abstract. We present a plasma source which works on the principle of the arc torch discharge. The powered electrode of the arc torch discharge was made from a thin pipe that simultaneously acts as the nozzle through which the working gas flows to the discharge region. The flow of the working gas stabilizes the arc torch discharge and a well defined plasma channel is created. The advantage of this system is that it is able to work at high pressure of working gas up to atmospheric pressure inside the plasma-chemical reactor and also in free space.

1. Introduction

Recently the RF low pressure plasma-chemical reactor with hollow cathode (radio-frequency plasma jet—RPJ) has been developed for the plasma surface and coating technologies, treatments of various materials and thin film deposition [1–4]. The primary RF discharge burning inside the reactor chamber induces the additional discharge inside the hollow cathode. The working gas flows through the hollow cathode that acts simultaneously as an inlet nozzle for the working gas. The incoming working gas forces the hollow cathode discharge supersonically from the nozzle into the reactor and a well defined plasma channel is created inside the primary RF plasma. This plasma channel can be used as a plasma source for the surface treatment technology and in particular cases fulfils special requirements necessary for deposition of thin films on internal walls of cavities, holes and on substrates with complex shapes. Further, by means of the RPJ reactor the thin films with defined stoichiometry Ge_3N_4 [5] and Cu_3N_4 [6] have been achieved. However, this reactor requires a relatively low pressure of the working gas from several Pa to several tens of Pa.

Sometimes it is desirable to have at our disposal a plasma source that generates at higher pressures a similar plasma channel like the low pressure RF reactor with hollow cathode [1–4]. Possible examples are the surface treatment and conservation of archaeological ancient artefacts or the plasma surface treatment of objects with large dimensions that cannot possibly be placed in the reactor chamber. Recently such a high-pressure plasma source that was based on the principle of a torch discharge was successfully created and investigated in [7]. A modification of this plasma source, where the thin pipe electrode of the arc torch discharge was fastened in the dielectric holder and used as a hand controlled plasma source, has been presented in [8]. This plasma source has already been used as an 'RF plasma pencil' for the treatment and conservation of archaeological artefacts in a free atmosphere. Already such an 'RF plasma pencil' has been further used for treatment of archaeological artefacts also in the liquid environment [8–10]. The preliminary investigation has shown that the 'RF plasma pencil' can be also used for the surface treatment of large dimension objects that are not possible to place inside a reactor chamber.

Up to date the torch discharge has been mainly used in spectral analysis, see e.g. [11–17]. The mentioned experiments with an RF arc torch plasma source have shown that such a system can represent, in particular cases, a useful tool for the plasma-aided surface treatment technology. Therefore we decided to study the properties of an arc torch plasma source based on the RF discharge. In the following part of our report at first the essential phenomena, that characterize the RF corona and the torch discharge and the transition between them, will be mentioned. After that the key properties of the plasma source that employs the high-pressure RF arc torch discharge and that we studied experimentally will be discussed.

2. The RF corona and the torch discharge

Generally the RF corona discharge is generated due to the strong intensity of the RF electric field in the neighbourhood of a sharp electrode edge where the discharge originates. The main ionization processes of neutral particles in the RF corona discharge are the ionizing collisions of electrons

0963-0252/99/010015+07$19.50

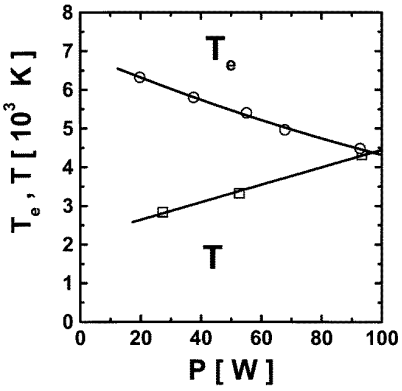

Figure 1. The dependence of neutral particle (T) and electron (T_e) temperatures on the RF power (P) absorbed in the corona and torch discharge in the polyatomic gases. From [19].

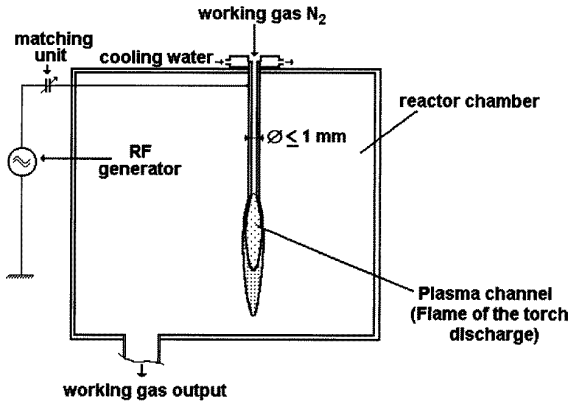

Figure 2. The experimental set-up of the plasma-chemical source with the torch discharge.

accelerated in the strong electric field region near the sharp electrode edge. This fact is confirmed by the emission spectrum of this discharge [19, 20]. If the RF power dissipated in the polyatomic working gas discharge increases then the vibrational temperature of excited neutral molecules also increases [18–20]. Due to this effect the role of thermal ionization of the excited neutral molecules (with higher vibrational temperature) increases too. This thermal ionization results in the decrease of the electric field intensity in the neighbourhood of the electrode. Consequently, the ionization caused by accelerated electrons also decreases. The resulting effect is that with increasing RF power absorbed in the discharge the electron temperature decreases and in contrast the vibrational temperature of the molecules increases. When the difference between the electron temperature and the vibrational temperature of the excited neutral molecules is small then the corona discharge changes into the torch one. The transition between the corona and the torch discharge does not occur stepwise, but gradually. The typical dependence of the neutral particle temperature T and the electron temperature T_e on the RF power in the transition region between the corona and the torch discharge is reproduced in figure 1 (from [19]). The RF corona discharge can then be characterized by the following criterion [19, 20]:

$$T_e/T > 1.$$

In the case of a discharge burning in molecular gas the temperature T_e can be approximated by the vibrational temperature T_v and the neutral gas temperature T by the rotational temperature T_r. The temperatures T_v and T_r are comparatively easy to estimate by means of spectroscopic measurements. In accord with the above mentioned mechanism and figure 1 the transition from the RF corona to the RF torch discharge occurs when the temperatures T_e and T approach each other. In other words small RF power absorbed in the discharge is characteristic for the corona discharge while at higher absorbed RF power the torch discharge occurs. Another characteristic of the corona and the torch discharge is the electric field in the vicinity of the sharp edge of the powered electrode. In the corona discharge this field ranges up to 14 000 V cm^{-1} as confirmed by the presence of the energetic states of molecules, and also by the calculations presented in this paper, see figure 3. In the torch discharge the electric field decreases down to 300 V cm^{-1} [19]. When the working gas is forced to stream fast around or through the electrode it is to be expected that it cannot reach thermal equilibrium. Hence, the temperature T of neutral particles will be smaller in comparison to the case when the gas flows slowly, only due to the temperature difference between the discharge core and the ambient environment. For this case it has been found experimentally in [19] that the torch discharge can transit back to the corona discharge.

It should be noticed that the plasma of the torch discharge burning in the monatomic working gas differs from that in the polyatomic gas where the energy levels up to 3 eV are excited at first, dependent on the energy levels and ionization potentials. The transfer of the electron energy to the neutral particles N, OH, NO in air has been studied in [21].

If the RF power dissipated in the torch discharge increases above a certain limit at which the temperature of the sharp electrode edge is high, the thermionic emission of the electrons from the electrode edge takes place. Then the properties of such a torch discharge do not resemble those of a glow discharge but they are more like those of an arc discharge. Hence the torch discharge at such a dissipated RF power level has been denoted as the arc torch discharge [19, 22]. In this type of discharge the significant source of charged particles is the thermionic electron emission from the electrode material. Hence, the small difference in temperatures T_e and T, which was the condition for sustaining the torch discharge in the absence of thermionic emission from the electrode, does not play as significant a role. This means that the arc torch discharge can burn even when the mentioned temperatures are not as close to each other. This fact has been demonstrated by our experiments described below. As already mentioned above the arc torch discharge has also its technological significance. In the following section the plasma source with the arc torch discharge, which has been developed in our laboratory, will be discussed in more detail.

3. The plasma source with the arc torch discharge

In order to study the plasma properties of the plasma source based on the arc torch discharge the experimental set-up

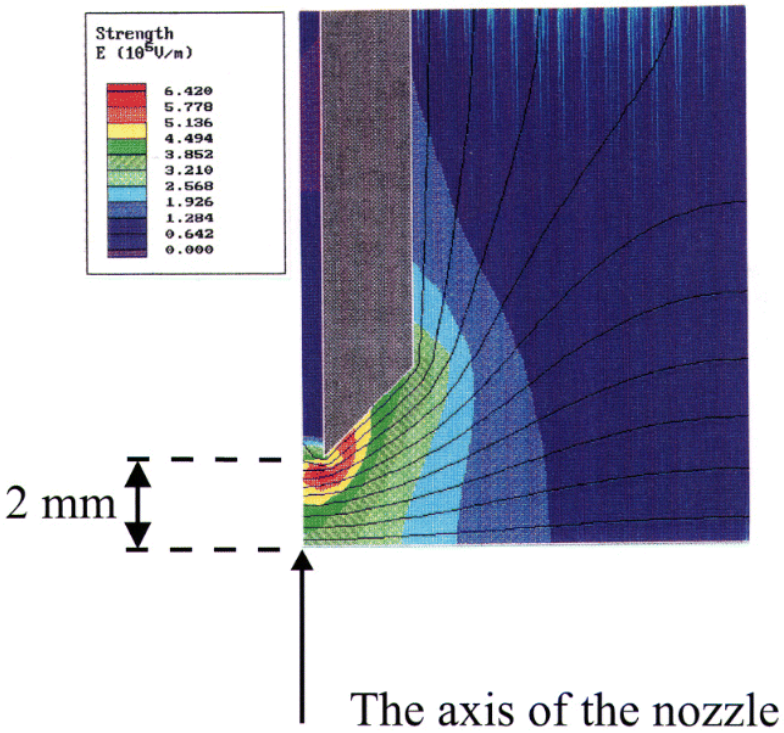

Figure 3. Model of the electric field distribution around the nozzle with a bevelled edge that points to a grounded plane. Cylindrical symmetry, only half of the nozzle cross-section is shown. Nozzle diameter 1 mm, distance nozzle–plane 5 mm, nozzle voltage 1000 V, in vacuum.

has been developed. The scheme of the set-up with the RF arc torch discharge is shown in figure 2. The powered electrode was made from thin pipe created from surgical needles with inner diameters of 0.5–1 mm and with length of several cm. The pipe edge is bevelled so a sharp point at the electrode edge is created. The pipe electrode is placed inside the reactor chamber. The electrode is fastened on a water-cooled support and is connected to the 13.56 MHz RF generator via a matching unit. The RF power has been measured using the conventional method of the difference between the incident and reflected power, i.e. when quoting the power absorbed in the discharge the power absorbed in the matching unit is neglected. The reactor chamber can be either continuously pumped by the rotary vane pump down to pressure in the kPa range or the reactor output can be opened to the environmental space in order to keep the gas inside the reactor chamber at atmospheric pressure. The gas flowing through the electrode pipe was technical argon with the throughput of approximately 750 standard cm^3 min^{-1}, i.e. the working gas in the reactor chamber was in our case a mixture of air and technical argon.

4. Model of the electric field near the electrode edge

In order to support the presence of the high electric field in the vicinity of the sharp (bevelled) nozzle edge we attempted to model the electric field in this region. The Quick Field program (shareware version 3.4 for modelling heat transfer, electrostatic and magnetostatic problems, solution of the Boltzmann equation in 2D and axisymmetric geometry) was used for this purpose. A sample of a typical result is presented in figure 3. In order to make the model as close to experiment as possible, the cylindrical configuration with the dimension corresponding to reality was used. The model calculates the electric field between the cylindrical pipe-like electrode with sharpened edges and the grounded planar electrode in vacuum. The voltage on the electrode was chosen as 1000 V; the distance between the electrode edge and the grounded plane was 2 mm. The model showed that in the region close to the bevelled electrode edge the electric field can reach values up to 10^6 V m^{-1}. In the model we did not suppose the thermionic emission from the electrode edge.

5. Experiment

The experiment has been performed at the pressure in the reactor chamber equal (a) to the atmospheric one and (b) to approximately 1 kPa. Under atmospheric pressure of the working gas (mixture of technical argon and air) the RF power absorbed in the torch discharge was adjusted just above 100 W in order to generate the arc torch discharge. However, at lower pressures of approximately 1 kPa the RF power of several tens of watts was sufficient for the creation of the arc torch discharge. At such lower pressures the working gas (argon) which flows from the nozzle stabilizes the arc torch discharge and a well defined plasma channel is created in the neighbourhood of the electrode edge.

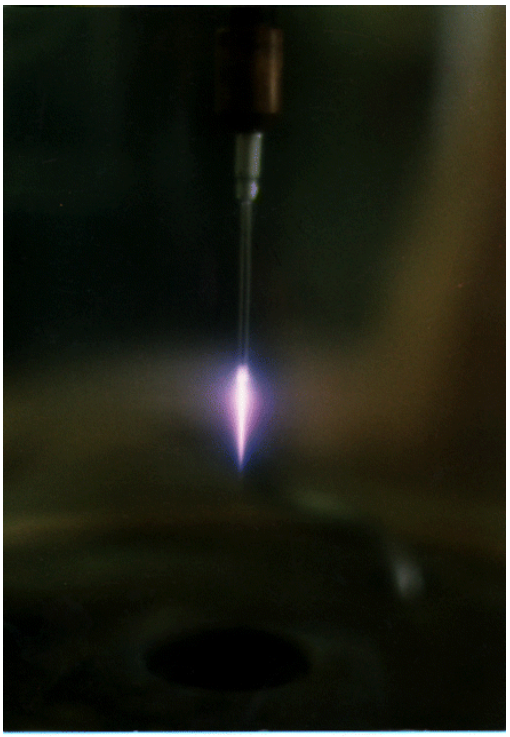

(a)

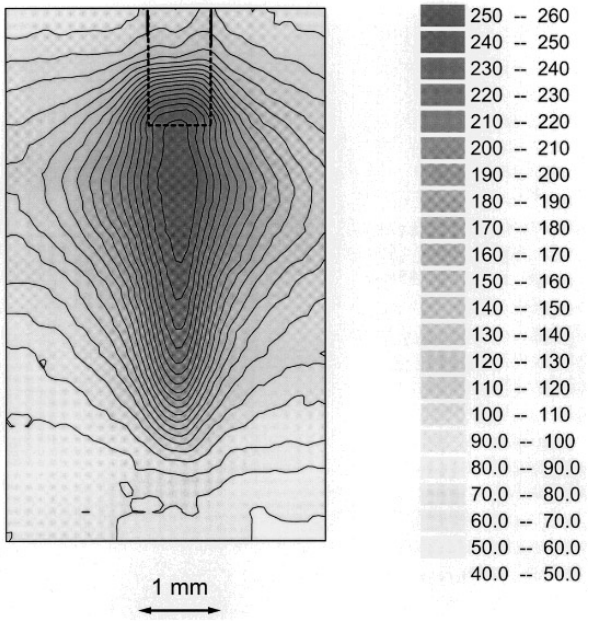

(b)

Figure 4. (a) A print of the plasma channel generated by the torch arc discharge that is stabilized by means of the Ar subsonic flow through the nozzle electrode. The throughput was approximately 750 standard cm^3 min^{-1}. The electrode is created from a surgical needle, outer diameter 0.7 mm, inner diameter 0.6 mm. RF power 125 W. The working gas was a mixture of air with Ar and was maintained inside the reactor at atmospheric pressure. (b) Curves of equal light intensities (isointensities) obtained by scanning and consequent computer processing of the print presented in figure 4 (enlarged detail of the electrode edge). The outer contour of the electrode is illustrated.

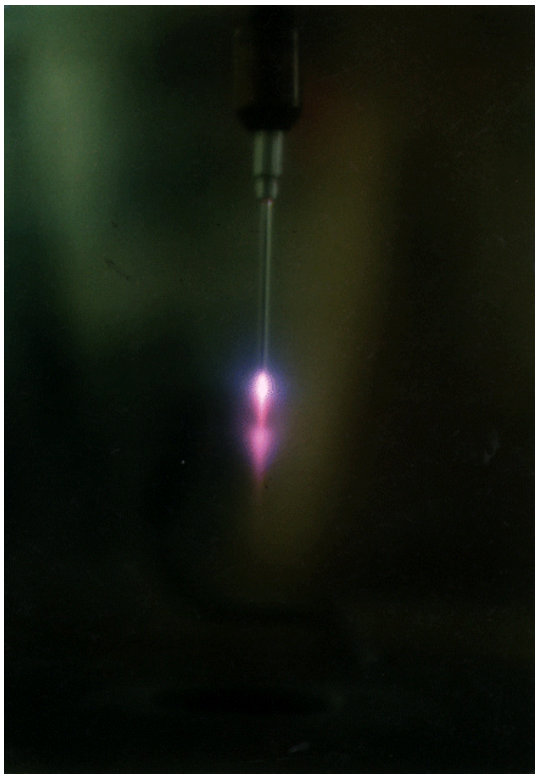

Figure 5. A print of the plasma channel generated by the torch arc discharge stabilized by means of supersonic Ar gas flow through the nozzle electrode. Throughput of the Ar gas was approximately 750 standard cm^3 min^{-1}. The electrode was created from a surgical needle with outer diameter 0.7 mm and inner diameter 0.6 mm. RF power 25 W. The working gas was a mixture of the air with Ar and was maintained inside the reactor approximately at pressure ∼1 kPa.

An example of a photographic print of the plasma channel that has been obtained at atmospheric pressure is presented in figure 4. The reactor chamber output was opened to the atmosphere during the measurement. We expect that similar results would have been observed if the electrode were placed in free space, i.e. outside the reactor chamber.

In order to receive more information about the plasma channel the photographic prints have been scanned and computer processed to obtain equiintensities (lines corresponding to the equal intensities of the light emitted by plasma). A typical result is given in figure 4(b). From both figures (figure 4(a) and especially from figure 4(b)) one can see that no barrel shock waves have been observed in the plasma channel and so one deduces as in [23] that the velocity of the working gas flow is subsonic. The edge of the electrode is hot which results in the creation of the arc torch discharge.

In order to increase the velocity of the working gas flow the reactor chamber was continuously pumped by the rotary vane pump. In this case the difference between the pressure at the input and output of the electrode was higher than in previous case. A photographic print of the plasma channel at a pressure inside the reactor chamber equal to approximately 1 kPa is shown in figure 5. From this picture one can see

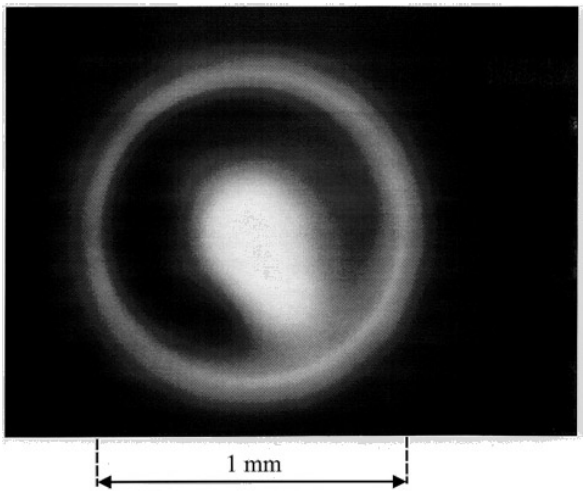

Figure 6. Radial distribution of the RF discharge in the nozzle. Snapshot by video camera with subsequent image processing. Argon gas flow 200 standard cm^3 min^{-1}, RF power 75 W.

two barrel shock patterns near the electrode output. Similar as in the RF reactor with hollow cathode [1–4] the presence of barrel shocks indicates that the velocity of the gas flow in the plasma channel at the neighbourhood of the electrode edge is supersonic. Note, however, that near atmospheric pressure the powered electrode (thin pipe) does not work as a hollow cathode and only the edge of the electrode influences the processes in the discharge. Due to this phenomenon the torch plasma source differs from the plasma source inside the RF low-pressure reactor using the hollow cathode [23]. This phenomenon is especially important for surface treatment technology because only sputtered or evaporated material of the electrode edge can take part in the plasma-aided technological process.

The radial structure of the discharge is shown in figure 6. This figure has been obtained by using a Panasonic NV-MS-5EG video camera (picture format S-VHS/VHS) with subsequent computer image processing. The exposure time has been adjusted manually in order to optimally match the range of the light intensity emitted from the discharge to the camera sensitivity (i.e. to prevent overexposure of the light parts and underexposure of the dark parts of the picture). The picture shows the axial view into the electrode nozzle from its output when the discharge was operational. It is seen in this figure that the discharge originates at the angular position of the nozzle electrode where the light emitted from the electrode edge has its maximum intensity. This is the position of the sharpest edge of the nozzle electrode. It is further seen that not only the sharpest electrode edge but all the outer circumference of the electrode shines. This effect proves the comparatively high temperature of the electrode edge (the electrode edge is 'white-hot'). Also, a relatively small increase of the incident RF power causes the electrode tip to melt. These facts further support our supposition that the thermionic electron emission from the electrode edge may also contribute as a source of charged particles for the observed discharge. The fact that the discharge originates at the sharpest electrode edge (that has the highest temperature) is probably the reason that no cathode spot formation is seen in figure 6.

The neutral vibrational and rotational temperature at the axis of the plasma channel has been determined by means of optical plasma diagnostic methods. During the measurements the electrode was placed outside the reactor chamber in free space, i.e. the presented data have been acquired at atmospheric pressure. The applied (measured) RF power was 150 and 200 W. A Jobin Yvon HR 640 monochromator with Spectrum-one air cooled CCD detector has been used for the determination of the molecular bands of N_2 and OH in the spectral range 280–900 nm. The vibrational temperature, which was assumed to be close to the electron temperature, $T_v \approx T_e$, has been determined from the molecular band of N_2, second positive system. The rotational temperature T_r has been determined from the OH 306.4 nm band. The rotational temperature can be used as an approximation of the neutral gas temperature T in the plasma channel. We investigated the part of the discharge downstream of the electrode edge within a distance of 0–10 mm from the electrode edge. The spatial resolution on the discharge axis was approximately 1 mm. We found the vibrational temperature T_v of N_2 to be about 2000 K and the average rotational one T_r to be about 500 K. The measured temperatures did not vary significantly (within the error limit $\pm 15\%$) within the whole investigated path up to 10 mm downstream from the electrode edge. The correction on the radial distribution of the light emitted by the plasma channel (Abel inversion procedure) has not been made and the quoted temperatures have been determined with an accuracy of 10–15%.

6. Discussion

The ratio of the temperatures $T_v/T_r \approx T_e/T$ measured by the emission spectroscopy has been found in our case close to (4 ± 1):1. This means that the working gas, that is forced to flow fast through the powered pipe electrode by the overpressure at the electrode entrance, does not have time to reach thermal equilibrium with the hot electrode edge. Without the presence of thermionic electron emission from the electrode edge the thermal ionization in the gas bulk would not suffice to sustain the torch discharge (characterized by comparatively low electric field at the electrode edge) and the discharge would return to the corona one. Hence, without the presence of thermionic electron emission from the electrode edge, the investigated ratio of temperatures would change very fast with increasing distance from the electrode edge. The fact that we did not find the above mentioned ratio to vary significantly with the distance from the electrode edge indicates that the thermionic emission of electrons from the electrode edge most probably plays a significant role in our plasma source. This fact is further supported by figure 7, where we plotted the dependence of the relative light intensity measured on the surface of the stainless steel electrode with respect to the distance from the electrode edge (its sharpest tip). This light intensity corresponds roughly to the black body radiation of the electrode surface and gives therefore information on the electrode temperature. The data have been taken from those in figure 4(b). It should be noted that the light emitted in the neighbourhood of the electrode edge is a superposition of the light emitted from the

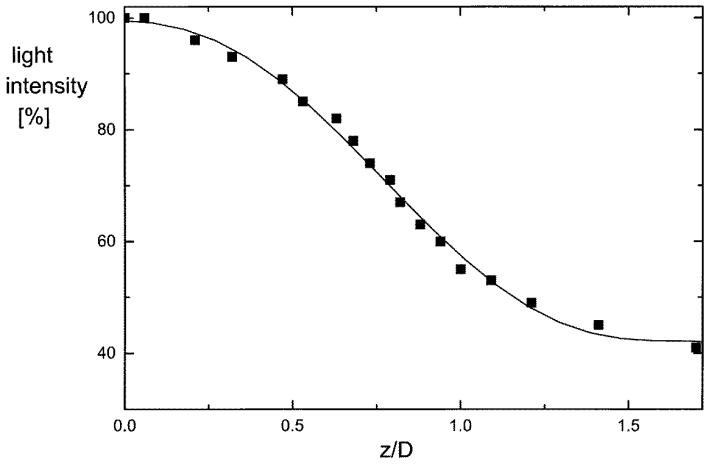

Figure 7. The dependence of the relative light intensity ε on the surface of the electrode with respect to the distance from the sharpest electrode edge. Obtained from the result presented in figure 4(b). z/D is the relative distance from the electrode edge; D is the outer diameter of the nozzle electrode.

hot electrode edge and from the torch discharge. However, it can be seen from the plot presented in figure 7 that the relative light intensity rises steeply in direction to its edge and that the discharge is concentrated close to the electrode edge. This fact supports our supposition that an additional source of charged particles might be the thermionic electron emission from the electrode edge and, consequently, that the presented plasma source has the features of an arc torch discharge.

In contrast to the low-pressure hollow cathode reactor [1–4] where the gas flow is laminar in case of the high-pressure torch discharge the gas flow is turbulent. This effect can influence the surface treatment in particular cases and imposes some restrictions to its applicability. We can state on the other hand, as an advantage of this plasma source, that it has been shown recently [8–10] that the arc torch discharge with the modified electrode can also work in a liquid environment.

7. Conclusion

We attempted to describe the novel plasma source that we call the high-pressure torch discharge plasma source. The principle of this discharge is based on the known principles of the corona and the torch discharge. The additional feature of this discharge is that it is stabilized by the flow of the working gas. Moreover the performed experimental study of this plasma source seems to support the supposition that the thermionic electron emission from the electrode edge contributes to the creation of charge carriers that are necessary to sustain the discharge even at atmospheric pressure. The following experimental facts seem to support this supposition:

- high light intensity emitted from the electrode edge that corresponds to the high temperature of the electrode edge,
- the discharge is formed close to the hottest electrode tip,
- there is no experimental evidence for the cathode spot formation,
- the ratio of the electron and the gas temperature is approximately 4:1 and does not vary significantly with the distance from the electrode.

Both the working gas flow and the thermionic electron emission from the electrode edge contribute therefore to the stable operation of the studied plasma source.

At present there is an urgent need for a plasma source that would enable the cleaning and/or the surface treatment of objects of larger dimensions preferably at atmospheric pressure. Such a plasma source would then replace the chemical or electrochemical methods that have mostly been used for these purposes up to now. The plasma source that was described and studied in this paper has already been successfully applied for cleaning of surfaces of comparatively large objects (archaeological artefacts) at atmospheric pressure and in a liquid environment [8–10].

Acknowledgments

This work has been done in the frame of the Association for Education, Research and Application in Plasma-Chemical Processes. The authors are grateful for the partial financial support afforded by the grants 202/95/1222 and 202/98/0666 of the Grant Agency of the Czech Republic, by the grants 181/1996/B FYZ/MFF and 75/1998/B FYZ/MFF of the Grant Agency of Charles University and by project COST 515.50.

References

[1] Šícha M, Bárdoš L, Tichý M, Soukup L, Jastrabík L, Baránková H, Soukup R J and Touš J 1994 *Contrib. Plasma Phys.* **34** 794
[2] Bárdoš L 1988 *Proc. Summer School on Thin Films (Skalský dvůr, 5–9 September, 1988)* ed Z Hájek and T Růžička (Union of the Czech Mathematicians and Physicists) p 73
[3] Bárdoš L 1993 *Proc. 21st ICPIG (Bochum, 19–24 September, 1993)* vol 3, ed G Ecker, U Arendt and J Böseler, p 98
[4] Soukup L, Šícha M, Jastrabík L and Novák M 1995 *Proc. 22nd ICPIG (Hoboken, 31 July–4 August, 1995)*

ed K H Becker, W E Carr and E E Kunhardt (New York: AIP) p 299
[5] Šícha M, Soukup L, Jastrabík L, Novák M and Tichý M 1995 *Surf. Coatings Technol.* **74** 212
[6] Fendrych F, Soukup L, Jastrabík L, Šícha M, Hubička Z, Chvostová D, Tarasenko A, Studnička V and Wagner T 1999 *Diamond and Related Materials* at press
[7] Brablec A, Slavíček P, Klíma M and Kapička V 1997 *Proc. 18th Symp. on Plasma Physics and Technology (Prague, 17–20 June, 1997)* ed J Píchal, p 193
[8] Brablec A, Slavíček P, Klíma M and Kapička V 1997 *Proc. 23rd ICPIG (Toulouse, 17–22 July, 1997)* vol I, ed M C Bordage and A Gleizes, p I-128
[9] Klíma M, Janča J, Zajíčková L, Brablec A, Sulovský P and Alberti M 1997 *Proc. 18th Symp. on Plasma Physics and Technology (Prague, 17–20 June, 1997)* ed J Píchal, p 285
[10] Klíma M, Zajíčková L and Janča J 1997 *Z. Schweiz. Arch. Kinstgesch.* **54** 31–4
[11] Baderau E, Giurgea M, Giurgea Ch and Trutia A T H 1957 *Spectrochim. Acta* **13** 441
[12] Mawrodineanu R and Hughes R C 1963 *Spectrochim. Acta* **19** 1209
[13] Tappe W and Calker J 1963 *Z. Anal. Chem.* **198** 13
[14] West D C and Hume D N 1964 *Anal. Chem.* **36** 415
[15] Dunken H, Pforr G, Mikkeleit W and Geller K 1964 *Spectrochim. Acta* **20** 1531
[16] Dunken H and Pforr G 1965 *Z. Phys. Chem.* **230** 48
[17] Pforr G and Kapička V 1966 *Collection Czech. Chem. Commun.* **31** 4710
[18] El Gammal M 1967 *Proc. 8th ICPIG (Vienna, 27 August–2 September, 1967)* ed F P Viehböck (Vienna: Springer) p 237
[19] Truneček V 1971 *Proc. Conf. on Unipolar High-Frequency Discharges (Brno) Folia Sci. Nat. Univ. Brno, Physica* **12** 3
[20] Janča J 1968 *Folia Fac. Sci. Nat. Univ. Brno* **9** 31
[21] Popov V and Stolov A L 1953 *Učon. Zap. Kazan. Univ.* **113** 53 (in Russian)
[22] Truneček V 1962 *Beitr. Plasmaphys.* **2** 598
[23] Tichý M, Šícha M, Bárdoš L, Soukup L, Jastrabík L, Kapoun K, Touš J, Mazanec Z and Soukup R J 1994 *Contrib. Plasma Phys.* **34** 765

Deposition of polymer films by rf discharge at atmospheric pressure

P. Slavíček, V. Buršíková, A. Brablec, V. Kapička, M. Klíma

Department of Physical Electronics, Faculty of Science, Masaryk University, Kotlarska 2, 611 37 Brno, Czech Republic

Received 24 April 2004

In this contribution we report some typical properties of the discharge which has been used for deposition of thin films and some mechanical parameters of thin films. RF plasma nozzle can burn very well even at atmospheric pressure. Special properties of RF discharges offer hopeful technological applications like deposition of thin solid films. The knowledge of physical parameters of plasma has been required. The parameters of the plasma were investigated by spectral and optical methods. The powered RF electrode of the torch discharge plasma source is made from the metal or dielectric pipe with an inner diameter of $1 \div 2$ mm and with a length of several centimeters. The electrode is connected through the matching unit to the RF generator driven at the frequency of 13.56 MHz. The mixture of argon and *n*–hexane or HMDSO (hexamethyldisiloxane, $C_6H_{18}Si_2O$) gas flows through the RF electrode at the pipe Fig. 1. Polymer films were deposited on the several substrates e.g. glass, brass polished plates and Si wafers.

PACS: 52.77.Dq, 52.80.Pi, 81.15.Jj
Key words: deposition of films, rf discharge, plasma diagnostics

1 Introduction

Special properties of RF discharges offer many hopeful technological applications like deposition of thin solid films, cleaning and treatment of surfaces, restoration of archaeological artefact's, etc. [1 – 4]. It was also demonstrated that this type of discharges could burn under the liquid level. They can interact with the material and then new chemical compounds can arise. This special plasma device so called "plasma pencil" was developed in our department. First results of deposition of thin films at atmospheric pressure by this plasma device were presented last year on XV Symposium on Physics of Switching Arc [1].

2 Experimental

The powered RF electrode of the torch discharge plasma source is made from the metal or dielectric pipe with an inner diameter of $1 \div 2$ mm and with a length of several centimeters [1 – 4]. The electrode is connected through the matching unit to the RF generator driven at the frequency of 13.56 MHz. The argon working gas flows through the RF electrode at the nozzle. The argon with an admixture of *n*–hexane or HMDSO goes directly to the discharge. The total gas flow ranged from 900 sccm/min to 5000 sccm/min. In case of the deposition from HMDSO/Ar

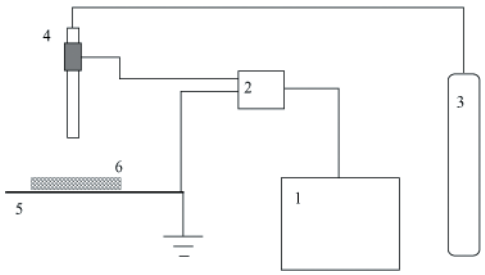

Fig. 1. Experimental set–up: 1 – rf generator, 2 – match unit, 3 – working gas, 4 – dilelectric plasma nozzle, 5 – grounded electrode with rotating substrate holder, 6 – substrate

mixture a rotating substrate holder was used in order to enhance the deposition homogeneity and to suppress the substrate heating.

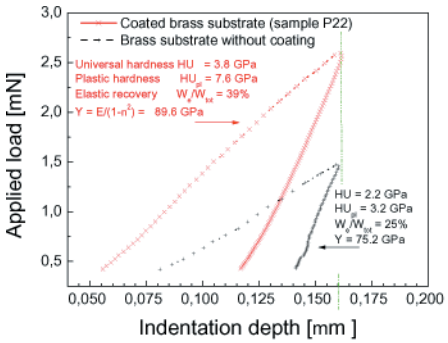

Fig. 2. Load–penetration curves for coated and uncoated brass substrate.

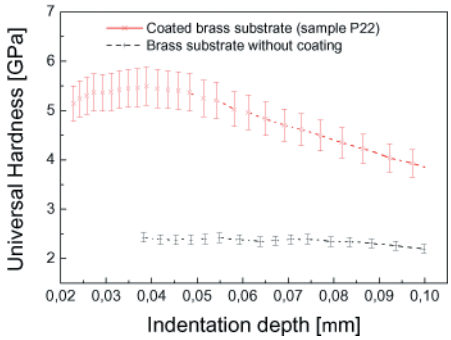

Fig. 3. Universal hardness dependence on the indentation depth.

The RF power absorbed in the torch discharge has been adjusted in the range from 50 W till 400 W. The length of the discharge was about 3 cm and the discharge has been not connected or connected with the substrate. Polymer films were deposited on the substrate of Al sheet, Cu and brass substrate polished plates, Si wafers and glass. This non–standard deposition source was used for deposition of thin films at atmospheric pressure and obtained films were tested by means of standard mechanical tools.

The nanoindentation tests were made by means of Fischerscope H100 tester. This equipment enables to record the indentation depth dependence on the applied load during both, the loading and unloading part of the indentation test. In our case the so–called Vickers indenter (square based pyramid) was used for hardness measurement. The universal hardness HU is defined [5, 6] as the measure of the resistance against elastic and plastic deformation. From the loading/unloading curves we obtained the elastic deformation work W_e and the irreversible dissipated

indentation work W_{irr}:

$$HU = \frac{L}{26.43\,h^2}, \tag{1}$$

$$W_{\mathrm{total}} = \int_{h=0}^{h_{\max}} L_1(h)dh \ \ , \ W_e = \int_{h_{min}}^{h_{\max}} L_2(h)dh \ \ , \ W_{\mathrm{irr}} = W_{\mathrm{total}} - W_{\mathrm{el}} \ \ , \tag{2}$$

where h is the penetration depth at applied load L, $L_1(h)$ is the loading curve and $L_2(h)$ is the unloading curve.

From the load–penetration curves it was possible to determine also the material resistance against plastic deformation H_{pl} (so called plastic hardness) and the elastic modulus Y.

$$H_{\mathrm{pl}} = \frac{L_{\max}}{26.43 h_{\mathrm{r}}^2}, \tag{3}$$

h_{r} is the depth of the remained indentation print created by irreversible deformation under maximum load $L_{\max}$. The indentation elastic modulus Y of the tested material can be calculated on the basis of the contact model in the following way:

$$\frac{1}{Y} = \frac{1}{E_{\mathrm{r}}} - \frac{(1-\nu_{\mathrm{i}}^2)}{E_{\mathrm{i}}} \ \ , \ E_{\mathrm{r}} = \frac{\sqrt{\pi} dL(h_{\max})/dh}{2\sqrt{A(h)}} \ \ . \tag{4}$$

Here E_{r} is the so called reduced elastic modulus, $dL(h_{\max})/dh$ is the slope of the unloading curve at maximum load (depth) and $A(h)$ is the projected contact area, when the maximum indentation depth is h. E_{i} and ν_{i} are the elastic modulus and the Poisson ratio of the indenter material.

3 Results

Each measurement was repeated at least nine times in order to check the reproducibility of the nanoindentation measurement. The indentation tests were provided at several different load and we studied also the fracture toughness of the coating/substrate systems. The coatings prepared on silicon substrate showed very low resistance against the indentation test.

Thin films on sample P22 and P29 were made by plasma device with metal nozzle and the discharge has been not connected with the substrate. The resistance of the coatings on brass substrates was much higher. Fig. 2, 3 shows the results of the nanoindentation tests on sample P22. In that case the test were provided on both coated and uncoated part of the brass substrate for the same maximum penetration depth $h_{\max} = 160$ nm, in order to get comparable load penetration curves. As it is shown in Fig. 2, 3, the coated part exhibited much higher resistance against penetration test as the uncoated part. The universal hardness HU increased from 2.2 to 3.8 GPa and the calculated plastic hardness increased from 3.2 to 7.6 GPa. There was also an increase in the elastic modulus Y from 75 to 90 GPa. The elastic to

total deformation work ratio W_e/W_{tot} increased from 25 to 39 %. These parameters characterize the whole system of the coating and the substrate. The films are very thin and there is still an influence of the substrate on the measured characteristics as it is shown in Fig. 2, 3 on the universal hardness dependence on the indentation depth.

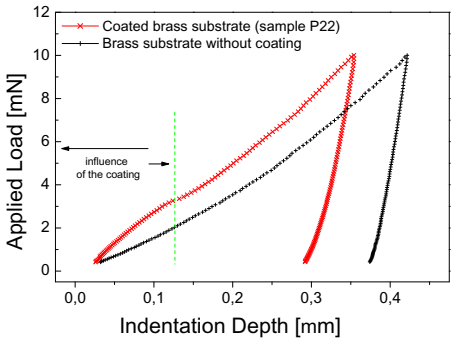

Fig. 4. Load–penetration curves obtained on sample P22 for maximum load of 10 mN. Deposition time 10 min, rf power 125 W.

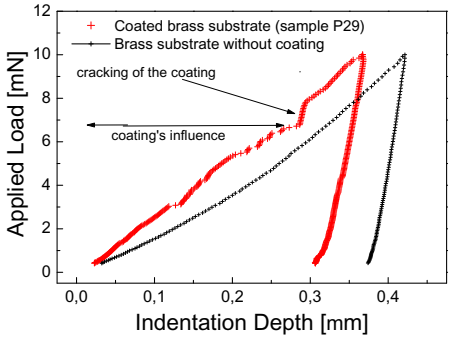

Fig. 5. Load–penetration curves obtained on sample P29 for maximum load of 10 mN (right). Deposition time 5 min, rf power 125 W.

The film resistance appeared on the measured universal hardness up to 60 nm (5 GPa) of the penetration depth, after that the influence of the substrate begun to be substantial. The nanoindentation tests were compared with microindentation tests. In Fig. 4 are shown the load–penetration curves obtained for maximum load of 10 mN for coated and uncoated part of the substrate (P22). The influence of the film resistance appeared on the part of the loading curve. The fracture toughness of the substrate was high, there were no cracks in the film or at the film/substrate interface. In Fig. 5, in the case of the sample P29, the influence of the film was substantial up to higher depths (250 nm), but after that coating fracture was observed. The cracking appeared on the loading curve as a significant jump. The hardness of the film P29 was about 8 GPa.

In case of the deposition from HMDSO/Ar mixture a rotating substrate holder was used. The HMDSO/Ar mixture proved to be suitable for preparation of porous silica-like films. These types of films are recently used for example for deposition of so-called low-k dielectrics. By the substrate rotation the film porosity was varied. The DSI tests enable to study also the film porosity on the basis of the "percolation theory" [7]. In case of films listed in Tab. 1 the deposition conditions were the same except the rotation rate of the substrate holder. So these films differed only in their porosity. As it can be seen in Tab. 1, the elastic modulus and plastic hardness differed for the films with different rotation rate. With lower rotation rate higher hardness and elastic modulus were achieved, what means that the degree of film porosity was lower as in the case of low rotation rate. The statistical distribution of the pores (see Fig. 6) was evaluated from the load–penetration curves. In Fig. 7

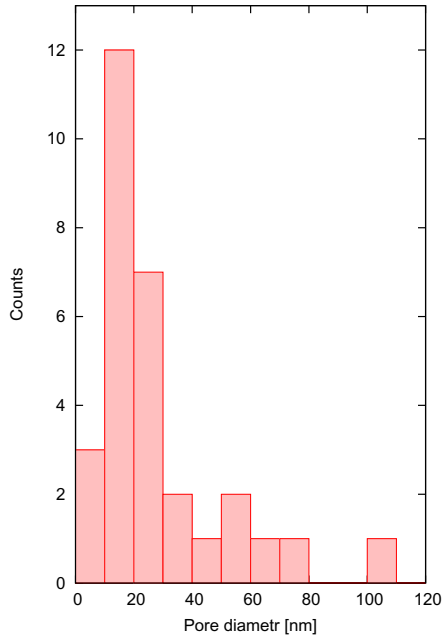

Fig. 6. Statistical distribution of the pore diameter for sample 5.

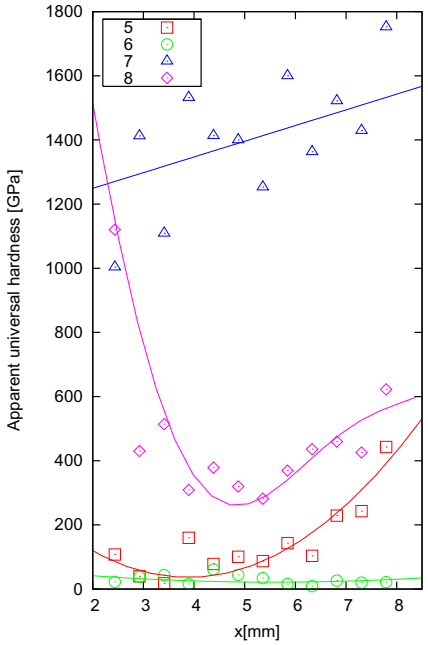

Fig. 7. Dependence of the apparent universal hardness on the distance x from the edge of the films No. 5 ÷ 8 deposited on glass substrates. The edge of the film was taken as zero.

the apparent universal hardness dependence on the distance from the film edge is illustrated. The values were obtained at maximum applied load of 4 mN.

No.	t[s]	v[m/s]	HU_{pl} [GPa]	Y [GPa]
5	11.31	0.063	0.08	2.7
6	18.26	0.025	0.15	7.8
7	2.62	0.063	1.2	4.5
8	7.84	0.025	0.11	14.2

Table 1. Deposition conditions (deposition time t and rotation rate v for porous silica–like films together with their apparent material parameters as plastic hardness H_{pl} and elastic modulus Y of the coating–substrate systems.

Emission UV–VIS spectra were obtained by means of the monochromator HR640 (1200 gr/mm) and Triax 550 (300 gr/mm, 1200 gr/mm, 3600 gr/mm). Optical emission spectra for two spectral ranges show that in pure argon we observe only

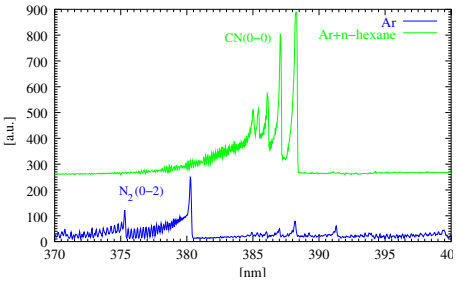

Fig. 8. Emission spectra of nitrogen and CN in pure Ar and mixture Ar + n–hexane.

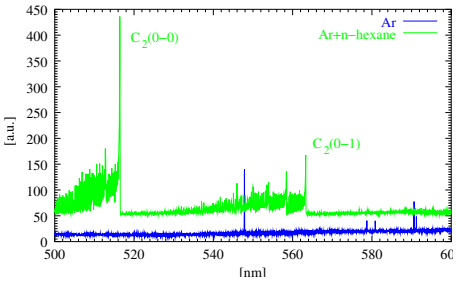

Fig. 9. Emission spectra of C2 in pure Ar and mixture Ar + n–hexane.

argon lines and nitrogen bands while in the mixture of argon and n–hexane we observe the molecular bands of CN and C_2, which originates from molecular n–hexane Fig. 8, 9.

4 Conclusions

The presented results show that RF discharges in atmospheric pressure is suitable for plasmachemical and technological processes. Namely, in this moment we conclude that to prepare thin films is less expensive and easier at atmospheric pressure then at low one.

This work has been financially supported by the research project MSM 143100003, projects COST OC 527.20, and by grant 202/03/0011 of Grant Agency of the Czech Republic.

References

[1] V. Bursikova, P. Slavicek, A. Brablec, V. Kapicka, M. Klima: Milos. XV Symposium on Physics of Switching Arc, Vol I. Contributed Papers, Brno, Czech Republic, 2003. p. 22-25,

[2] K. Wiesemann: in Book of Invited Lectures. 20th SPIG. (Eds. by N. Konjevic, Z. Lj. Petrovic and G. Malovic), 2000, Zlatibor, Yugoslavia, p. 307.

[3] M. Klima, J. Janca, V. Kapicka, P. Slavicek, P. Saul: it The Method of Making a Physically and Chemically Active Environment by Means of a Plasma Jet and the Related Plasma Jet. Czech patent No. 286310 (prior. 12.5.1998) or PCT/CZ99/00012

[4] A. Brablec, P. Slavicek, M. Klima, V. Kapicka, J. F. Behnke, M. Sicha: Czech. J. Phys. (2002) 561–566.

[5] W. C. Oliver and G.M. Pharr, J. Mater: Res. 7. (1992), 1564.

[6] W. C. Oliver, G.M. Pharr and F.R. Brotzen, J. Mater: Res. 7 (1992) 613.

[7] L. Gibson and M. Ashby: Cellular solids. 2nd Ed. (1997)

RF DISCHARGE AT ATMOSPHERIC PRESSURE – DIAGNOSTICS AND APPLICATIONS

PAVEL SLAVICEK[*a], MILOS KLIMA[a], DANA SKACELOVA[a], EVA KEDRONOVA[a], ANTONIN BRABLEC[a], and VLADIMIR AUBRECHT[b]

[a] Department of Physical Electronics, Faculty of Science, Masaryk University, Kotlarska 2, 611 37 Brno, [b] Department of power electrical and electronic engineering,Brno University of Technology, Technicka 8, budova A3, 61600, Brno, Czech Republic
ps94@sci.muni.cz

1. Introduction

Low temperature plasmas are extensively used for the plasma processing[1], light sources, various plasma technologies[2] etc. During several last years different plasma discharges with nozzle and powered by rf generator driven at frequency 13,56 MHz have been investigated. Plasma pencil is a special type of plasma nozzle working at atmospheric pressure, which is interesting for possible applications[6,8] such as local treatment of surface, deposition of thin films, change surface energy, cutting in surgery, etc. Through this nozzle, which is made from quartz tube with typical inner diameter 2 mm, flows working gas (argon with water vapour). The powered electrode is connected through the maching unit to the rf generator.

In the contribution, we present diagnostics of unipolar discharge channel generated by the plasma pencil at atmospheric pressure. For different electrical parameters and various construction design of the plasma pencil the parameters of the plasma channel are estimated from optical emission spectra in the spactral range 200–900 nm: rotation temperature from OH rotational lines, vibrational temperature from nitrogen bands as well as concentration of electons and temperature of neutral gas from Stark and Doppler broadening of hydrogen lines, resp.

Fig. 1. **Photograph of plasma pencil**

2. Experimental setup

The plasma pencil is shown in Fig. 1. The powered electrode of was separated by the dielectric quartz tube, nozzle with the inner diameter 2 mm and the outer diameter 4 mm and 50 mm length. As an active medium flowing through the hollow electrode of the plasma pencil argon with purity 99.996 % was used. Note, that the working gas flowing from the nozzle stabilises the dischrge. The hollow electrode was connected through the matching network to the rf generator Cesar – 1310 by Dresler driven at frequency 13,56 MHz[5–7].

Optical emission spectroscopy was accomplished by means of the monochromator FHR 1000 by Jobin-Yvon-Horiba supplied with CCD detector and ICCD (Intensified Charge Couple Device) system. CCD detector in "continual" regime was used, ICCD system in pulse regime was chosen whereas square pulse modulation frequency of 27 kHz by means of external triggering generator Agilent 33220A was adjusted.

The spectra was recorded perpendicularly to the plasma channel for different discharge parameters.

The rotational temperature from rotational lines of OH, the electron temperature from Ar lines in the plasma channel at different conditions of discharge (power supply, frequency, length) were determined. Rotational and electron temperature were calculated from Boltzmann plot[3,4].

The most frequently used technique for determination of electron concentration N_e is based on the half-width and shape of the hydrogen Balmer beta (H_β = 486.13 nm) spectral line.

Electron concentration was estimated by approximate formula e.g.() by Weise et al[9,10,12] .

$$N_e[m^{-3}] = 10^{22}\left(\frac{W_s}{4.7333}\right)^{1.49}$$

W_s is the Stark halfwidth at half maximum (HWHM) of line. In case when Stark width, W_s, is small and comparable

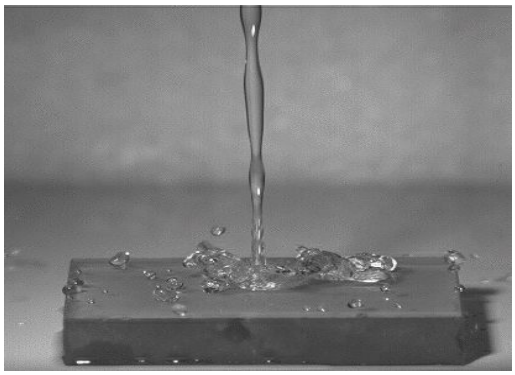

Fig. 2. **Thin hydrophobic layer on glass**

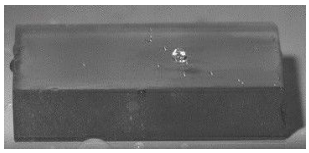

Fig. 3. **Drop of water on thin hydrophobic layer surface.** This layer was deposited by plasma pencil at atmospheric pressure

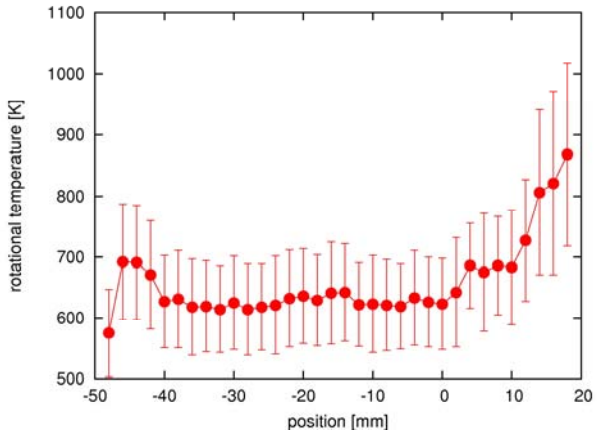

Fig. 4. **Rotational temperature estimated from OH lines as a function of the distance from the end of the nozzle for fixed gas flow of 1 l min^{-1} and fixed hf power input of 125 W.** The negative distance was taken in the nozzle while the positive values were taken out of the nozzle.

with Doppler and/or instrumental broadening it may be determined by using an approximate deconvolution formula[11].

In calculation of electron concentration other broadening mechanism such as resonance and Van der Waals broadening were ignored, because Stark broadening was dominant.

3. Results and discussion

A typical distribution of rotational temperature estimated from OH lines as a function of the distance from the end of the nozzle for fixed gas flow of 1 l min^{-1} and fixed hf power input of 125 W is shown in Fig. 4. The negative distance was taken in the nozzle while the positive values were taken out of the nozzle and the lenth of nozzle was 50 mm. The rotational temperature is aproximately constant along the nozzle. In side the nozzle rotational temperature insreases fast.

Fig. 5 shown a distribution of concentration of electrons as function of the distance from the end of the nozzle for fixed gas flow of 1 l min^{-1} and fixed hf power input of 125 W. The negative distance was taken in the nozzle while the positive values were taken out of the nozzle. Concentration of electrons, calculated from the half-width and shape of the hydrogen Balmer beta line H_β = 486,13 nm, decreases along the nozzle from electrode to the end of the nozzle.

A typical distribution of electron temperature and rotational temperature as a function of the delay while using ICCD system in pulse regime, square pulse modulation frequency of 27 kHz and duty cycle 50 % is shown in Fig. 6. and Fig. 8. Gas flow of 1 l min^{-1} and hf power input of 135 W in the end of the nozzle. Is evidently, that the temperature is measurable only in the range of modulation pulse.

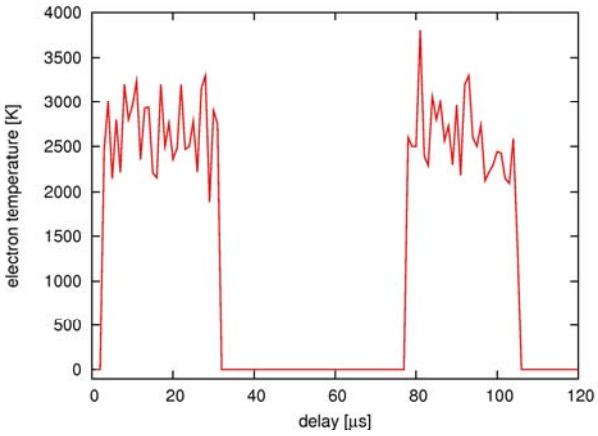

Fig. 6. **Electron temperature calculated from Ar lines as a function of the delay while using ICCD detector for fixed gas flow of 1 l min^{-1} and fixed hf power input of 135 W in the end of the nozzle.** Pulse modulation frequency of 27 kHz was adjusted

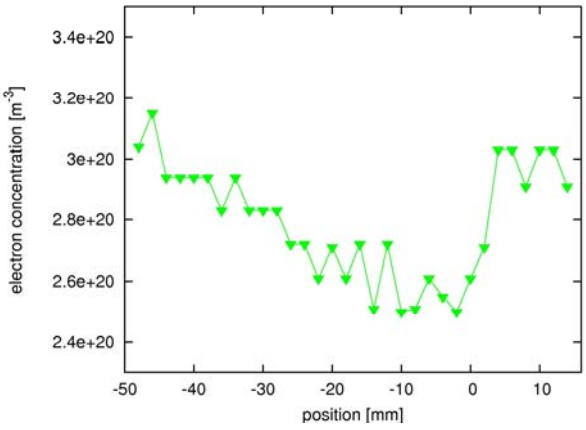

Fig. 5. **Concentration of electrons as function of the distance from the end of the nozzle for fixed gas flow of 1 l min^{-1} and fixed hf power input of 125 W.** The negative distance was taken in the nozzle while the positive values were taken out of the nozzle

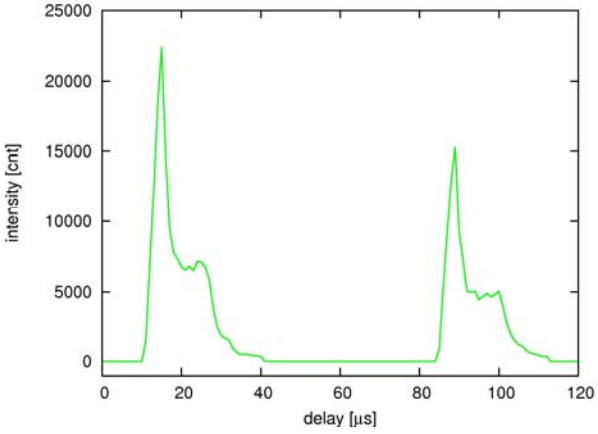

Fig. 7. **Intensity of OH lines as a function of the delay while using ICCD detector for fixed gas flow of 1 l min^{-1} and fixed hf power input of 135W in the end of the nozzle.** Pulse modulation frequency of 27 kHz was adjusted

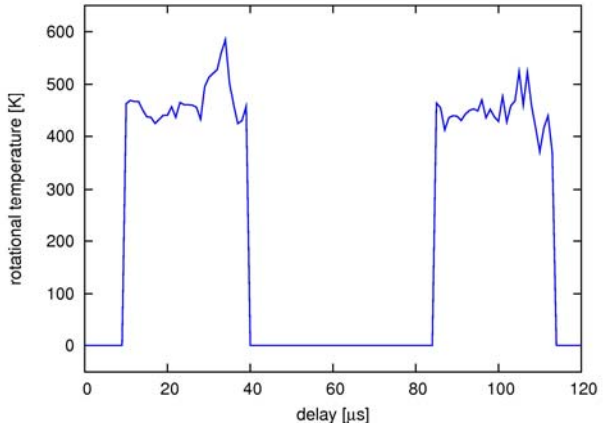

Fig. 8. **Rotational temperature calculated from OH lines as a function of the delay while using ICCD detector for fixed gas flow of 1 l min^{-1} and fixed hf power input of 135 W in the end of the nozzle.** Pulse modulation frequency of 27 kHz was adjusted

Fig. 7 shows a distribution of intinsity of one rotational line of OH molecul as a function of delay in pulse regime of discharge.

Pulse regime of discharges are perspective for deposition of thin layer on thermal sensitive materials and for other applications..

This discharge in „continual" regime was used for deposition thin layers on glass substrates. For this deposition mixture of Ar and hexamethyldisiloxane (HMDSO) was used as working gas.

High speed camera Olympus i-SPEED-2 was used for demonstration of properties of this thin films. Record speed 1000 frames per second was used. Fig. 2 and Fig. 3 show pictures accompilshed by this camera. Pictures show drops of water on hydrophobic thin films deposited on glass substrates. This are first hydrophobic films deposited by this plasma device at atmospheric pressure.

4. Conclusion

In this article results of electron concentration, rotational and electron temperature in discharge generated by plasma pencil at atmospheric pressure were presented for „continual" and pulse regime.

First results of deposition of hydrophobic thin films on glass substrates by plasma pencil were presented too.

In this contribution the single nozzle was used, but several nozzles can be applied simultaneously in one device, which is more convenient for practical application.

This research has been supported by the grant 202/07/1207, by the Czech Science Foundation and by the research intent MSM:0021622411 funding by the Ministry of Education of the Czech republic and Grant Agency of Academy of Science of Czech Republic contract No. KAN101630651.

REFERENCES

1. Rahel J., Simor M., Cernak M., Stefecka M., Imahori Y., Kando M.: Surf. Coat. Technol. *169-170*, 604 (2003).
2. Sira M., Trunec D., Stahel P., Bursikova V., Navratil J.: Phys. D *41*, 015205 (2008).
3. Griem H. R.: *Principles of Plasma Spectroscopy*. Academic Cambridge Univ. Press, New York 1997.
4. Lochte-Holtgreven Ed W.: *Plasma Diagnostics*. American Institute of Physics, New York 1995.
5. Cada M., Hubicka Z., Sicha M., Churpita A., Jastrabik L., Soukup L., Tichy M.: Surf. Coat. Technol. *174-175*, 530 (2003).
6. Slavicek P., Klima M., Janca J., Brablec A., Kadlecova J., Smekal P.: Czech. J. Phys., B 56 (2006).
7. Slavicek P., Bursikova V., Brablec A., Kapicka V., Klima M.: Czech. J. Phys. *54*, C586 (2004).
8. Hubicka Z.: Plasma Sources Sci. Technol. *11*, 195 (2002).
9. Zikic R., Gigisos M. A., Ivkovic M., Gonzales M. A., Konjevic N.: Spectrochim. Acta, Part B *57*, 987 (2002).
10. Kelleher D. E. : J. Quant. Spectrosc. Radiat. Transfer *25*, 191 (1981).
11. Ivkovic M., Jovicevic S., Konjevic N.: Spectrochim. Acta, Part B *59*, 591 (2004).
12. Zikic R., Gigisos M. A., Ivkovic M., Gonzales M. A., Konjevic N.: Spectrochim. Acta, Part B *57*, 987 (2002).

Journal of
APPLIED
BIOMEDICINE

J Appl Biomed **8**:55–66, 2010
DOI 10.2478/v10136-009-0013-9
ISSN 1214-0287

REVIEW

Gas plasmas and plasma modified materials in medicine

Sadiqali Cheruthazhekatt[1], **Mirko Černák**[2], **Pavel Slavíček**[2], **Josef Havel**[1, 2]

[1]Department of Chemistry, Faculty of Science, Brno, Czech Republic
[2]Department of Physical Electronics, Faculty of Science, Brno, Czech Republic

Received 8th February 2010.
Revised 25th March 2010.
Published online 19th April 2010.

Summary
The applications of gas plasma and plasma modified materials in the emerging fields of medicine such as dentistry, drug delivery, and tissue engineering are reviewed. Plasma sterilization of both living and non-living objects is safe, fast and efficient; for example plasma sterilization of medical equipment quickly removes microorganisms with no damage to the tiny delicate parts of the equipment and in dentistry it offers a non-toxic, painless bacterial inactivation of tissues from a dental cavity. Devices that generate plasma inside the root canal of a tooth give better killing efficiency against bacteria without causing any harm to the surrounding tissues. Plasma modified materials fulfill the requirements for bioactivity in medicine; for example, the inclusion of antimicrobial agents (metal nano particles, antimicrobial peptides, enzymes, etc.) in plasma modified materials (polymeric, metallic, etc) alters them to produce superior antibacterial biomedical devices with a longer active life. Thin polymer films or coating on surfaces with different plasma processes improves the adherence, controlled loading and release of drug molecules. Surface functionalization by plasma treatment stimulates cell adhesion, cell growth and the spread of tissue development. Plasma applications are already contributing significantly to the changing face of medicine and future trends are discussed in this paper.

Key words: plasma; sterilization; dentistry; surface functionalization; drug delivery; tissue engineering

Abbreviations

DBD, dielectric barrier discharge
B. cereus, Bacillus cereus
E. coli, Escherichia coli
NPs, nanoparticles
PA, porous alumina
PAA, polyacrylic acid
P. aeruginosa, Pseudomonas aeruginosa
PE, polyethylene
PEG, poly(ethylene glycol)
PHBV, poly(3-hydroxybutyric acid-co-3-hydroxyvaleric acid)
PIII, plasma immersion and ion implantation
PP, polypropylene
PSDVB, polystyrene-divinylbenzene
PU, polyurethanes
RF, radio frequency
S. aureus, Staphylococcus aureus
S. mutans, Streptococcus mutans

✉ Josef Havel, Department of Chemistry, Faculty of Science, Masaryk University, Kotlářská 2, 611 37 Brno, Czech Republic
💻 Havel@chemi.muni.cz
☎ +420 549 494 114
🖷 +420 549 492 494

INTRODUCTION

Plasma is considered as the fourth state of matter and it is the most abundant state in the universe. It exists in a variety of forms among which is 'fire', known for millions of years, since the early stone age. Plasma is not a human invention, and is present in nature, as fire

in the sun, stars, in the tails of comets and as flashes of lightning (Conrads and Schmidt 2000). In medicine and biology 'plasma' refers to the non-cellular fluid component of blood. The term was introduced into physics by Irving Langmuir in 1928, because it resembles the ionic liquids in biology and medicine.

The number of applications of plasma technology in many fields including microelectronics, metallurgy, polymer engineering, and biomedical engineering, is growing rapidly. One of the advantages of this technology is that surface properties such as hardness, corrosion resistance and other chemical and physical properties can be selectively modified without affecting the bulk characteristics of the materials. The use of synthetic materials in biomedical applications has increased dramatically during the past few decades. However some synthetic biomaterials, for example polymeric implants, can, in biosystems, cause problems, such as microbial growth and/or adsorption of bioorganisms. The simple addition or deposition of bioactive molecules to such materials can offer less stability and uniformity than covalently bonded species. In comparison with other methods for surface modification (layer by layer deposition, dipping, etc.) plasma surface modification offers a shorter and more economical method for the covalent attachment of bioactive molecules to the substrate without obstructing the bulk properties (Chu et al. 2002, Oehr 2003). Thus plasma technology has great importance in the development of new biomaterials. In medicine direct plasma treatment for sterilization, deactivating pathogens, blood clotting, wound healing, cancer treatment, etc. is more effective than any other method. Thus, plasma and plasma modified materials play an important role in our daily live, making it more convenient and healthier.

Several reviews of the biomedical application of plasma and plasma treated materials have been published (Fridman et al. 2008, Gomathi et al. 2008, Laroussi 2008, Desmet et al. 2009), but to date, none gives an overview of modern applications of plasma and plasma modified materials in medicine; the aim of this review is therefore to present a survey of recent advances of plasma and plasma modified materials in this field.

PLASMA FORM OF MATTER AND METHODS FOR GENERATION

On the application of sufficient heat, a solid material transforms firstly into a liquid and then. at a higher temperature, into a gas. As the energy supplied is increased, the electrons receive sufficient energy to separate from the atoms or molecules of gas and become electrically conductive. In this way gas undergoes a phase transition to a partially or completely ionized gas, called the plasma state. Fig. 1 illustrates the phase transformations of matter by changes in the energy of the system under processes such as melting, vaporization, ionization, etc.

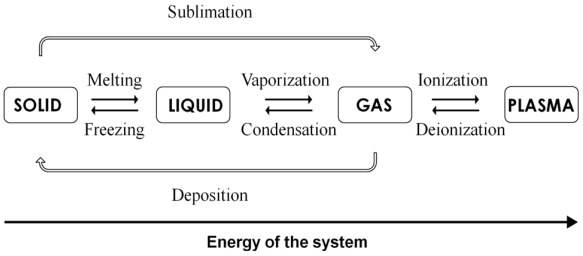

Fig. 1. **Different states of matter.**

Plasma consists of a mixture of positively and negatively charged ions, electrons and neutral species (atoms, molecules). It can be divided into two main categories; hot plasma (near-equilibrium plasma) and cold plasma (non-equilibrium plasma). Hot plasma consists of very high temperature particles and they are close to the maximal degree of ionization. Cold plasma is composed of low temperature particles and relatively high temperature electrons and they have a low degree of ionization (Tendero et al. 2006). Cold plasma can be further subdivided into low pressure and atmospheric pressure cold plasma. Atmospheric pressure cold plasma is the basis of one of the most promising methods of achieving a more flexible, reliable, less expensive and continuous method of surface modification (Bogaerts et al. 2002). Different forms of energy (thermal, electric current, electromagnetic radiations, light from a laser, etc.) are used to create the plasma regardless of the nature of the energy source. Depending on the type of energy supplied and the amount of energy transferred to the plasma, the properties of the plasma change in terms of electron density or temperature (Braithwaite 2000). In common, man made, plasma, electrical energy is usually injected into a system in a continuous manner in order to avoid stoppage of the plasma discharge. Plasma is most commonly produced by passing an electric current through the gas. Different frequencies of power sources – direct current, alternating current, low frequency, radio frequency, microwave, etc. are used for the generation of discharges such as atmospheric and low pressure glow discharge, corona, magnetron and dielectric barrier discharge (DBD) (Conrads and Schmidt 2000, Denes and Manolache

2004). An example of a high frequency plasma jet pencil is given in Fig. 2 (Klíma et al. 1998, 2003, 2005) and plasma generated by a surface coplanar barrier discharge in ambient air atmosphere is given in Fig. 3. Plasma parameters must be designed specifically for a given application asplasma sources have their own peculiarities, advantages, and disadvantages. The selection of a plasma source and design for the production of novel material is a great challenge for scientists and industry.

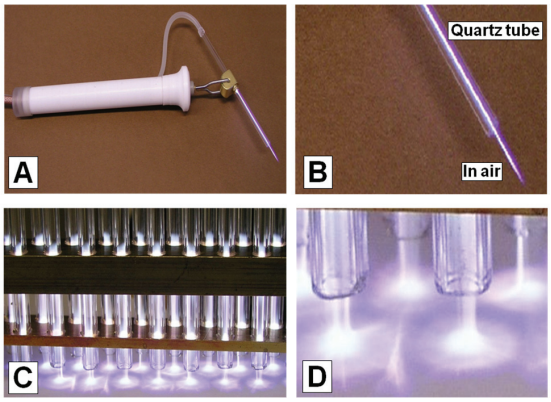

Fig. 2. **(A)** Plasma pencil device. **(B)** Magnified plasma pencil torch glowing in a quartz tube and in air. **(C)** Multi jet system. **(D)** Magnified multi jests modifying the surface. *Photo: M. Klíma (reproduced with permission).*

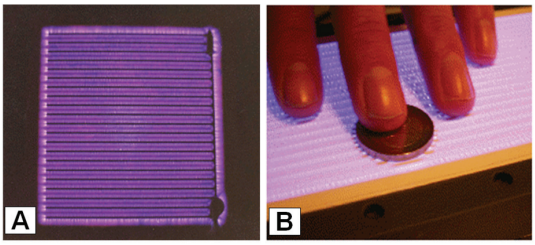

Fig. 3. **Scheme of barrier discharge generation.** (A) Plasma of surface barrier discharge and (B) Illustration of safety of the surface coplanar barrier discharge burning in ambient air atmosphere.

PLASMA TREATMENT IN MEDICINE

Heat and high temperature (steam, hot metal objects) have been used in medicine for a significant length of time: in tissue removal, blood clotting, wound healing and for the disinfection of both living and non-living biomedical articles. Direct contact with hot metal will affect the surrounding tissues in living organisms by tissue adhesion, restarting of bleeding, charring of the neighbouring tissues and causes damage to heat sensitive biomedical articles. Treatment with low temperature plasma provides an alternative method of avoiding the difficulties associated with this ancient method (Hayashi et al. 2006, Fridman et al. 2008), because the ions and the neutral species in low temperature plasma are relatively cold and do not cause any thermal damage to articles which come in contact with the plasma. This non-thermal behavior recommends the use of gas plasma for the treatment of heat sensitive materials including biological matter, such as cells and tissues (Laroussi 2005). In recent years, non-thermal atmospheric plasma effects have been developed to extend the plasma treatment of living tissue. These can be selective in achieving a desired result for some living matter, while having little or no effect on the surrounding tissue (Fridman et al. 2008), and have found application in low heat surface modification of polymers (Gomathi et al. 2008), clinical instrument sterilization, tissue engineering and dental cavity treatment (Shenton and Stevens 2001, Denes and Manolache 2004, Laroussi 2005). Many different types of plasma devices including plasma pencils, radio frequency plasma needles, direct current plasma brushes and plasma jets have been developed for non-thermal atmospheric pressure plasma generation (Laroussi et al. 2008, Nie et al. 2009). A brief overview of gas plasma applications in medicine is given in Fig. 4.

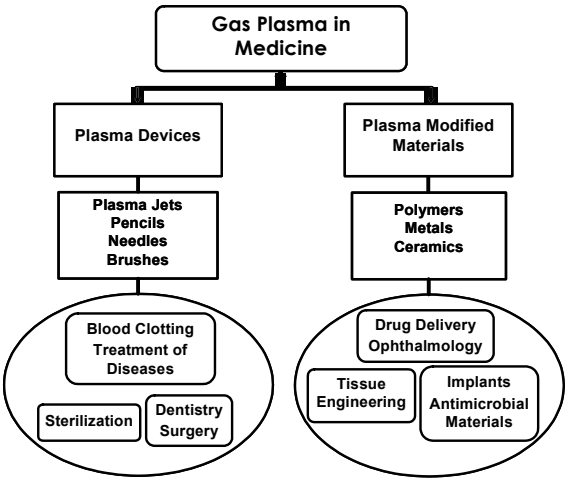

Fig. 4. **Gas plasma uses in medicine.**

Plasma sterilization

Plasma sterilization is a well established technology in medicine. Plasma, in the form of fire, was used for sterilization thousands of years ago. The sterilization

of living objects, such as human, animal, and plant tissues is of much interest in medicine (Crow and Smith 1995). Plasma sterilization works at the atomic/molecular level and therefore it helps to reach all surfaces, including the interior parts of medical equipment (catheters, needles, syringes, etc.) and other regions which are not accessible to fluid disinfectants (Fridman et al. 2007). It has several advantages (see Fig. 5) over commonly used sterilization methods such as heat, chemical solutions, or gas and radiation bombardment which cause thermal, chemical, or irradiation damage to both living and non-living objects. The parametric study of plasma for sterilization is of importance in understanding and controlling the deactivation of microbes, because the main sterilizing factors are strongly dependent on the plasma source type and/or the plasma characteristics. Nowadays non-thermal atmospheric pressure plasma is more frequently used for the sterilization of both living and non-living materials (Lerouge et al. 2001, Trompeter et al. 2002, Xingmin et al. 2006, Fridman et al. 2008, Moreau et al. 2008).

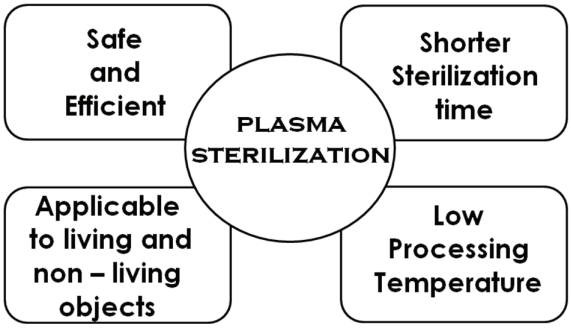

Fig. 5. **Some advantages of plasma sterilization.**

Sterilization of living materials

Several types of plasma device have been reported for the sterilization of living animal and human tissues. An electrically safe DBD plasma with a floating electrode set up has been reported for the sterilization of living tissue. This method provides complete tissue sterilization within seconds, with no damage to skin samples (Fridman et al. 2006). Recently a new DBD non-thermal plasma at atmospheric pressure with conical geometry structured electrodes was developed for evaluating the bactericidal effect against *Pseudomonas aeruginosa (P. aeruginosa)*, *Bacillus cereus (B. cereus)* and *Escherichia coli (E. coli)* bacteria. The complete removal of these microorganisms was effected within an exposure time of 10 min for *P. aeruginosa*, and 15 min for *E. coli* and *B. cereus*, respectively (Sohbatzadeh et al. 2009). Low power radio frequency (RF) plasma at atmospheric pressure with a helium flow is used for the no damaging sterilization of living tissues. This plasma has the capacity to kill different kinds of bacteria: *E. coli, P. aeruginosa* and *Staphylococcus aureus (S. aureus)* with a decimal reduction time of 1–2 minutes, while preserving the living cells of the substrate (Martines et al. 2009). Gweon et al. (2009) studied the sterilization mechanisms and the major sterilization factors of RF plasma, with *E. coli* as the target. They found that sterilization is more effective (up to 40%) with 0.15% oxygen added to the helium gas supply. Moon et al. (2009), generated a relatively large area (110 mm × 25 mm) of RF discharges with low current and low gas temperature at atmospheric pressure to carry out treatment on living tissue. They investigated possible electrical and thermal damage and also the sterilization efficiency for living cell treatment which was tested with microorganisms inoculated on pork and human skin surfaces.

Sterilization of non-living materials

The sterilization of medical equipment is an important procedure for disinfection in hospitals, and a number of medical plasma sterilizer devices have been introduced (Griffiths 1993, Herrmann et al. 1999, Lin et al. 1999, Montie et al. 2000, Gaunt et al. 2006, Laroussi et al. 2006).

The removal of protein residues from surgical instruments is quite difficult and commonly used sterilization and decontamination techniques can cause major damage to the objects treated. Kylián et al. (2008) developed a low pressure inductively coupled (Ar/O_2 mixture) plasma discharge for the removal of model proteins from different substrate materials ranging from metallic surfaces to polymeric materials. Ar/O_2 mixture represents a favorable option compared to the discharges sustained in other gases or gas mixtures, since it allows for the fast elimination of proteins and killing of bacterial spores. Moreover, the application of this mixture overcomes the environmental and safety drawbacks of mixtures containing fluorine which is found to be capable of sterilizing and etching organic materials.

It is important to find appropriate plasma sterilization conditions for modern polymeric medical devices, because under some conditions sterilization will destroy the surfaces by degradation of the chains and produce some low molecular volatiles. Halfmann et al. (2007) introduced double inductively coupled low pressure plasma for sterilization of three dimensional biomedical materials. The short

treatment time and low temperature allow for the sterilization of heat sensitive materials such as ultra high molecular weight polyethylene (PE) and polyvinyl chloride (PVC). In the experimental study of Miao and Jierong (2009), the germicidal effect of *E. coli* on the surface of medical PVC in remote oxygen plasma and the effective inactivation of the *E. coli* by this plasma was observed. Compared with direct oxygen plasma sterilization, remote plasma can enhance the hydrophilic property and limits the degradation of the PVC surface.

Plasma in dentistry

A number of methods, such as mechanical drilling, laser techniques and chemical reagents have been employed for the cleaning and disinfection of the tissue in dental cavities or in root canals. However, most of these methods have disadvantages such as heating, the destruction of healthy tissues, and undesirable side effects including a disagreeable taste and staining by chemotherapeutic agents such as chlorhexidine (Goree et al. 2006). Plasma bacterial inactivation of tissues in a dental cavity or in a root canal is of importance and a tissue saving method in dentistry. The exposure of enamel to the plasma is painless and the heating of the pulp is tolerable. Furthermore, plasma is non-toxic and it does not cause damage to the mineralized matrix of the tooth.

Several types of nonthermal atmospheric plasma devices have been used for dental treatment (Sladek et al. 2004). A low power, millimeter sized, atmospheric pressure glow discharge plasma needle was developed to kill *Streptococcus mutans (S. mutans)* which is the main microorganism causing dental caries. This plasma can effectively kill the bacteria with a treatment time of ten seconds within a solid circle of 5 mm diameter, demonstrating its site specific treatment capabilities (Goree et al. 2006). Atmospheric pressure DBD plasma needles with a funnel shaped nozzle were used for the inactivation of *S. mutans*. Oxygen was injected downstream in the plasma afterglow region through a powered steel tube (Zhang et al. 2009). Jiang et al. (2009), introduced a safe and novel technique for endodontic disinfection with a hollow electrode based, 100 ns pulsed plasma dental probe. It generates a room temperature, tapered cylindrical plasma plume in ambient atmosphere. The plasma plume causes minimal heating of biological materials and is safe to touch with bare hands without causing a burning sensation or pain. Greater sterilization depth and surface coverage were achieved by optimizing the width and length of the plasma plume. A no-thermal atmospheric pressure helium plasma jet device was developed to enhance the tooth bleaching effect of hydrogen peroxide. The combination of the plasma with hydrogen peroxide improves the bleaching efficacy by a factor of three compared to sterilization by hydrogen peroxide alone (Lee et al. 2009).

Due to the narrow channel shape geometry of the root canal of a tooth, the plasma generated by some devices is not efficient in delivering reactive agents into the root canal for disinfection. Therefore, to have a better killing efficacy, plasma has to be generated inside the root canal. Recently Lu et al. (2009), constructed a cold plasma jet device which can generate plasma inside the root canal and which efficiently kills *Enterococcus faecalis* (one of the main types of bacteria causing failure of the root canal) within several minutes.

PLASMA MODIFIED MATERIALS IN MEDICINE

The surface properties of materials play an essential role in determining their biocompatibility, strongly influence their biological response and determine their long term performance *in vivo* (Chu et al. 2002). Many synthetic biomaterials such as metals, alloys, ceramics, polymers and composites have a different environment from the natural environment consisting of neighbouring cells or extra cellular matrix components. So it is important to design biomaterials with the right surface properties, especially chemical binding properties to achieve the biocompatibility of artificial biomaterial surfaces. For surface modification in the medical field, very thin layers with a thickness of some ten to hundred nanometers are mainly required (Favia et al. 2008). The treatment of the surfaces of materials with non-thermal plasma can lead to surface activation and functionalization. This creates unique surface properties often unobtainable with conventional, solvent based chemical methods. Thus plasma surface modification can improve biocompatibility and biofunctionality. Appropriate selection of the plasma source enables the introduction of diverse functional groups on the target surface to improve biocompatibility or to allow subsequent covalent immobilization of various bioactive molecules (Gupta and Anjum 2003, Oehr 2003, Denes and Manolache 2004). Polymers are common medical materials because of their superior properties such as easy processing, ductility, impact load damping and excellent biocomparability (Gomathi et al. 2008). A list of polymeric and metallic plasma treated biomaterials and their uses is given in Table 1.

Table 1. **Plasma modified materials and their applications.**

Plasma modified materials	Applications
Polymers	
Polyethylene Polypropylene Polyvinylchloride Polyurethanes	Catheters, anti-microbial coatings, implants
Polytetrafluoroethylene	Implants, vascular grafts
Poly(methyl methacrylate) Silicone rubber	Contact lenses, artificial corneas
Poly(ethylene terephthalate) Polystyrene	Implants, tissue culture dishes
Polylactic acid Polyglycolic acid	Sutures, drug delivery matrix
Metals and alloys	
Ti Ti-Ni alloys Co-Cr alloys	Implants
Steel	Stents

Types of plasma surface modification processes

A number of plasma processes have been developed to attain specific surface properties for biomaterials and some are listed below

a) surface functionalization by gas plasma (O_2, CO_2, N_2, NH_3, etc.);
b) formation of thin films by plasma polymerization;
c) inclusion of metal ions in the surface by plasma induced ion implantation.

Analytical techniques such as optical microscopy, 3D laser profiling, scanning electron microscopy, atomic force microscopy, contact angle, X-Ray photoelectron spectroscopy, static time of flight secondary ion mass spectrometry and dynamic secondary ion mass spectrometry have been used to characterize the surface properties of plasma modified materials.

Antimicrobial materials

The biomaterials used for the treatment of diseases and for implants must possess good antimicrobial properties. So it is important to improve the antibacterial properties of such materials by the incorporation of antimicrobial agents in, or by the application of surface coatings to the materials used. The antimicrobial properties of metals and metal ions (silver, copper, etc.) have been well known since ancient times. Nowadays, metal nanoparticles (NPs) are widely employed to improve the antimicrobial activity of many synthetic biomaterials (Weir et al. 2008). This bactericidal effect of metal NPs has been attributed to their small size and high surface to volume ratio which allow them to interact closely with microbial membranes. Metal NPs with bactericidal activity can be immobilized and coated onto surfaces which may find application in medical instruments and devices (Kim et al. 2007, Ruparelia et al. 2008). Plasma processes such as plasma sputtering, plasma induced ion implantation and plasma enhanced chemical vapor deposition among others, are relatively simple and efficient methods for the incorporation of such agents. In this way the antimicrobial properties of the biomaterials made from metals, polymers, and other materials have been improved.

Metallic biomaterials

Copper is known to be active against bacteria and fungi (Silver and Phung 1996, Noyce et al. 2006). An antibacterial nanocomposite of copper containing organosilicon thin films, has been successfully

synthesized on stainless steel using a mixed plasma enhanced chemical vapor deposition-sputtering deposition technique. The antimicrobial properties were evaluated with a solution containing *E. coli* microorganisms for 24 h, the *E. coli* concentration decreased to the minimal detectable value. The process parameters were optimized to control the quantity of incorporated copper in the layer (Daniel et al. 2009).

Silver ions are widely used as a bactericide in catheters, burn wounds and dental work. The incorporation of silver into implants is a most promising method in reducing the infection rate, while exhibiting low toxicity towards cells and tissues. Some harmful effects of silver nanoparticles and their toxicity for human health have been reviewed (Panyala et al. 2008). The inhibitory effect of silver on bacteria is generally believed to be caused by silver reacting with thiol groups in protein which induce the inactivation of the bacterial proteins (Rai et al. 2009, Sharma et al. 2009). A plasma sprayed nano-titania/silver coating was deposited on titanium substrates for the prevention of bacterial infections. The experimental results confirmed that the plasma sprayed nano-titania/silver coating has good bioactivity, cytocompatibility and antibacterial properties, which makes it a promising application against postoperative infections in the replacement of hard tissues (Li et al. 2009). The inclusion of silver into the chemical treatment of the surface of vacuum plasma sprayed titanium coatings plays an important role in inhibiting the proliferation of bacteria. The treated titanium coatings exhibit a prominent antibacterial effect against *E. coli, P. aeruginosa* and *S. aureus* (Chen et al. 2009b). The antibacterial properties of doped silver on biocompatible silica based glass have also been studied. Firstly the glass powders were coated on titanium alloy and stainless steel substrates by a plasma spray process in air. *In vitro* test results showed an antimicrobial action against tested bacteria without disturbance of the biocompatibility of the glass (Miola et al. 2009). Stainless steel dental device plates were modified by the plasma based fluorine and silver ion implantation-deposition method. Due to the presence of both fluoride and silver ions, the brushing abrasion resistance of the deposited or mixing layer was improved and the hydrophobic properties remained even after brushing with a toothbrush. This simultaneous fluoride and silver ion implantation-deposition could provide a possible antimicrobial property to medical and dental devices (Shinonaga and Arita 2009).

A nanolayer biofilm of polyacrylic acid (PAA) was uniformly coated on the surface of magnetic nickel NPs using a dielectric barrier discharge glow plasma fluidized bed. The PAA acting as an adhesion layer was used to immobilize a certain concentration of antimicrobial peptide (LL-37) to kill the bacteria *E. coli*. The results indicated that the modified nickel NPs immobilizing a certain concentration of LL-37 could kill the bacteria effectively (Chen et al. 2009a).

Polymeric biomaterials

Medical polymers are widely used in biomedical applications because of their excellent mechanical and biological properties. However, the infection in medical polymers is a major clinical complication. Recently plasma surface modification techniques have been employed in the development of anti-infective medical polymers for the biomedical industry (Sodhi et al. 2001, Ji et al. 2007).

A comparative study has been carried out on single and dual copper plasma immersion and ion implantation (PIII) to produce an antibacterial surface on polyethylene (PE). Compared with the single copper PIII process, the dual plasma implantation process (Cu/N_2 PIII) can better regulate the copper release rate and improve the long term antibacterial properties of PE against *E. coli* and *S. aureus* (Zhang et al. 2007). The improved antimicrobial activity of plasma treated PE films after chemical immobilization of an antimicrobial enzyme (lysozyme) has also been investigated. Plasma conditions and enzyme solution concentrations were optimized for the effective immobilization on the PE surface (Conte et al. 2008). A tunable antimicrobial polypropylene (PP) surface with a controllable strength against *Pseudomonas putida* and *S. aureus* has been recently reported. Microwave plasma reaction in the presence of maleic anhydride results in the formation of acid groups on the surface of PP. This modification of the plasma surface helps the attachment of antibiotics such as penicillin V (PEN) and gentamicin (GEN) to the modified PP surface through the reaction of the acid group on the PP surface and polyethylene glycol (PEG), diglycidyl PEG respectively (Aumsuwan et al. 2009).

Drug delivery

Plasma surface modification provides sufficient adherence to metallic and polymeric materials for the binding of drug molecules. The bioabsorbable materials can act as drug carriers by controlling the release rate of the drug initially loaded in an application for drug delivery systems. Fig. 6 shows the schematic illustration of a drug molecule grafting on an O_2 plasma treated substrate.

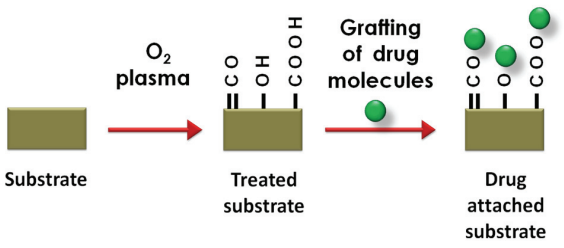

Fig. 6. **Incorporation of drug molecules to plasma treated substrate for drug delivery** (● Drug molecule).

Nanoporous membranes have attracted considerable interest for application in drug delivery. The deposition of heptylamine plasma polymer coatings onto porous alumina (PA) membranes has been investigated with the aim of adjusting the surface chemistry and the pore size of the membranes. The structural (pore size) properties of PA membranes can be altered systematically by adjusting the deposition time during the polymerization process. The resultant PA membranes with active amino groups and controlled pore size are applicable for molecular separation and drug delivery (Losic et al. 2008). The polylactic acid ultrasound contrast agent has significant importance in ultrasound imaging and eventually in drug treatment for cancer. It has an additional advantage, because ultrasound in drug delivery may induce cavitations, increase cell membrane permeability and facilitate drug release. Plasma surface modification improves drug loading for ultrasound-triggered drug delivery. Plasma treatment appears to both sterilize and beneficially modify the agent for increased doxorubicin adsorption (Eisenbrey et al. 2009). The macroporous structure of polystyrene-divinylbenzene (PS-DVB) solid foams materials with high pore volume makes them interesting for the design of new drug delivery systems. The wettability of the highly hydrophobic PS-DVB films was improved by a short post discharge plasma treatment with different gases with a view to opening new possibilities for the absorption of hydrophilic compounds (Canal et al. 2009). The surface functionalization of TiO_2 nanotubes by plasma polymerization generates a thin and chemically reactive polymer film rich in amine groups on top of the substrate surface. The tailoring of surface functionalities on nanotube surfaces has potential for significantly improving the properties of this attractive biomaterial and promoting the development of new biomedical devices such as drug eluting medical implants with multiple functions (orthopedic implants, dental, coronary stents). This will provide an elegant route to the prevention of infection, clotting control or to a decrease in inflammation as a result of these implants (Vasilev et al. 2010).

Tissue engineering

Artificial materials are of growing importance in medicine and biology. A modern scientific interdisciplinary field known as tissue engineering has been developed to design artificial biocompatible materials to substitute irreversibly damaged tissues and organs. Cells can sense the physical properties and chemical composition of these materials and regulate their behavior accordingly (Bačáková et al. 2004). Cell affinity is the most important factor to be considered when biodegradable polymeric materials are utilized as a cell scaffold in tissue engineering. A plasma technique can easily be used to introduce desired functional groups or chains onto the surface of materials, so it has a special application in improving the cell affinity of scaffolds.

The copolymer, poly(3-hydroxybutyric acid-co-3-hydroxyvaleric acid) (PHBV) has been intensely studied as a tissue engineering substrate. Plasma treatment of PHBV films increases the nano roughness pattern and results in a moderate hydrophilicity on the film surface. This physicochemical change modifies the behaviour of the vero cells by stimulating cell adhesion, cell growth and spreading, etc. (Lucchesi et al. 2008). Poly(methylmethacrylate) films were modified by the application of glow discharge oxygen plasma. An increase in the hydrophilicity and surface free energy and an increase in the plasma power and application time was observed. This improves the surface properties of the implants (at the molecular level) in order to enhance the cell attachment to the materials (Ozcan et al. 2008).

Plasma treatment with acrylic acid is an attractive way of introducing carboxylic groups to a polyurethane (PU) surface and subsequently of immobilizing natural or synthetic molecules carrying amino groups in their structure, through the formation of amide bonds. The plasma treatment allows a monolayer of PAA, which is then functionalized with a biomacromolecule. The PU treated with macromolecules is a good candidate as a cell substrate. In particular, functionalization with poly (L-lysine) performs extremely well in the activation of cellular processes and shows optimum cell proliferation with increasing time (Sartori et al. 2008). A variety of extracellular matrix protein components such as gelatin, collagen, laminin and fibronectin could be immobilized onto the plasma treated surface

to enhance cellular adhesion and proliferation. Electrospun nanofibres composed of polyglycolic acid, poly-L-lactic acid or poly(lactic-co-glycolic acid) were modified with carboxylic acid groups through plasma glow discharge with oxygen and gas phased acrylic acid. Such hydrophilized nanofibres were shown to enhance fibroblast adhesion and proliferation without compromising physical and mechanical bulk properties (Yool et al. 2009). Starch based scaffolds treated by argon plasma were shown to be a good support when used in bone tissue engineering. Higher proliferation rates, because of the novel protein surface interaction by plasma treatment were observed on the scaffolds (Santos et al. 2009).

CONCLUSION

Modern plasma tools employed in medical treatments are found to be more efficient and flexible in use. The plasma sterilization of both living and non-living objects offers non destructive removal of the microorganisms in a shorter treatment time. The use of different types of plasma jets in dentistry offers a painless treatment for the cleaning of dental cavities. The incorporation of the antimicrobial agents to plasma treated polymeric and metallic material enhances superior antimicrobial activity which significantly increases the convenience of these objects in medicine. Surface functionalization of artificial biomaterials (implants and scaffolds) by plasma treatment illustrates an improved rate of drug loading and controlled release even long term. This surface modification technique helps the introduction of bioactive species on the scaffolds, and promotes cell adhesion and proliferation which play an important role in tissue development. Thus the plasma treatment of materials represents an unusually convenient and versatile technique for surface activation and functionalization, which creates unique surface properties, often not obtainable by other methods. Plasma applications and plasma modified materials in medicine are undergoing fast development and plasma-medicine is becoming an important part of modern health care.

ACKNOWLEDGEMENT

Financial aid from the research grant of the Academy of Science of the Czech Republic (Project KAN 101630651), project MSM0021622411 and LC 06035 are greatly acknowledged.

REFERENCES

Aumsuwan N, McConnell MS, Urban MW: Tunable antimicrobial polypropylene surfaces: simultaneous attachment of penicillin (Gram +) and gentamicin (Gram –). Biomacromolecules 10:623–629, 2009.

Bačáková L, Filová E, Rypáček F, Svorčík V, Starý V: Cell adhesion on artificial materials for tissue engineering. Physiol Res 53:35–45, 2004.

Bogaerts A, Neyts E, Gijbels R, Mullen J: Gas discharge plasmas and their applications: Review. Spectrochim Acta Part B 57:609–658, 2002.

Braithwaite NSJ: Introduction to gas discharges. Plasma Sources Sci Technol 9:517–527, 2000.

Canal C, Gaboriau F, Vílchez A, Erra P, Celma MG, Esquena J: Topographical and wettability effects of post-discharge plasma treatments on macroporous polystyrene-divinylbenzene solid foams. Plasma Process Polym 6:686–692, 2009.

Chen G, Zhou M, Chen S, Guohua L, Yao J: Nanolayer biofilm coated on magnetic nanoparticles by using a dielectric barrier discharge glow plasma fluidized bed for immobilizing an antimicrobial peptide. Nanotechnology 20:465706, 2009a.

Chen Y, Zheng X, Xie Y, Ji H, Chuanxian D: Antibacterial properties of vacuum plasma sprayed titanium coatings after chemical treatment. Surf Coat Technol 204:685–690, 2009b.

Chu PK, Chen JY, Wang LP, Huang N: Plasma-surface modification of biomaterials. Mater Sci Eng R Rep 36:143–206, 2002.

Conrads H, Schmidt M: Plasma generation and plasma sources. Plasma Sources Sci Technol 9:441–454, 2000.

Conte A, Buonocore GG, Sinigaglia M, Lopez LC, Favia P, Agostino R, Del Nobile MA: Antimicrobial activity of immobilized lysozyme on plasma-treated polyethylene films. J Food Prot 71:119–125, 2008.

Crow S, Smith JH: Gas plasma sterilization: Application of space-age technology. Infect Control Hosp Epidemiol 16:483–487, 1995.

Daniel A, Pen LC, Archambeau C, Reniers F: Use of a PECVD-PVD process for the deposition of copper containing organosilicon thin films on steel. Appl Surf Sci 256:82–85, 2009.

Denes FS, Manolache S: Macromolecular plasma-chemistry: An emerging field of polymer science. Prog Polym Sci 29:815–885, 2004.

Desmet T, Morent R, Geyter N, Leys C, Schacht E, Dubruel P: Nonthermal plasma technology as a versatile strategy for polymeric biomaterials

surface modification: A Review. Biomacromolecules 10:2351–2378, 2009.

Eisenbrey JR, Hsu J, Wheatley MA: Plasma sterilization of poly lactic acid ultrasound contrast agents: surface modification and implications for drug delivery. Ultrasound Med Biol 35:1854–1862, 2009.

Favia P, Sardella E, Lopez L, Laera S, Milella A, Pistillo B, Intranuovo F, Nardulli M, Gristina R, D'Agostino R: Plasma assisted surface modification processes for biomedical materials and devices. NATO ASI Ser A 10:203–225, 2008.

Fridman G, Peddinghaus M, Ayan H, Fridman A, Balasubramanian M, Gutsol A, Brooks A, Friedman G: Blood coagulation and living tissue sterilization by floating-electrode dielectric barrier discharge in air. Plasma Chem Plasma Process 26:425–442, 2006.

Fridman G, Brooks AD, Balasubramanian M, Fridman A, Gutsol A, Vasilets VN, Ayan H, Friedman G: Comparison of direct and indirect effects of non-thermal atmospheric-pressure plasma on bacteria. Plasma Process Polym 4:370–375, 2007.

Fridman G, Friedman G, Gutsol A, Shekhter AB, Vasilets VN, Fridman A: Applied plasma medicine. Plasma Process Polym 5:503–533, 2008.

Gaunt LF, Beggs CB, Georghiou GE: Bactericidal action of the reactive species produced by gas-discharge nonthermal plasma at atmospheric pressure: A review. IEEE Trans Plasma Sci 34:1257–1269, 2006.

Gomathi N, Sureshkumar A, Neogi S: RF plasma-treated polymers for biomedical applications. Curr Sci 94:1478–1486, 2008.

Goree J, Liu B, Drake D, Stoffels E: Killing of S. mutans bacteria using a plasma needle at atmospheric pressure. IEEE Trans Plasma Sci 34:1317–1324, 2006.

Griffiths N: Low-temperature sterilization using gas plasmas. Med Device Technol 4:37–40, 1993.

Gupta G, Anjum N: Plasma and radiation-induced graft modification of polymers for biomedical applications. Adv Polym Sci 162:35–61, 2003.

Gweon B, Kim DB, Moon SY, Choe W: *Escherichia coli* deactivation study controlling the atmospheric pressure plasma discharge conditions. Curr Appl Phys 9:625–628, 2009.

Halfmann H, Bibinov N, Wunderlich J, Awakowicz P: A double inductively coupled plasma for sterilization of medical devices. J Phys D Appl Phys 40:4145–4154, 2007.

Hayashi N, Guan W, Tsutsui S, Tomari T, Hanada Y: Sterilization of medical equipment using radicals produced by oxygen/water vapor RF plasma. Jpn J Appl Phys 10B 45:8358–8363, 2006.

Herrmann HW, Henins I, Park J and Selwyn GS: Decontamination of chemical and biological warfare agents using an atmospheric pressure plasma jet. Phys Plasmas 6:2284–2289, 1999.

Ji J, Zhang W: Bacterial behaviors on polymer surfaces with organic and inorganic antimicrobial compounds. J Biomed Mater Res Part A 10:448–453, 2007.

Jiang C, Chen MT, Gorur A, Schaudinn C, Jaramillo DE, Costerton JW, Sedghizadeh PP, Vernier PT, Gundersen MA: Nanosecond pulsed plasma dental probe. Plasma Process Polym 6:479–483, 2009.

Kim JS, Kuk E, Yu KN, Kim JH, Park SJ, Lee HJ, Kim SH, Park YK, Park YH, Hwang CY, Kim YK, Lee YS, Jeong DH, Cho MH: Antimicrobial effects of silver nanoparticles. Nanomed Nanotechnol Biol Med 3:95–101, 2007.

Klíma M, Janča J, Kapička V, Slavíček P, Saul P: Způsob vytváření fyzikálně a chemicky aktivního prostředí plazmovou tryskou a plazmová tryska. Patent CZ 147698, 12. 5. 1998.

Klíma M, Janča J, Kapička V, Slavíček P, Saul P: The method of making a physically and chemically active environment by means of a plasma jet and the related plasma jet. Patent US 6, 525, 481, 2003; Patent EP 1077021, 2005. Prior 12. 5. 1998.

Kylián O, Rauscher H, Gilliland D, Bretagnol F, Rossi F: Removal of model proteins by means of low-pressure inductively coupled plasma discharge. J Phys D Appl Phys 41:095201, 2008.

Laroussi M: Low lemperature plasma-based sterilization: Overview and state-of-the-art. Plasma Process Polym 2:391–400, 2005.

Laroussi M: The biomedical application of plasma: A brief history of the development of a new field of research. IEEE Trans Plasma Sci 36:1612–1614, 2008.

Laroussi M, Tendero C, Lu X, Alla S, Hynes WL: Inactivation of bacteria by the plasma pencil. Plasma Process Polym 3:470–473, 2006.

Laroussi M, Hynes W, Akan T, Lu X, Tendero C: The plasma pencil: A Source of hypersonic cold plasma bullets for biomedical applications. IEEE Trans Plasma Sci 36:1298–1299, 2008.

Lee HW, Kim GJ, Kim JM, Park JK, Lee JK, Kim GC: Tooth bleaching with nonthermal atmospheric pressure plasma. J Endod 35:587–591, 2009.

Lerouge S, Wertheimer MR, Yahia LH: Plasma sterilization: A review of parameters,

mechanisms, and limitations. Plasmas Polym 6:175–188, 2001.

Li B, Liua X, Menga F, Chang J, Dinga C: Preparation and antibacterial properties of plasma sprayed nano-titania/silver coatings. Mater Chem Phys 118:99–104, 2009.

Lin SM, Swanzy, Jacobs PT: Method of hydrogen peroxide plasma sterilization. U S patent 5 876 666, 1999.

Losic D, Cole MA, Dollmann B, Vasilev K, Griesser HJ: Surface modification of nanoporous alumina membranes by plasma polymerization. Nanotechnology 19:245704, 2008.

Lu X, Cao Y, Yang P, Xiong Q, Xiong Z, Xian Y, Pan Y: An RC plasma device for sterilization of root canal of teeth. IEEE Trans Plasma Sci 37:668–673 2009.

Lucchesi C, Ferreira BMP, Duek EAR, Santos AR Jr., Joazeiro PP: Increased response of vero cells to PHBV matrices treated by plasma. J Mater Sci Mater Med 19:635–643, 2008.

Martines E, Zuin M, Cavazzana R, Gazza E, Serianni G, Spagnolo S, Spolaore M, Leonardi A, Deligianni V, Brun P, Aragona M, Castagliuolo I, Brun P: A novel plasma source for sterilization of living tissues. New J Phys 11:115014, 2009.

Miao H, Jierong C: Inactivation of *Escherichia coli* and properties of medical poly(vinyl chloride) in remote-oxygen plasma. Appl Surf Sci 255:5690–5697, 2009.

Miola M, Ferraris S, Nunzio SD, Robotti PF, Bianchi G, Fucale G, Maina G, Cannas M, Gatti S, Massé A, Brovarone CV, Verne E: Surface silver-doping of biocompatible glasses to induce antibacterial properties. Part II: Plasma sprayed glass-coatings. J Mater Sci Mater Med 20:741–749, 2009.

Montie C, Kelly WK, Roth R: Overview of research using the one-atmosphere uniform glow discharge plasma for sterilization of surfaces and materials. IEEE Trans Plasma Sci 28:41–50, 2000.

Moon Y, Kim DB, Gweon B, Choe W, Song HP, Jo C: Feasibility study of the sterilization of pork and human skin surfaces by atmospheric pressure plasmas. Thin Solid Films 517:4272–4275, 2009.

Moreau M, Orange N, Feuilloley MGJ: Non-thermal plasma technologies: New tools for bio-decontamination. Biotechnol Adv 26:610–617, 2008.

Nie QY, Cao, Ren CS, Wang DZ, Kong MG: A two-dimensional cold atmospheric plasma jet array for uniform treatment of large-area surfaces for plasma medicine. New J Phys 11:115015, 2009.

Noyce JO, Michels H, Keevil CW: Potential use of copper surfaces to reduce survival of epidemic methicillin-resistant staphylococcus aureus in the healthcare environment. J Hosp Infect 63:289–297, 2006.

Oehr C: Plasma surface modification of polymers for biomedical use. Nucl Instrum Methods Phys Res B 208:40–47, 2003.

Ozcan C, Zorlutuna P, Hasirci V, Hasirci N: Influence of oxygen plasma modification on surface free energy of PMMA films and cell attachment. Macromol Symp 269:128–137, 2008.

Panyala NR, Peña-Méndez EM, Havel J: Silver or silver nanoparticles: A hazardous threat to the environment and human health? J Appl Biomed 6:117–129, 2008.

Rai M, Yadav A, Gade A: Silver nanoparticles as a new generation of antimicrobials. Biotechnol Adv 27:76–83, 2009.

Ruparelia JP, Chatterjee AK, Duttagupta SP, Mukherji S: Strain specificity in antimicrobial activity of silver and copper nanoparticles. Acta Biomater 4:707–716, 2008.

Santos MI, Pashkuleva I, Alves CM, Gomes ME, Fuchs S, Unger RE, Reisab RL, Kirkpatrick CJ: Surface-modified 3D starch-based scaffold for improved endothelialization for bone tissue engineering. Mater Chem 19:4091–4101, 2009.

Sartori S, Rechichi A, Vozzi G, D'Acunto M, Heine E, Giusti P, Ciardelli G: Surface modification of a synthetic polyurethane by plasma glow discharge: Preparation and characterization of bioactive monolayers. React Funct Polym 68:809–821, 2008.

Sharma VK, Yngard RA, Lin Y: Silver nanoparticles: Green synthesis and their antimicrobial activities. Adv Colloid Interface Sci 145:83–96, 2009.

Shenton MJ, Stevens GC: Surface modification of polymer surfaces: Atmospheric plasma versus vacuum plasma treatments. J Phys D Appl Phys 34:2761–2768, 2001.

Shinonaga Y, Arita K: Surface modification of stainless steel by plasma-based fluorine and silver dual ion implantation and deposition. Dent Mater 28:735–742, 2009.

Silver S, Phung LT: Bacterial heavy metal resistance: New surprises. Annu Rev Microbiol 89:753–789, 1996.

Sladek REJ, Stoffels E, Walraven R, Tielbeek PJA, Koolhoven RA: Plasma treatment of dental cavities: A feasibility study. IEEE Trans Plasma Sci 32:1540–1543, 2004.

Sodhi RNS, Sahi VP, Mittelman MW: Application of electron spectroscopy and surface modification techniques in the development of anti-microbial coatings for medical devices. J Electron Spectros Relat Phenomena 121:249–264, 2001.

Sohbatzadeh F, Colagar AH, Mirzanejhad S, Mahmodi S: E. coli, P. aeruginosa, and B. cereus bacteria sterilization using afterglow of non-thermal plasma at atmospheric pressure. Appl Biochem Biotechnol 10:1–7, 2009.

Tendero C, Tixier C, Tristant P, Desmaison J, Leprince P: Atmospheric pressure plasmas: A review. Spectrochim Acta Part B 61:2–30, 2006.

Trompeter FJ, Neff WJ, Franken O, Heise M, Neiger M, Shuhai L: Reduction of bacillus subtilis and aspergillus niger spores using nonthermal atmospheric gas discharges. IEEE Trans Plasma Sci 30:1416–1423, 2002.

Vasilev K, Poh Z, Kant K, Chan J, Michelmore A, Losic D: Tailoring the surface functionalities of titania nanotube arrays. Biomaterials 31:532–540, 2010.

Weir E, Lawlor A, Whelan A, Regan F: The use of nanoparticles in anti-microbial materials and their characterization. Analyst 133:835–845, 2008.

Xingmin S, Yukang Y, Yanzhou S, Wang Y, Fengling P, Yuchang Q: Experimental research of inactivation effect of low-temperature plasma on bacteria. Plasma Sci Technol 8:569–572, 2006.

Yool HS, Kim TG, Park TG: Surface-functionalized electrospun nanofibers for tissue engineering and drug delivery. Adv Drug Delivery Rev 61:1033–1042, 2009.

Zhang W, Zhang Y, Ji J, Yan Q, Huang A, Chu PK: Antimicrobial polyethylene with controlled copper release. J Biomed Mater Res Part A 83:838–844, 2007.

Zhang X, Huang J, Liu X, Peng L, Guo L, Lv G, Chen W, Feng K, Yang S: Treatment of streptococcus mutans bacteria by a plasma needle. J Appl Phys 105:1063, 2009.

INSTITUTE OF PHYSICS PUBLISHING JOURNAL OF PHYSICS D: APPLIED PHYSICS

J. Phys. D: Appl. Phys. **38** (2005) 3188–3193 doi:10.1088/0022-3727/38/17/021

Planar UV excilamp excited by a surface barrier discharge

N N Guivan[1], J Janča[2], A Brablec[2,3], P Šťahel[2], P Slavíček[2] and L L Shimon[1]

[1] Department of Quantum Electronics, Uzhgorod National University, Pidgirna 46, Uzhgorod 88000, Ukraine
[2] Department of Physical Electronics, Masaryk University, Kotlářská 2, Brno 61137, Czech Republic

E-mail: abr92@elanor.sci.muni.cz (A Brablec)

Received 11 November 2004, in final form 15 February 2005
Published 19 August 2005
Online at stacks.iop.org/JPhysD/38/3188

Abstract
In this paper, the typical characteristics of a planar excilamp based on KrCl* and XeCl* exciplex molecules are presented. The excitation of the working mixture $Kr/Xe/Cl_2$ is realized by means of the surface barrier discharge at pressures of 0.1–1 bar. The following properties are measured and discussed: spectra emitted by the plasma in the UV/VIS/NIR spectral range, intensity of emitted light versus total pressure in the discharge, the composition of the working mixture and the power of emitted light. The radiation power versus input electric power, and space distribution of the emitted light including basic electrical parameters of the discharge were also measured. It was shown that the characteristic power of UV radiation emitted in the spectral range 200–400 nm is about 6 mW cm^{-2} while the efficiency could be about 8%.

1. Introduction

There has been increased interest in new types of light sources including excimer and exciplex lamps (excilamps) [1–3] emitting spontaneous radiation in the UV and VUV spectral range, which cover both measurements of basic physical parameters and possible applications. In the last decade, excilamps excited by means of the dielectric barrier discharge (DBD) at near atmospheric pressures have been used in different applications, such as UV-induced metal deposition, dielectric thin film deposition, oxidation of silicon, surface modification and pollution control [1, 4]. The DBD driven excilamps appear to be one of the simplest devices in terms of the design of the light sources; there exist two basic configurations of DBDs [5]. The first configuration is the 'volume barrier discharge' (VBD) arrangement, when one or both separated electrodes are covered by a dielectric layer (e.g. two parallel plates or coaxial cylinders). The second one is the 'surface barrier discharge' (SBD) arrangement, where a plane dielectric with the electrode is placed on one surface and the metallic cover on its reverse side. The SBD is promising for surface engineering at atmospheric pressure. Plasma chemical reactors with the SBD arrangement are already used for protective hydrophobic film deposition [6] and surface modification [7].

The excilamps operate almost at one fixed wavelength, which can be changed only if the working mixture is used with another composition. For some specific applications of excilamps in ecology, biophysics and biochemistry, it appears to be sensible to use the multiwave regime when the bands corresponding to individual B → X transitions in molecules of halogenides of inert gases are visible in the spectrum simultaneously at different wavelengths . The multiwave low-pressure (up to 40 mbar) excimer source for the spectral region of 170–310 nm excited by a longitudinal dc glow discharge was investigated in [8]. The results of the development and optimization of the transverse electric-discharge lamp based on fluorides and chlorides of heavy inert gases were already presented in [9]. In this case, the multiwave mode occurs in the lamp due to the use of $He/Xe(Kr)/CF_2Cl_2$ working mixtures. The optimization of the lamp design and applications requires a knowledge of the electrical and optical performance characteristics and the output spectrum. These parameters have been reported in detail only for

[3] Author to whom any correspondence should be addressed.

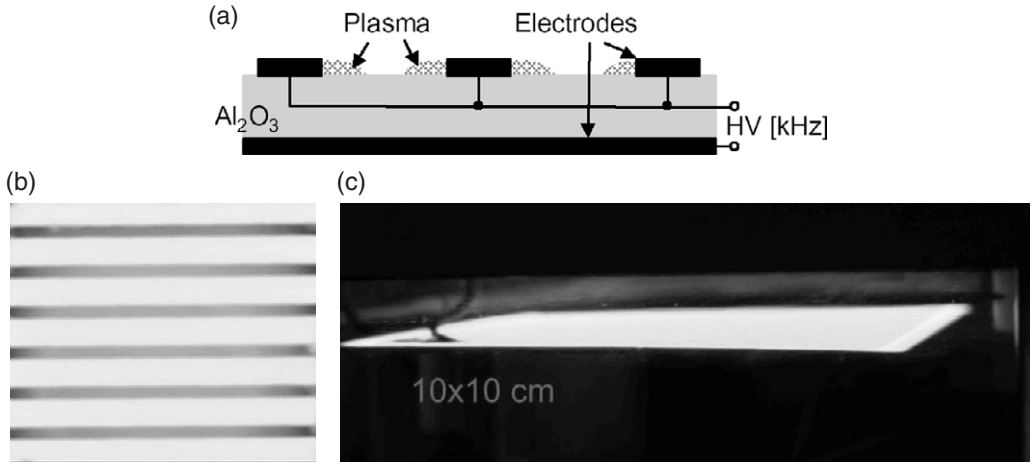

Figure 1. Schematic drawing of the SBD (*a*) and photographs of the discharge in the $Kr/Xe/Cl_2 = 920/80/1$ mbar mixture: from above (*b*), from the side (*c*).

excilamps driven in the VBD arrangement, radiated on one intensive molecular band (see [3] and references therein), while the properties of the multi-wavelength mode, when the mixture contains two working heavy inert gases (Kr, Xe), were not investigated. Excilamps with planar geometry also appear to be interesting for obtaining a homogeneous flat radiation flux.

In this paper, an experimental study of the UV excilamp with planar geometry of electrodes, operated in $Kr/Xe/Cl_2$ gas mixtures at a total pressure within the limits of 0.1–1 bar, and excited by the SBD has been carried out.

2. Experiment

The SBD module consists of two tungsten electrodes of different forms, which are separated by a high purity Al_2O_3 $100 \times 100\,mm^2$ ceramic plate (relative permittivity: $\epsilon = 9.5$) with a thickness of 0.5 mm. One electrode was in the form of a comb, and the second one had the form of a square plate (figure 1). The discharge visually appears as a rather uniform plasma sheet with dimensions of $90 \times 90\,mm^2$ covering the surface of the dielectrics. The electrode system was mounted inside a chamber of 1.5 litre in volume. Before the filling of working gases, the chamber was pumped down below 0.1 mbar by a rotary pump and passivated by chlorine. The partial pressure for Cl_2 ranged from 0.5 to 10 mbar and the total pressure of the $Kr/Xe/Cl_2$ mixtures used was varied between 0.1 and 1 bar. For the excitation of working mixtures the generator of high voltage sinusoidal pulses was used, with peak-to-peak voltage V_{p-p} up to 22 kV and frequency from 1 to 10 kHz. The frequency was matched for the resonance of the electrical circuit consisting of the output transformer coil and electrode module with a capacitance of 400 pF. The measurements were performed for an excitation frequency of typically 3 kHz and V_{p-p} up to 4 kV. The time evolution of the lamp voltage was measured using a voltage divider. The lamp current was measured by means of the voltage drop across a resistor, placed in series with the lamp. Both quantities were registered by the HP Infinium digital oscilloscope (500 MHz, $2\,GSa\,s^{-1}$).

The radiation was monitored in the direction perpendicular to the surface of the ceramics through a quartz window and it was analysed in the spectral range 200–900 nm. The spectra were recorded by the TRIAX 550 monochromator (grating 1200 grooves mm^{-1}, quartz optical fibre, CCD Spectrum ONE detector cooled by liquid nitrogen, spectral resolution of the system was about 0.05 nm). The registration system was calibrated within the wavelength region 200–900 nm by means of the Quartz Tungsten Halogen lamp emitting a continuous spectrum. The absolute optical power was measured by the Lab Master Ultima powermeter with two exchangeable sensor heads (for 250–400 and 400–1100 nm). As the powermeter was not sensitive to wavelengths $\lambda < 250$ nm, the power of the emitted radiation in the range 200–250 nm has been estimated using the spectral characteristics as a ratio of corresponding areas, $k_1 = S_{(250\text{–}400\,nm)}/S_{(200\text{–}400\,nm)}$. The emitted radiation collected from a small area of the source surface, which was confined by a diaphragm D with area 1 cm^2, and the sensor head was located at a distance $L = 25$ cm from the ceramic plate. For the measurement of the UV radiation power versus distance the position of the sensor head was varied from 7 to 30 cm. At $L > 10D$ this area can be considered as a point radiation source. In this case, the part of the radiation power, registered by the powermeter, was calculated as $k_2 = \Omega_1/\Omega_2$, where $\Omega_1 = 2\pi$—the total space angle, $\Omega_2 = S_h/L^2$—the space angle corresponding to the sensor head of the powermeter, $S_h = \pi r^2$—the input aperture of the sensor head and $r = 0.03$ cm. So, the specific radiation power (in $mW\,cm^{-2}$) can be estimated by means of the formula $P = P_0 k_2/k_1$, where P_0 is the power measured by the powermeter.

Finally, the efficiency of the conversion from electrical power to emitted radiation can be defined as $\eta = (P/P_{el}) \times 100\%$, where P_{el} is the electrical power applied to the electrode system. As the calculation of the power supplied to the electrode system from the measured voltage and current time courses shows a large error, only the input power to the high voltage power supply was measured. The power to the electrodes was then calculated by multiplying the input power by the conversion coefficient (estimated at 90%).

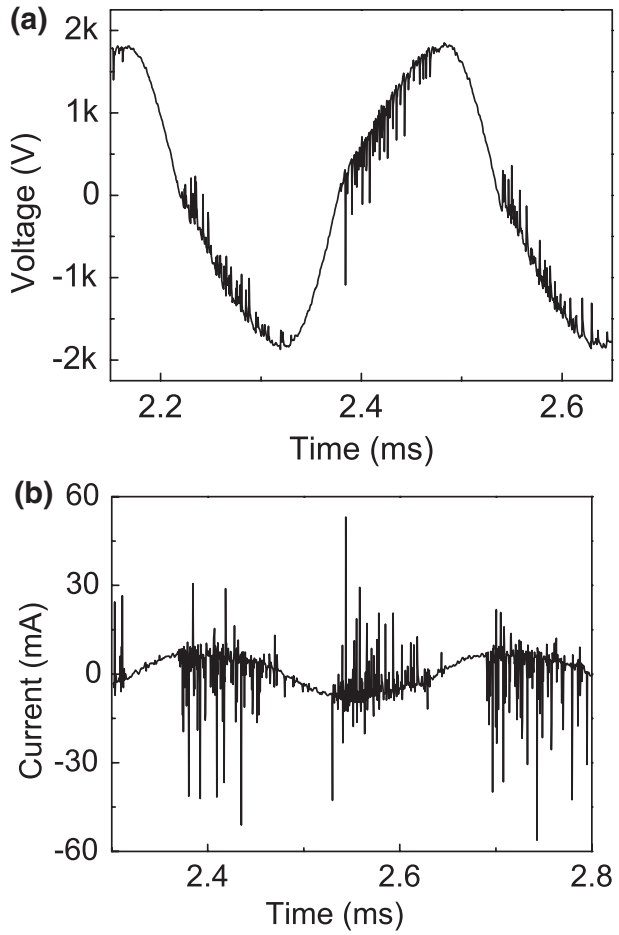

Figure 2. Oscilloscope traces of voltage across the discharge (*a*) and discharge current (*b*) in the $Kr/Xe/Cl_2 = 920/80/1$ mbar mixture.

3. Results and discussion

High-purity gases (Kr, Xe and Cl_2) were used for studying the excilamp. Not only the optical diagnostics, but the electrical characteristics were also measured. In figure 2, we present typical waveforms of the voltage (*a*) and discharge current (*b*) in SBD. It can be seen that the current pulse consists of two parts: capacitive current and a set of sharp peaks (with a duration of several nanoseconds), which are characteristic of a filamentary discharge. These short current pulses reflect the transferred charge. In the SBD arrangements the charges are distributed on the dielectric surface. The length of the charged area depends on the amplitude of the applied voltage, and an increase in the voltage leads to an enlargement of the discharge area. Taking into account [5], the charge transfer takes place in the thin layer close to the dielectric surface. The outer boundary of the charged area is determined by the first positive half-cycle of the applied voltage. In the succeeding negative half-period, the negatively charged layer is extended by the outer positive charges on the surface, enhancing the field strength component parallel to the surface.

In the UV emission spectra of the SBD the molecular bands corresponding to 222 nm of KrCl(B $\rightarrow$ X), 236 nm of XeCl(D $\rightarrow$ X), 258 nm of Cl_2(D′ $\rightarrow$ A′), 308 nm of XeCl(B $\rightarrow$ X) and 345 nm of XeCl(C $\rightarrow$ A, B $\rightarrow$ A) were observed simultaneously. Similar results were already observed in the case of the DBD discharge in the cylindrical configuration [10] and the sliding discharge [11]. The maximal brightness among these bands corresponds to XeCl(B $\rightarrow$ X) (figure 3—top). The radiation brightness of the molecular band J was considered to be proportional to the area below the corresponding curve in the spectrum. It was estimated that upper limit in the error in the brightness was about 5%.

The optimization of the discharge with respect to the partial pressure of components was done and it was found that the maximal brightness of the XeCl(B $\rightarrow$ X) band occurs at $p(Cl_2) = 1$–3 mbar, p(92% Kr + 8% Xe) = 500–1000 mbar. The Kr/Xe ratio was chosen as 92% Kr + 8% Xe in order to obtain approximately the same brightness of KrCl(B $\rightarrow$ X) and XeCl(B $\rightarrow$ X) bands in the $Kr/Xe/Cl_2$ mixture, i.e. $J_{KrCl}/J_{XeCl} = 0.7/1$. Note, that approximately the same brightness of the bands KrCl(B $\rightarrow$ X) and XeCl(B $\rightarrow$ X) was observed at pressures of Kr, which were higher by about one order than pressures of Xe. The feature of the brightness distribution in the emission spectra of the plasma containing Kr and Xe, can be explained by efficient energy transfer from atoms and molecules of Kr to Xe atoms as well as via the displacement reaction [12]

$$Kr^* + Xe \longrightarrow Kr + Xe^*, \quad k = 1.6 \times 10^{-10}\,cm^3\,s^{-1}, \tag{1}$$

$$Kr_2^* + Xe \longrightarrow 2Kr + Xe^*, \quad k = 4.4 \times 10^{-10}\,cm^3\,s^{-1}, \tag{2}$$

$$KrCl^* + Xe \longrightarrow Kr + XeCl^*. \tag{3}$$

The brightness of the XeCl(B $\rightarrow$ X) band increased to its maximum value when the working gas (92% Kr + 8% Xe) pressure increased to 500 mbar, and remained at this level up to 1000 mbar (figure 4—left ordinate). Similar dependences of brightness versus p(Kr + Xe) were observed for XeCl(D $\rightarrow$ X, C $\rightarrow$ A, B $\rightarrow$ A) molecular bands, whereas the brightness of the Cl_2(D′ $\rightarrow$ A′) excimer band decreases linearly. For an increase of p(Kr + Xe) within the limits 92/8–920/80 mbar the full-width at half-maximum of the XeCl(B $\rightarrow$ X) band decreases from 3.3 to 1.4 nm (figure 4—right ordinate). This result indicates that the selective narrow band incoherent UV radiation source can be successfully realized in a $Kr/Xe/Cl_2$ mixture operating in the SBD arrangement at near atmospheric pressure.

In the blue-green spectral range, the broad continuum with the maximum at a wavelength $\lambda = 480 \pm 10$ nm emitted by the plasma containing Xe and Kr at pressures p(Kr + Xe) > 500 mbar is overlapped by the line spectrum of atoms and ions of inert gases, which was also observed in [13]. When the pressure of the working mixture changes within the range 0.1–1 bar the intensity of the overlapped lines decreases 3–4 times as the continuum increases (figure 3—bottom). The most probable process, which results in this continuum, is the radiation of triple molecules Xe_2Cl^*. The molecules are created in the reaction as follows [12]:

$$XeCl^* + 2Xe \longrightarrow Xe_2Cl^* + Xe. \tag{4}$$

Another possibility can be realized via the recombination radiation

$$e + R^+ \longrightarrow R^* + h\nu. \tag{5}$$

The intensity of the continuum radiation is about two orders lower in comparison with the intensity of XeCl(B $\rightarrow$ X) and KrCl(B $\rightarrow$ X) bands. The most intensive atomic

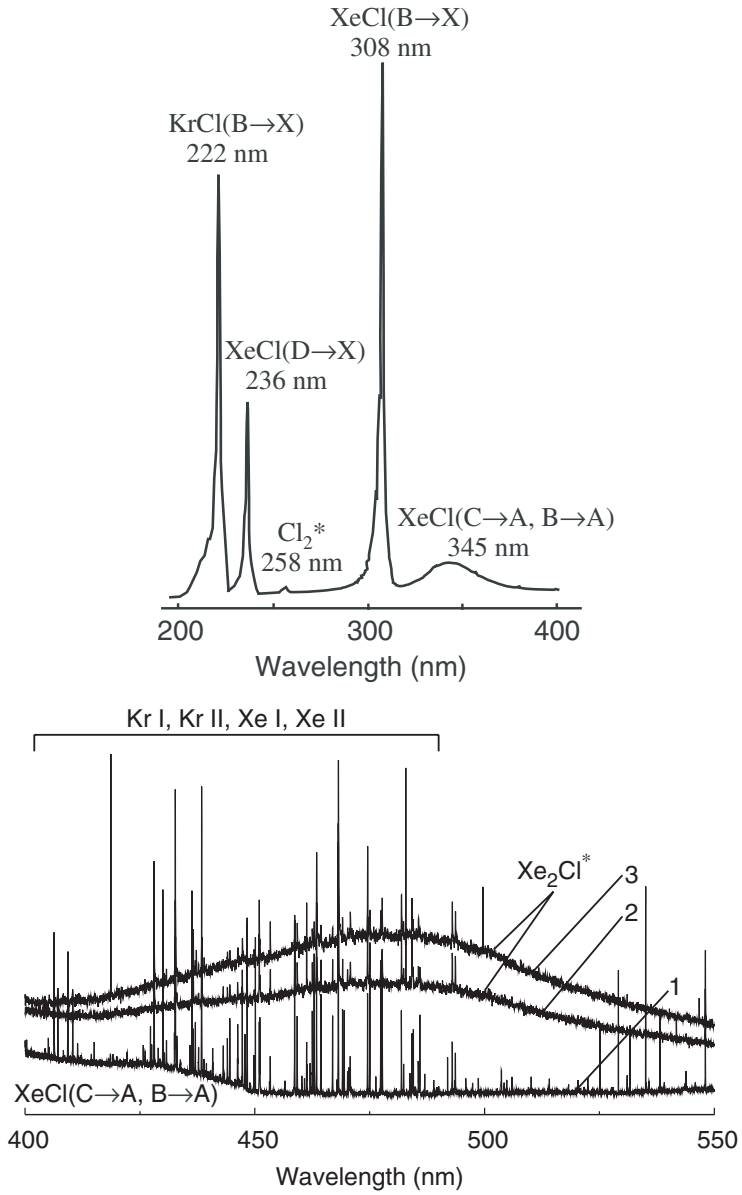

Figure 3. Typical spectra emitted by the SBD in the UV range for the mixture $Kr/Xe/Cl_2 = 920/80/1$ mbar (top) as well as in the visible range (bottom) for the following mixtures: 1—$Kr/Xe/Cl_2 = 92/8/1$ mbar; 2—$Kr/Xe/Cl_2 = 644/56/1$ mbar; 3—$Kr/Xe/Cl_2 = 920/80/1$ mbar.

lines correspond to the transitions Xe(6s–7p), Xe(6s′–6p′), Kr(5s–6p) and Kr(5s′–6p′). Except these lines, in the spectral range 750–850 nm at near atmospheric pressures of the working mixture, intense lines of Kr(5s–5p) and Xe(6s–6p) were observed.

It was also observed that the radiation power increases linearly when the input electrical power increases in the range of 5–15 W, whereas the efficiency of the conversion of electrical energy into the emitted radiation is not monotonic (figure 5). Note, that in the case of DBD excilamps based on $XeCl^*$ or $KrCl^*$ molecules, the efficiency (conversion coefficient) decreases as the input electrical power increases [2].

The measurements of average radiation power of the SBD have shown that at atmospheric pressure of the mixture, the contribution of visible and NIR light is rather significant (figure 6), while in the $Kr/Xe/Cl_2 = 460/40/1$ mbar mixture the power of visible and NIR radiation (400–1100 nm) is equal to 25% of the UV radiation power density.

In figure 7, we show the UV radiation power versus distance from the emitting surface. The radiation flux decreases approximately as L^{-2}, where L is the distance. In order to achieve a high intensity at effective utilization of the generated radiation, it is necessary to place the irradiated object close to the output window of the excilamp. As discussed in [14], the thickness of the plasma generated by the DBD in the excilamp with the cylindrical configuration does not influence significantly the density of emitted radiation.

4. Conclusion

We have studied the multi-wavelength planar $KrCl^*$ and $XeCl^*$ excilamps operated in mixtures of krypton and xenon with

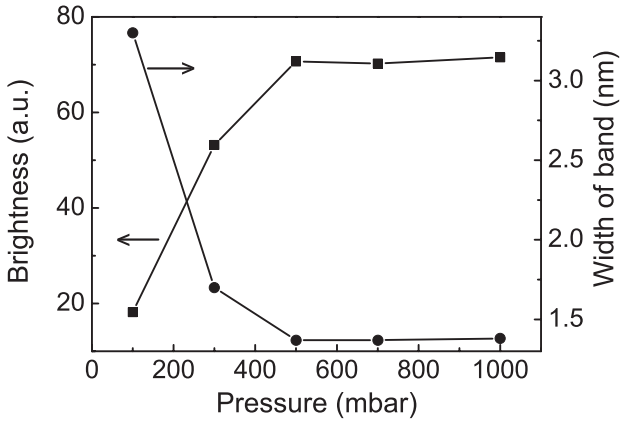

Figure 4. The brightness (left Y—axis) and full-width at half-maximum (right Y—axis) of the XeCl(B → X) band versus working gas (92% Kr + 8% Xe) pressure in the Kr/Xe/Cl_2 mixture at $p(Cl_2) = 1$ mbar.

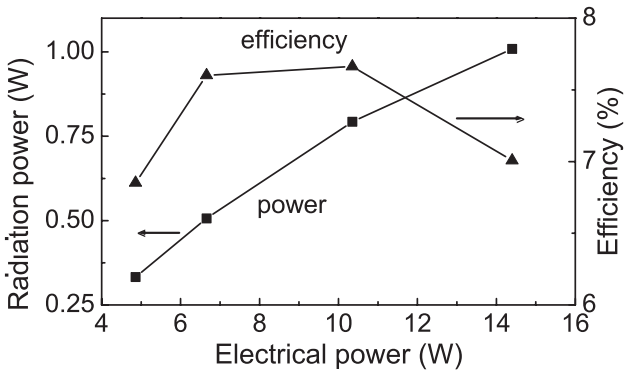

Figure 5. Mean radiation power as well as efficiency (conversion coefficient) versus input electrical power for the mixture Kr/Xe/Cl_2 = 920/80/1 mbar.

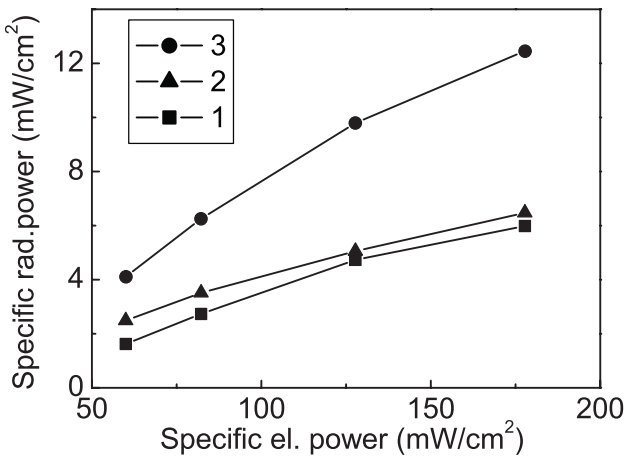

Figure 6. Radiation power density versus electrical power density for the Kr/Xe/Cl_2 = 920/80/1 mbar mixture: 1—UV radiation, 2—visible and NIR radiation, 3—total.

chlorine excited by the SBD. The main characteristics of the source in the pressure region of 0.1–1 bar have been investigated. The increase in voltage results in the enlargement of the discharge area on the dielectric surface. The power

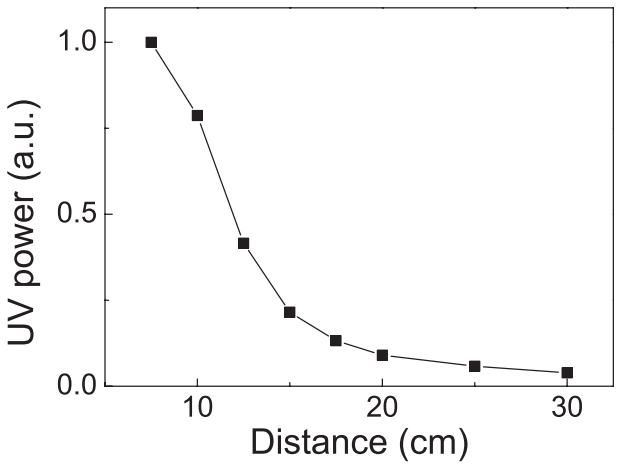

Figure 7. Space power distribution of UV radiation measured in the direction perpendicular to the surface of the electrodes.

density of UV radiation was 6 mW cm^{-2} in Kr/Xe/Cl_2 = 920/80/1 mbar mixture. The maximal power of UV radiation at the minimal power of visible and NIR was achieved at a total pressure of around 500 mbar (Kr/Xe/Cl_2 = 460/40/1). The conversion efficiency of the lamp varied with the electrical power, reaching maximum values of around 8%. This multi-wavelength excilamp with homogeneous output radiation flux adds to the commercial UV sources available to initiate various photo-chemical reactions.

Note, that even if the planar system shows remarkable properties, such a system is sensitive to sparks that can appear at the edge of the dielectrics and so a higher conversion coefficient cannot be achieved without effective suppression of this phenomenon. As mentioned before other configurations are possible [10, 11]. A comparison with the planar UV excilamp is in progress.

Acknowledgments

This work has been financially supported by the Grant Agency of the Czech Republic under the contract numbers 202/03/0708, 202/03/0011 and by research intent MSM: 143100003 funding by the Ministry of Education of the Czech Republic.

References

[1] Kogelschatz U, Esrom H, Zhang J-Y and Boyd I W 2000 *Appl. Surf. Sci.* **168** 29
[2] Boyd I W and Zhang J-Y 1996 *J. Appl. Phys.* **80** 633
[3] Lomaev M I, Skakun V S, Sosnin E A, Tarasenko V F, Shitz D V and Erofeev M V 2003 *Phys.—Usp.* **46** 193
[4] Boyd I W and Zhang J-Y 1997 *Nucl. Instrum. Methods Phys. Res.* B **121** 349
[5] Gibalov V I and Pietsch G J 2000 *J. Phys. D: Appl. Phys.* **33** 2618
[6] Šťahel P, Buršíková V, Navrátil Z, Záhoranová A, Janča J and Buršík J 2003 *Proc. 16th ISPC (Department of Chemistry, University of Bari)* p 10
[7] Šimor M, Ráhel J, Černák M, Imahori Y, Štefečka M and Kando M 2003 *Surf. Coat. Technol.* **172** 1
[8] Shuaibov A K, Shimon L L, Dashchenko A I and Shevera I V 2002 *Instrum. Exp. Tech.* **45** 95

[9] Shuaibov A K, Shimon L L and Shevera I V 1998 *Instrum. Exp. Tech.* **41** 427
[10] Guivan N N, Janča J, Sťahel P, Slavíček P, Brablec A and Malinin A N 2004 *Proc. 15th Int. Conf. on Gas Discharges and Their Applications (University of Toulouse)* p 773
[11] Guivan N N, Janča, Slavíček P, Brablec A and Sťahel P 2004 *Proc. 9th Int. Symp. on High Pressure, Low Temperature Plasma Chemistry (University of Padova)* 2P-04
[12] Rhodes Ch K 1979 *Excimer Lasers* vol 30 *Topics in Applied Physics* (Berlin: Springer)
[13] Shuaibov A K and Minya A I 1997 *J. Appl. Spectrosc.* **64** 523
[14] Boichenko M, Skakun V S, Tarasenko V F, Fomin E A and Yakovlenko S I 1993 *Quantum Electron.* **20** 613

Excitation of phosphors by UV XeI excimer radiation

M. M. Guivan, A. N. Malinin

Uzhgorod National University, Department of Quantum Electronics, Pidgirna 46, Uzhgorod, Ukraine
e-mail: m_guivan@rambler.ru

A. Brablec, J. Janča, P. Šťahel, P. Slavíček

Department of Physical Electronics, Masaryk University, Kotlářská 2, 611 37 Brno, Czech Republic
e-mail: {abr92, jan92, pstahel, ps94}@physics.muni.cz

Received 1 May 2006

The experimental study of excitation of green, red, and white phosphors by UV excimer radiation has been carried out. Generation of excimer radiation was realized by means of diffuse coplanar surface discharge (DCSD) sustained in Xe(Ne, Ar)/I_2 or Ne(Kr)/Xe/I_2 mixtures at pressures $1 \div 100$ kPa. Spectral characteristics of gas–discharge plasma as well as a composition compound of the working media have been investigated in order to obtain the maximal yield of XeI excimer radiation.

PACS: 52.80.Yr
Key words: diffuse coplanar surface discharge, excimer molecules, phosphor, emission spectrum, UV radiation

1 Introduction

Cheap and intense UV sources are of interest to the different applications such as surface modification, water sterilization or primary sources for the excitation of the luminescent lamp phosphor [1]. As it is well known, discharges in the rare gas – halogen mixtures can generate excimer radiation [2]. Plasma on the rare gas – iodine mixtures is investigated less in comparison with other halogens (chlorine, fluorine). Iodine is the least aggressive at interaction with materials and the most harmless substance from all halogens. It increases service life of iodine–based light sources and provides ecological safety of processes of their manufacture, operation and recycling. As to the development of new light sources the great interest attracts attention a xenon-iodine mixture because of effective formation of XeI^* molecules. The wavelength of $B - X$ transition of the XeI^* excimer molecules ($\lambda = 253$ nm) coincides with the brightest line of Hg at $\lambda = 253.6$ nm. The experimentally obtained efficiency (conversion of input electrical to output optical energy) reaches 22 % at using of the dielectric barrier discharge (DBD) [3], that allows to replace, fully or at least partially, the Hg–lamps by the mercury–free excimer ones. The mercury–free light sources radiate in the same wavelength range as mercury, which makes possible to apply the phosphors developed for mercury sources.

In this contribution the excitation of green, red and white phosphors by UV excimer radiation generated in diffuse coplanar surface discharge (DCSD) is studied experimentally.

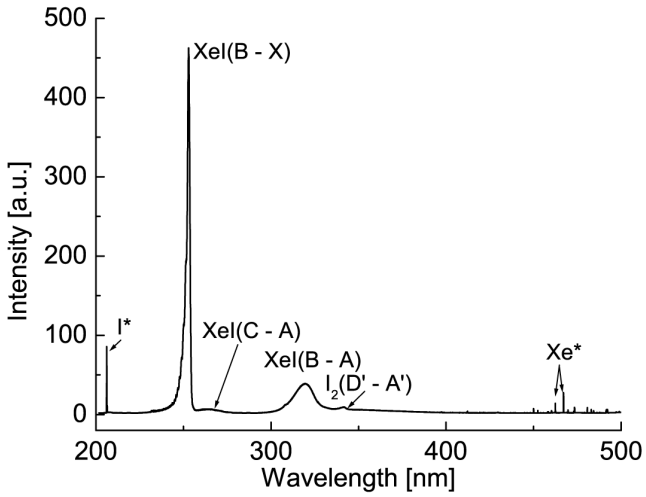

Fig. 1. Emission spectrum of the DCSD in the $Xe/I_2 = 15$ kPa/40 Pa working mixture.

2 Experiment

The diffuse coplanar surface discharge is a type of DBD generated on the surface of a dielectric barrier with embedded electrodes in planar design [4]. The DCSD electrode module was manufactured on the glass plate under the description presented in [4]. Strip–like electrodes have width 2 mm and distance between strips was 1 mm, thickness of a glass layer above electrodes 0.14 mm. The plasma consists of numerous H–shaped elementary discharges with brighter streamer–like filamentary plasma that bridges two clouds of diffuse plasma formed over the embedded electrodes. The distance between glass plate covered by phosphor and plasma sheet could change within the limits of $0.5 \div 20$ mm. The electrode system was mounted inside a chamber of 1.5 l in volume.

To excite working mixture the generator of high voltage AC pulses was used; peak–to–peak voltage up to 10 kV, frequency range was taken from 1 to 100 kHz. The frequency is matched for the resonance of the electrical circuit consisting of the transformer coil and the electrode module capacity. The measurements of the current and voltage across the DCSD were performed for an excitation frequency of typically 9 and 85 kHz, discharge voltage up to 7 kV by a current shunt and voltage divider Tektronix P6015A, resp. Both quantities were registered by digital oscilloscope HP Infinium (500 MHz, 2 GSa/s).

Prior to filling of gases the chamber is pumped down below 10 Pa. Iodine crystals were dried by means of resublimation cycles. The working mixture of rare gases with iodine vapors was prepared directly inside the chamber. Radiations were measured perpendicularly to the surface of dielectrics through quartz window and they were

analyzed in spectral range $200 \div 900$ nm. The spectra were recorded by the Jobin Yvon TRIAX 550 monochromator (grating 1 200 grooves/mm, quartz optical fiber) with the high–speed CCD Spectrum ONE detector cooled by liquid nitrogen [5]. Spectral resolution of the system was about 0.05 nm. Registration system was calibrated within the wavelength regions $200 \div 400$ nm and $400 \div 900$ nm by means of the Deuterium lamp and Quartz Tungsten Halogen lamp emitting continuous spectra.

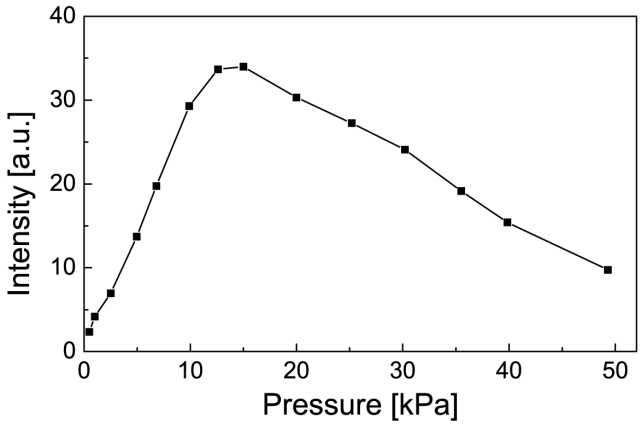

Fig. 2. Brightness of the XeI($B - X$) band as a function of xenon pressure in the Xe/I_2 mixture at $p(I_2) = 40$ Pa.

3 Results and discussion

In UV range, the emission spectra of the DCSD generated in the Xe/I_2 or $Ne(Kr)/Xe/I_2$ mixtures were recorded and molecular bands were observed such as XeI($B \rightarrow X$) – 253 nm, XeI($B \rightarrow A$) – 320 nm and $I_2(D' \rightarrow A')$ – 342 nm. The maximal brightness among them corresponds to XeI($B \rightarrow X$) (Fig. 1).

The radiation brightness of molecular band was considered to be proportional to the area below corresponding curve in the spectrum. The full width at half maximum (FWHM) of XeI($B \rightarrow X$) band decreases from 2.6 to 1.5 nm within the pressure range $5 \div 100$ kPa. The optical emission at 206.2 nm corresponds to the atomic iodine transition ($^2P_{3/2} \rightarrow ^2P_{1/2}$). A very low intensity emission was observed at 265 nm that correlates to XeI($C \rightarrow A$) while the wide molecular band in the range $350 \div 400$ nm with the maximum around 375 nm corresponds to Xe_2I^* excimer at pressure $p(Xe) > 25$ kPa. Its brightness grows while the pressure increases. The low intensity atomic lines of Xe($7p \rightarrow 6s$) were revealed at 462 and 467 nm (Fig. 1).

The working mixtures were optimized for maximal yield of UV excimer radia-

tion. For example, Fig. 2 shows the brightness of the XeI($B - X$) band vs. xenon pressure in the Xe/I_2 mixture with a fixed I_2 pressure $p(I_2) = 40$ Pa. The XeI($B-X$) emission increased to a maximum value with gas pressure, and then decreased when

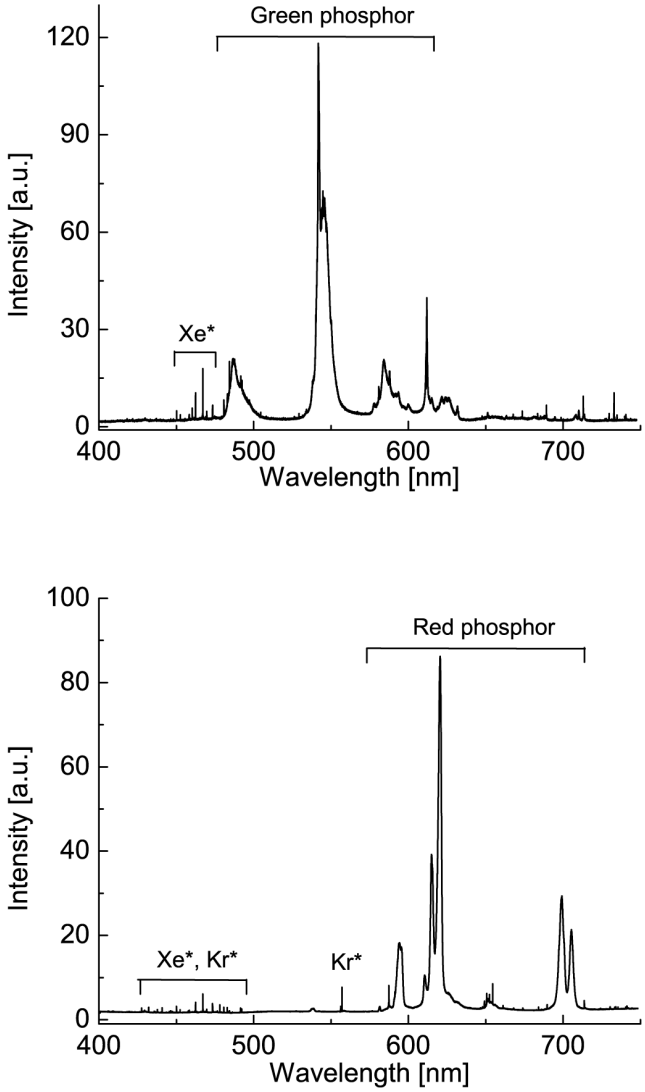

Fig. 3. Emission spectrum of the $MgAl_{11}O_{19}$:(Ce, Tb) green phosphor (top) and the Y_2O_3:Eu red phosphor (bottom) with XeI* excitation (top: $Xe/I_2 = 15$ kPa/40 Pa, bottom: $Kr/Xe/I_2 = 51$ kPa/4 kPa/40 Pa working mixtures).

the gas pressure was more than 15 kPa. Similar result were obtained in case of the Xe/I_2 mixture in DBD [3] but optimal xenon pressure was about 50 kPa. Probably, it is because of larger partial pressure of iodine used (about 1 kPa) in [3]. The decrease of XeI^* fluorescence at $\lambda_{max} = 253$ nm for high total pressures was caused by quenching of XeI^* by Xe in the reaction

$$XeI^* + 2Xe \longrightarrow Xe_2I^* + Xe. \tag{1}$$

In the $Kr/Xe/I_2$ mixture, the UV output initially increases with gas pressure, up to a maximum value in the range of $40 \div 60$ kPa, and then some decreases. Unlike to the Xe/I_2 mixture, in the emission spectra of $Kr/Xe/I_2$ mixture it was observed that intensity of $I_2(D' \to A')$ band was more higher than intensity of $XeI(B \to A)$.

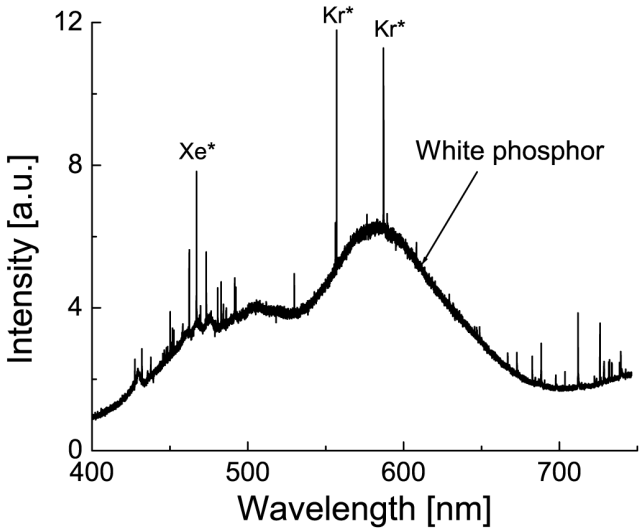

Fig. 4. Emission spectrum of the white phosphor upon XeI^* excitation ($Kr/Xe/I_2 = 51$ kPa/4 kPa/40 Pa working mixture).

Using the different phosphors, the intense visible radiation has been only observed in xenon–containing mixtures, such as Xe/I_2 or $Ne(Kr)/Xe/I_2$, capable to form XeI excimer molecules (Figs. 3 and 4). The best results were obtained when the $MgAl_{11}O_{19}$:(Ce, Tb) green phosphor emitted the maximum intensity at 541 nm was used (Fig. 3, top). In visible range, a weak fluorescence was only registered when Ne/I_2 or Ar/I_2 mixtures were used. It was revealed, that optimal distance between plasma and phosphor was $3 \div 5$ mm for obtaining intense homogeneous visible light. The homogeneity was worse at smaller distance and at large distance the intensity falls.

4 Conclusion

We investigated the possibility of using a XeI($B - X$) excimer radiation generated by diffuse coplanar surface discharge at middle pressures for the excitation of phosphors. The working mixtures were optimized to obtain maximal output of UV radiations. It has been shown that Xe/I_2 or $Ne(Kr)/Xe/I_2$ discharges have the potential to be used in the mercury–free fluorescent lamps. It was revealed that optimal distance between DCSD plasma sheet and phosphor to achieve the intense homogeneous luminescence in the visible range is $3 \div 5$ mm.

This work has been financially supported by Czech Science Foundation under the contract numbers 202/03/0708, 202/03/0011 and by research intent MSM0021622411, Ministry of Education, Czech Republic.

References

[1] U. Kogelschatz: Plasma Chemistry and Plasma Processing. **23** (2003) 1.

[2] M. I. Lomaev, V. S. Skakun, E. A. Sosnin, V. F. Tarasenko et al: Phys. Usp. **46** (2003) 193.

[3] J.-Y. Zhang, I. W. Boyd: J. Appl. Phys. **84** (1998) 1174.

[4] M. Šimor, J. Ráhel, P. Vojtek, M. Černák, A. Brablec: Appl. Phys. Lett. **81** (2002) 2716.

[5] N. N. Guivan, J. Janča, P. Slavíček, A. Brablec, P. Sťahel: IX Int. Symp. on High Pressure, Low Temperature Plasma Chemistry (Hakone IX), Padova, Italy. (2004) 2P–04.

Underwater pulse electrical diaphragm discharges for surface treatment of fibrous polymeric materials

A. Brablec, P. Slavíček, P. Sťahel, T. Čižmár, D. Trunec,

Dep. of Phys. Electronics, Masaryk University, Kotlářská 2, 611 37 Brno, Czech Republic

M. Šimor, M. Černák

Institute of Physics, Comenius University, Mlynská dolina F2, 842 48 Bratislava, Slovakia

Received 30 May 2002

Preliminary results on physical characteristics of pulsed underwater diaphragm electrical discharges are presented. The discharges burning in tap water, water–chelaton solutions, and some other water–based solutions were studied as a potential atmospheric–pressure H_2O – plasma source for surface activation of polyester cord threads. The discharge plasma parameters have been measured by means of optical emission spectroscopy. Electron number density of roughly 2×10^{18} cm^{-3} and an electron temperature of 1×10^4 K were estimated from broadening of hydrogen lines (H_α), and vibrational temperature of 2500 K was determined from the vibrational band of nitrogen. A significant increase in the surface energy and wettability of the cord threads due to the plasma treatment was obtained.

PACS: 52.75.Hn, 52.80.–s
Key words: underwater discharge, H_2O plasma, surface treatment, polyester cord

1 Introduction

Materials applications of polymers have become increasingly specialized relying on specific combination of properties. In particular, applications in adhesion and coatings require specific surface properties such as bondability, hydrophilicity, and surface energy. However, common polymers very often do not posses the surface properties needed for these applications. Thus, surface modifications are used to transform these inexpensive materials into valuable finished products.

It is known that hydroxyl radicals generated in low–pressure H_2O plasma may be used to incorporate hydroxyl functionality onto a polymer surface [1 – 4] and that preferred polymers, which can be treated to increase their surface energy and reactivity, are polyaromatic polymers [1 – 3] as, for example, polyester (PES) used in manufacturing of high performance tire cord. The works [1 – 4] were made at reduced pressures on the order of 10^{-3} – 10^3 Pa, where the low–temperature H_2O plasma can easily be generated and brought into direct contact with surfaces of polymer materials in form of fabrics, films, fibres, powders, etc. However, the use of expensive vacuum systems that force batch processing has discouraged these applications of low–pressure plasmas, where on–line surface treatments of polymer products with the low added value in large amounts are required. As a consequence,

it is apparent that atmospheric pressure operation is desired for practical applications.

Underwater pulsed corona discharges generated in liquid water matrix at atmospheric pressure have been demonstrated to be effective in the production of hydrated electrons and hydroxyl radicals [5 – 12]. Following the pioneering work of Clements et al. [5] on pulsed streamer corona generated using point–to–plane geometry of electrodes in water, various types of underwater electrical discharges producing hydrated electrons and hydroxyl radicals in liquid water–based media have been tested for the removal of low levels of non biodegradable organic pollutants from ground waters and industrial waste waters [6 – 12]. Very few results, however, have been published on interactions of the active species generated in pulsed electrical discharges in water with polymer materials [13 – 15].

Preliminary results presented in Refs. [14] and [15] indicate that a promising technique for atmospheric–pressure plasma surface activation of polymeric materials in the form of threads can be based on the use of underwater diaphragm electrical discharges. In contrast to other types of underwater electrical discharges, in diaphragm electrical discharges the discharge plasma is not in a direct contact with the metallic electrodes, which helps to eliminate potential problems with electrode oxidation and erosion due to a direct contact of the electrodes with highly reactive H_2O plasma. The main object of the present paper is to report an extension of the earlier works [14, 15] focused on a more detailed study of the discharge physical properties and its H_2O plasma parameters. For purpose of comparison with the existing results [14, 15] on the surface activation of PES cord threads, the same material was used in the present experiments. The diaphragm discharge was generated in a tap water, in water–chelaton (always used Chelaton 3), and in other water–based solutions.

2 Experimental apparatus and results

The H_2O–plasma was generated using the diaphragm discharge arrangement illustrated by Figs.1(a) and 1(b). The discharge occurred in the vicinity and inside of a 1.2 mm–diam. hole in the diaphragm made from a plexiglass desk of 3 mm thickness, which was inserted in the gap between two stainless steel planar electrodes in conductive water–based solution. Several conductive water–based solutions as tap water and water–chelaton were tested. In contrast to the known results for the pulsed underwater corona arrangement, where the discharge was initiated on an electrode surface [9, 10], the results obtained with the diaphragm discharge were not sensitive to the solution conductivity and its chemical composition. Therefore, for the sake of brevity, the data to be reported her were confined to those taken in water–chelaton solutions and tap water. The water–chelaton solutions are of practical interest also because their use as a medium for plasma cleaning of archeological artefacts [16]. A picture illustrating the discharge visual appearance is shown in Fig. 2. The discharge appearance did not depend significantly on the solution used. It is seen that the discharge plasma took the form of streamers propagating on the

thread surface to the distance several millimetres from the diaphragm.

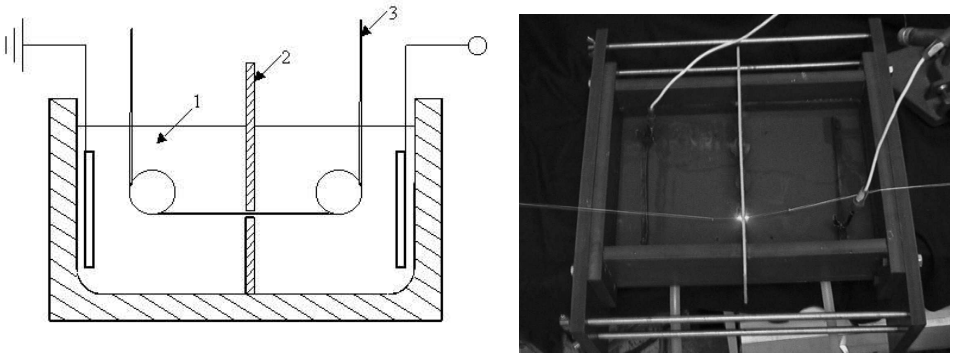

Fig. 1. Experimental arrangement for the underwater diaphragm discharge: (a) Schematics: 1– water–based solution, 2 – diaphragm, 3 – treated cord, (b) Photo of the arrangement (right).

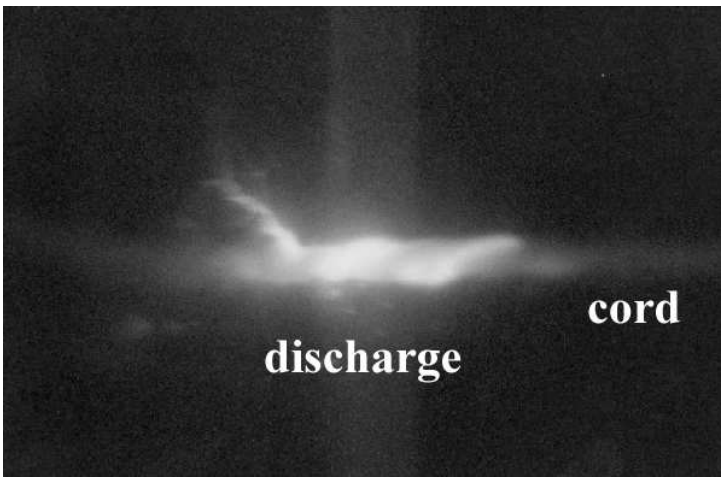

Fig. 2. Photo of the underwater discharge plasma.

The treated polyester PES cord thread moved in the hole with a speed of 5 cm/s. One of the electrodes was connected with a HV pulse power supply. The power supply consisted of a variable voltage 0 – 60 kV DC source, a low inductance storage capacitor of 3 nF, and a rotating double spark gap similar to that described in [10]. The double spark gap was used to separate the charging and discharging phases of the storage capacitor. The gap voltage and discharge current pulse waveforms were

measured using a TEKTRONIX P6015A HV probe and a PERSON 2877 current probe with a home–made current divider and recorded using a HP 54820A Infinium digital oscilloscope (500 MHz, 2 GSa). The HV pulse power supply was operated at 25 Hz, which was given by a limited power (150 W) of the DC source used. Typical HV pulse and discharge current waveforms that, as already mentioned, were not critically dependent on the water–based solution conductivity and chemical composition, are shown in Fig. 3.

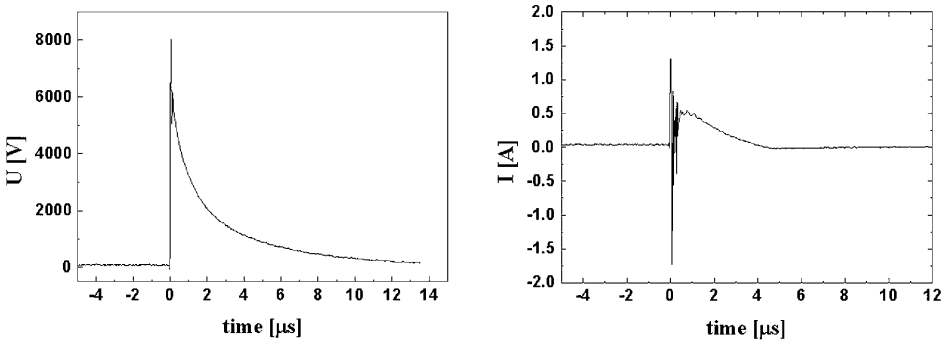

Fig. 3. Typical gap voltage and current temporal developments of the discharge pulse in tap water. The peak power, the total energy dissipated in the pulse, and the discharge onset voltage were 770 kW, 0.58 J, and 18.5 kV, respectively.

Spectral analysis of the light emitted by the discharge was done using TRIAX 550 spectrometer by Jobin – Yvon with the CCD detector (cooled by liquid nitrogen, 2000 × 800 pixels) using a grating with 1200 gr/mm.

Typical spectra measured in a water–chelaton solution and in tap water are compared in Fig. 4. The most striking observation is that while in the water–chelaton solution and other solutions studied a strong H_α line radiation was observed, this was nearly absent in the case of discharge in tap water. This is clearly illustrated by Fig.5, where H_α lines measured for the discharge in several solutions are shown in detail. To determine electron temperatures and densities standard Griems table (which takes into account the impact broadening by electron and quasi–static broadening by ions) of H_α line profile [17] was used.

Note that mercury lines as well as a background radiation (continuum) originating from an outer light source are discernible in Fig. 4 and Fig. 5. The continuum was seen when long integration times were used mainly around 580 nm. The weak nitrogen vibrational bands observed between 300 and 400 nm indicate that the discharge burnt also in bubbles containing air.

Since the measured H_α line profile was not symmetrical the temperature and electron density were estimated approximately from one half of the profile. It also indicate that other broadening mechanisms could play a non–negligible role and, consequently, the actual electron densities and temperatures can be somewhat lower

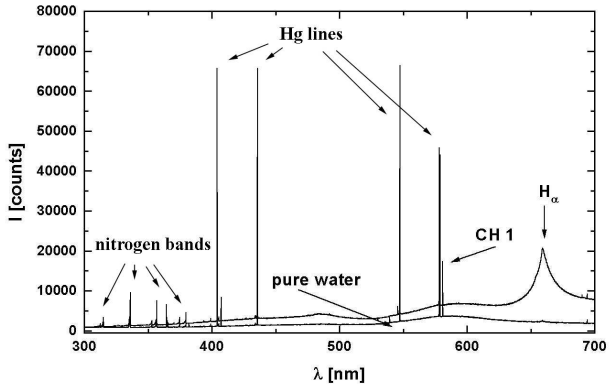

Fig. 4. A typical spectrum for tap water and saturated solution of chelaton (CH 1). The diameter of diaphragm was 1.2 mm. The peak power was estimated on 770 kW, total energy absorbed in one pulse was about 0.58 J, starting HV on the capacitor in equivalent circuit was estimated 18.5 kV.

Table 1. Typical values of electron temperature and electron density estimated from the H_α line profile for various water based solution. CH 1 is the saturated solution of chelaton, CS 1.5 is the water solution with 1.5 g/l of copper sulphate and CS 3 is the solution with 3 g/l of copper solution, resp.

	electron temperature K	electron density cm^{-3}
CH 1	1.1×10^4	2.30×10^{16}
CS 1.5	1.0×10^4	2.51×10^{16}
CS 3	1.1×10^4	2.34×10^{16}

than those shown in Table 1.

Surprisingly, no OH bands were not found in the emission spectra at 305 – 311 nm. It is not clear if it is because they were absent completely or were hidden by noise. Thus, rotational temperatures of OH radicals was not determined. On the second hand the nitrogen bands were used for estimation of vibrational temperatures of nitrogen component in the discharge. It was found that the vibrational temperature determined from the nitrogen bands (0 – 2 system, second positive) were practically the same both for the tap water and for the chelaton solution, i.e. 2448 ± 260 K and 2507 ± 330 K, respectively (correlation – 0.99).

To avoid of a complex chemistry involved, and to obtain data complementary to the results presented in Refs. [14] and [15], we limited our preliminary study of

the chemical effects of the discharge to simple measurements of surface properties PES cord treated in tap water: To gain some information on the changes in surface properties of the PES cord thread due to the H_2O plasma treatment the contact angle was measured by means of imaging of the cord surface–liquid meniscus shape. Alternatively, the observation of the spreading time of known volume of the liquid in the cord was correlated to the cord thread wettability. Even when it is difficult to record the size of the drop immediately after setting on the cord surface, it was possible to estimate the initial drop size by the observation of a dynamic evolution of the drop size in time.

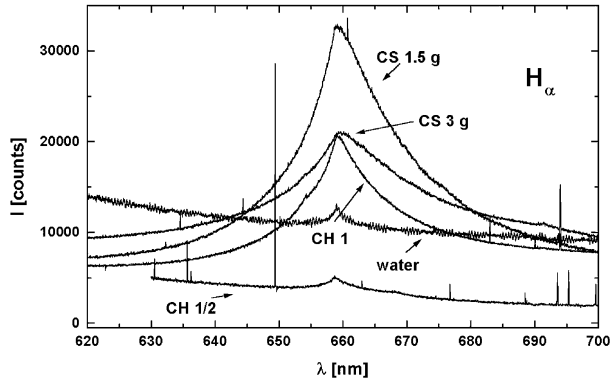

Fig. 5. Spectral line profile of H_α tap water and several typical solutions: saturated solution of chelaton (CH 1) and half concentration of chelaton (CH 1/2), water based solution of copper sulphate (CS) with 1.5 g/l and 3 g/l. Data for the pure water and CH 1/2 were multiplied by a constant for better reading their structure.

As reported by Grundke [18], when the wettability of a fiber bundles is measured, following points have to be taken into account:

– the direct measurement of the equilibrium contact angle of fiber bundles is not possible, since there is always a capillary penetration of the liquid into the sample

– deviations from equilibrium contact angle are observed when using the indirect dynamic methods for the determination of contact angles.

In spite of the above mentioned difficulties, we used the dimension of the drop (height and width) to estimate approximately the contact angle. If the height is larger for the given drop volume, the corresponding surface energy of the solid will be smaller. Our measurements are based on the following model: According to [19] the initial spreading coefficient can be defined in terms of the difference of the solid

surface tension and the liquid surface tension together with the interfacial tension by the following equation:

$$S_O = \gamma_s - \gamma_l - \gamma_i. \tag{1}$$

The initial spreading coefficient S_O can also be defined as the difference between the work of adhesion and work of cohesion and is equal to the negative of the Gibbs free energy per unit area:

$$S_O = W_{a0} - W_c = -\Delta F_{s0}. \tag{2}$$

The liquid l spreads spontaneously on the solid s when the initial spreading coefficient $S_O > 0$, i.e. surface energy of the solid is greater than the sum of liquid surface tension and interfacial tension (see Eq. (1)). The liquid forms a lens resulting in a partial wetting, when $S_O < 0$.

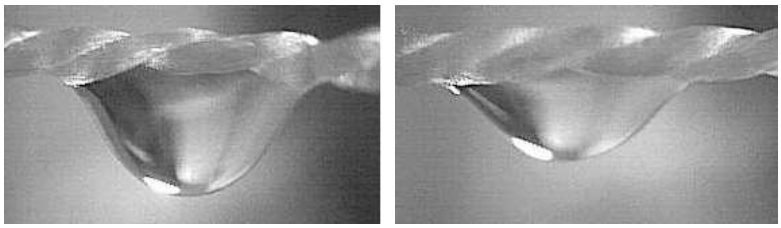

Fig. 6. The snapshot of the cord fiber with water drop: without plasma treatment (left) and after the plasma treatment recorded 2 s after the application of the drop (right).

The experimental procedure used is illustrated by Fig. 6, where the cord suspended horizontally with a known tension can be seen. Liquid drops (in our case the volume of the drop was 5 μl) were made by micropipette. The images of the liquid drop in successive time steps were recorded by CCD camera. It can be seen that, in comparison with the plasma treated cord, a bigger drop was set on the untreated cord thread surface. The bigger drop indicates that the water get soaked inside the fiber essentially slower than in case of non–treated fiber. One can see that for practically the same width of both drops the drop on treated cord fiber is less than for non–treated one, i.e. the contact angle is substantially higher and surface energy lower than for the cord fiber treated by diaphragm plasma.

Table 2. Initial height and spreading time of treated and untreated samples. Plasma treatment was made by mens of diaphragm plasma discharge burning in water.

plasma treatment	yes	no
initial height [pixels]	51	61
spreading time [seconds]	17	35

In Fig. 7 the drop height as a function of spreading time measured on the untreated and plasma treated cord threads are shown. The spreading times and initial heights of the drops are shown in the Table 2. From the results it is clear that the plasma treatment increased the wettability of the cord (see the decrease in time necessary for the complete spreading of 5 μl of water with respect of the corresponding reference). Moreover, the plasma treatment resulted in a pronounced decrease in water contact angle i.e. an increase in surface energy. This fact is indicated by the decrease in initial height of 5 μl drop formed on horizontally suspended cord.

3 Discussion

The visual appearance of the discharge indicate that the discharge mechanism is identical with those described in [20 – 21] where, however, diaphragm discharges without any fibrous dielectric material, such as a PES cord thread were studied. We believe that a general picture of the discharge development can be described as follows: After the HV pulse application the whole ion current flowing in the water due to its conductivity is concentrated to the hole in diaphragm and heats and evaporates water there. As indicated by nitrogen bands (see Fig. 4) the water vapour generated there is mixed with air bubbles trapped in cavities inside the cord thread, where the water did not penetrate since the thread fibres are not wettable by water. In such a way a gas–filled region inside the hole and in its immediate vicinity is formed. Neglecting a voltage drop on the water layers between both electrodes and the diaphragm, nearly whole HV pulse applied to the electrodes appears on the gas region surface, resulting in its electrical breakdown and creation of a highly conductive plasma streamers propagating along the cord thread surface (see Fig. 2). This physical picture indicates that all gas discharge processes occur in a water vapour/air mixture, without any expected dependence on the conductivity and chemical composition of the water solution used. This is in conformity with the observed insensitivity of the discharge current and plasma parameters to the water solution properties.

It is possible that because of a complex chemistry involved in the generation and decay of various radicals in atmospheric pressure plasmas [9], the solution chemical composition can have a significant effect on the radicals densities and, consequently, on chemical effects of the discharge plasma. Also, at the moment we have no plausible explanation for the observed sensitivity of H_α line to composition of the solution used. Such effects apparently can result from a very complex chemistry of the active species in water vapour plasma at atmospheric pressure. A detailed study of the discharge plasma chemistry is beyond the scope of this article and could be an interesting subject for some future studies. It is believed that the fundamental plasma parameters of the diaphragm discharge measured probably for the first time can form a basis for such a more detailed future studies. Discussing the plasma parameters measured it is of interest to note that the electron density of 2×10^{18}cm-3 is nearly identical with that measured by Sunka et al. [10] for a different underwater corona discharge type.

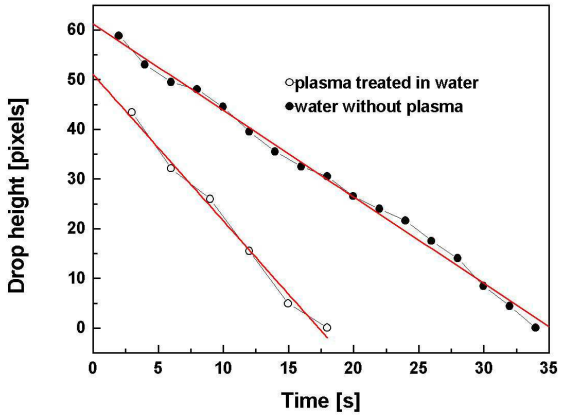

Fig. 7. The drop height as a function of time measured on treated and untreated polyester cord. Measured data fulfill linear fits.

As for the effect of the discharge plasma on the PES cord surface properties, the data reported here are confined to the observed increase in the wettability and surface energy of the plasma–treated PES cord. It is known that the practical adhesion, or bondability, between polymer surfaces and other materials deposited onto them cannot always be correlated with wettability and surface energy [22]. Nevertheless, it appears that the increase in the wettability and surface energy observed in our experiments offers a plausible explanation for an enhancement of the adhesive strength between a rubber matrix and PES cord threads plasma treated in similar conditions [14, 15].

4 Conclusions

Basic physical characteristics of the underwater diaphragm discharge in a configuration designed for the H_2O plasma treatment of polymeric threads and filaments do not depend critically on the conductivity and chemical composition of the water solution used. Over the range of water solutions studied the following plasma parameters were determined: the electron density of 2×10^{18} cm^{-3}, electron temperature of 1×10^{4} K, and vibrational temperature of 2500 K. A significant increase in the surface energy and wettability of the cord threads due to the plasma treatment was obtained, without any reproducible effect of the water solution conductivity and chemical composition.

This work has been financially supported by grant 202/00/D057, 202/01/P017 of Grant Agency of the Czech Republic, research intent CEZ J07/98:143100003 funding by

the Ministry of Education of the Czech Republic and by project No. 1/8316/01 of Slovak Grant Agency VEGA.

References

[1] C. M. Chan, T. M. Ko and H. Hiraoka: Surface Sci. Reports **24** (1996) 1.

[2] S. Okazaki et al. (E. C. Chemical Co., Ltd.): JP 34425092 (1992).

[3] N. J. Chou et al.: US 5,019,210 (1991).

[4] U. Hayat: GB 9124467 (1993).

[5] J. S. Clements, M. Sato, R. H. Davis: IEEE Trans. Ind. Appl. **IA–23** (1987) 224.

[6] S. A. Slobodskoi et al.: *Vopr. Technol. Ulavlivania i Pererab. Prod. Koksovania* (1978) 71.

[7] A. K. Sharma, B. R. Locke, P. Arce, W. C. Finney: Hazardous Waste & Hazardous Materials **10** (1993) 209.

[8] D. R. Grimonpre, A. K. Sharma, W. C. Firney, B. R. Locke: Chem. Engineering Journal **82** (2001) 189.

[9] P. Lukes, Ph.D. Thesis, Prague 2001.

[10] P. Sunka, V. Babicky, M. Clupek, P. Lukes, M. Simek, J. Schmidt, M. Cernak: Plasma Sources Sci. Technol. **8** (1999) 258.

[11] P. Sunka, V. Babicky, M. Clupek, K. Kolacek, P. Lukes, M. Ripa, M. Cernak: in *Proc. of 18th Symp. Plasma Physics and Technology*, Prague, 1997 144.

[12] P. Sunka: Physics of Plasmas **8** (2001) 2587.

[13] M. Mikula, J. Panak, V. Dvonka: Plasma Sources Sci. Technol. 6 (1997) 179.

[14] H. Krump, M. Simor, J. Rahen, I. Hudec, M. Cernak: *Improvement of PES cord/rubber adhesion by atmospheric–pressure H_2O plasma treatment*, in press.

[15] M. Simor, M. Cernak, H. Krump, J. Hudec, M. Stefecka: in *Proc. of XXV Int. Conf. on Phenomena in Ionised Gases* Nagoya, **4** 2001 63.

[16] M. Klima, J. Janca et all: Czech Patent No. 286310 (Prague, 2000).

[17] H. R. Griem: *Spectral line broadening by plasmas*, Academia Press, New York, 1974.

[18] K. Grundke, M. Boerner, H. J. Jacobasch: Colloids and Surfaces **58** (1991) 47.

[19] W. D. Harkins, A. Feldman: J. Am Chem. Soc. **44** (1992) 2665.

[20] E. M. Drobishevhii, Yu. A. Dunyajev, S. I. Rozov: Zh. Tech. Phys. 43 (1973) 1217.

[21] I. E. Boguslavskii, E. V. Krivickii, V. N. Petrishenko: Elektron. Obrob. Mater. 183 (1995) 33.

[22] E. M. Liston, L. Martinu, M. R. Vertheimer: J. of Adhesion Science Technology **7** (1993) 1091.

STUDY OF POLYPROPYLENE NON-WOVEN FABRICS TREATMENT IN UNDERWATER ELECTRICAL DIAPHRAGM DISCHARGE

GABRIELA NEAGOE[a]*, ANTONÍN BRABLEC[a], JOZEF RÁHEĽ[a,b], PAVEL SLAVÍČEK[a], and MIROSLAV ZAHORAN[b]

[a] *Dep. of Physical Electronics, Faculty of Science, Masaryk University, Kotlářská 2, 61137 Brno, Czech Republic,* [b] *Dep. of Experimental Physics, Comenius University, Mlynská dolina F2, 84248 Bratislava, Slovak Republic*
gabriela.pirpiliu@yahoo.com

Introduction

Plasma treatment has an explosive increase in interest and use in industrial applications as for example in medical, biomedical, automobile, electronics, semiconductor and textile industry. A lot of intensive basic research has been performed in the last years, also in the field of textiles and technical textiles. This has resulted in an increasing knowledge of the possibilities of this process regarding demands as wettability, dyeability, printability, coating and washability of conventional and technical textile. All day problems of wettability and adhesion, together with the environmental driven forces have increased the interest of industry today. This delivers new materials with new possibilities, which opens perspectives to resolve production or even develop complete new applications.

Production problems are mainly caused by the substitution of the base material to new materials for example polymers, which have not the correct surface behavior for further processing.

Plasma treatment of textiles is becoming more and more popular as a surface modification technique. Plasma treatment changes the outermost layer of a material without interfering with the bulk properties. Textiles are several millimeters thick and need to be treated homogeneously throughout the entire thickness. It is known that hydroxyl radicals generated in low-pressure H_2O plasma may be used to incorporate hydroxyl functionality onto a polymer surface to increase their surface energy and reactivity. Underwater pulse diaphragm discharge is an effective tool in the production of hydrated electrons and hydroxyl radicals, which can be used for material surface modification (bondability, hydrophilicity, surface energy).

Preliminary results on physical characteristics of pulsed underwater diaphragm electrical discharge[1,2] have shown that the discharges burning in tap water, water-chelaton solutions, and some other water based solutions can be used as a potential atmospheric-pressure H_2O – plasma source for surface activation of various materials in the form of fabrics, films, fibers, etc. The discharge burning at atmospheric pressure can substitute low-pressure plasma sources[3–6] when atmospheric pressure on-line surface treatments of polymer products with the low added value in large amounts are required.

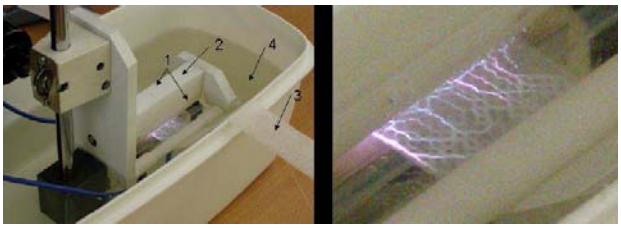

Fig. 1. **Experimental arrangement (left) for underwater diaphragm discharge:** 1 – electrodes; 2 – diaphragm; 3 – polypropylene nonwoven fabric; 4 – water-based solution. **A detail of the discharge treating the textile is also shown (right)**

Underwater pulsed corona discharges generated in liquid water matrix at atmospheric pressure have been demonstrated to be effective in the production of hydrated electrons and hydroxyl radicals[7–11,13,14]. Following the pioneering work of Clements et al.[7] on pulsed streamer corona generated using point-to-plane geometry of electrodes in water, various types of underwater electrical discharges producing hydrated electrons and hydroxyl radicals in liquid water-based media have been tested for the removal of low levels of non biodegradable organic pollutants from ground water and industrial waste water[14]. Very few results, however, have been published on interactions of the active species generated in pulsed electrical discharges in water with polymer materials[1,15,16]. Few applications are helpful for fixing metallic atoms on the polypropylene (PP) surface for metal coating.

In contrast to other types of underwater electrical discharges, in diaphragm electrical discharge the discharged plasma is in a direct contact with the metallic electrodes.

While in ref.[1] and ref.[2] the common features and chemical effects including promising application of this discharge for surface treatment of polymer materials are presented and discussed, the main object of the present paper is to report a more detailed study of the discharge physical properties. Using optical emission spectroscopy the electron number densities have been determined from broadening of hydrogen lines (H_α) *vs.* solution conductivity, frequency of high voltage pulses, speed of fiber movement for fixed applied voltage, length of the slit in dielectric diaphragm, and the diaphragm thickness.

Experiment

The H_2O-plasma treatment was performed using a diaphragm discharge apparatus illustrated by Fig. 1. The discharge was generated in a narrow slit of 0.1×1 mm positioned between two metallic electrodes at 2 cm mutual distance. Both electrodes and the slit (diaphragm) were immersed in water medium. Polypropylene nonwoven fabrics of 50 gsm and 30 mm width was fed trough the slit with an adjustable speed. The electrodes were connected to a pulsed HV power supply based on the double rotating spark gap. The maximum peak voltage was 40 kV DC. The maximum repetitive rate of pulses was 60 Hz. The duration of the electrical pulses was given by the water conductivity. Different water based media were used in this study: deionized water, Cu^{2+} solution with the concentration C = 0.0075 M of $Cu(NO_3)_2$. 3 H_2O; and

CO_2 saturated mineral water. Similar experiment was already realized in ref.[2].

Results and discussion

Initially the plasma starts within the air bubbles trapped inside the porous structure of nonwovens. After the air voids are filled with water a different discharge breakdown mechanism takes place. The high intensity electrical current flowing through the narrow slit is capable of initiating the water vaporization. The discharge starts in the water vapour bubbles created by that vaporization. The discharge manifests itself as thin plasma filaments propagating along the textile surface up to the distance where the metallic electrodes are positioned. The length of propagation is given by the conductivity of water solution and amplitude of the applied voltage.

Typical profiles of H_α are shown in Fig. 2a. To determine electron temperature and density the standard Griem's table (which takes into account the impact broadening by electron and quasi-static broadening by ions) of H_α line profile[17] and the procedure for data processing presented in ref.[1] were used. Note, that all profiles were symmetrical. In our case (rectangular discharge slit) the electron density changes from $1\cdot10^{22}$ m^{-3} to $2\cdot10^{24}$ m^{-3} while the electron temperature was practically constant $\approx 4\cdot10^4$ K in all experimental conditions studied. The same results were obtained as in the previous experiments (for diaphragm discharge). This is an interesting phenomenon and it means that comparable high density of electrons can be reached in the rectangular configuration. The error of the measured electron density was less than 5 %. The error of electron temperature was much higher, which is due to the weak dependence of the line profile on the electron temperature.

In Fig. 2b, the change of electron number density *vs.* conductivity of Cu^{2+} solution is presented. Taking into account the possible dispersion in the electron number density (for example, the corresponding error is always about 5 %), it

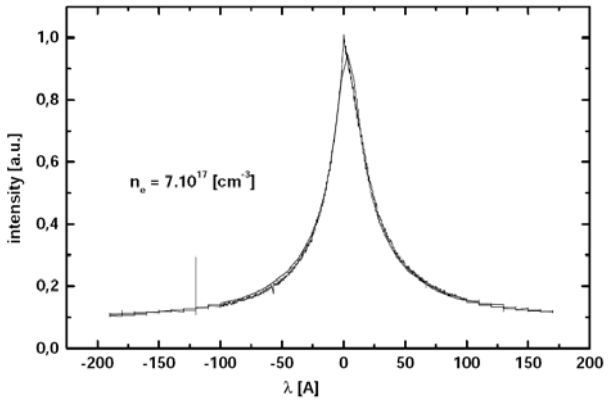

Fig. 2a. **The typical H_α line profile fitted with a model based on Stark broadening**

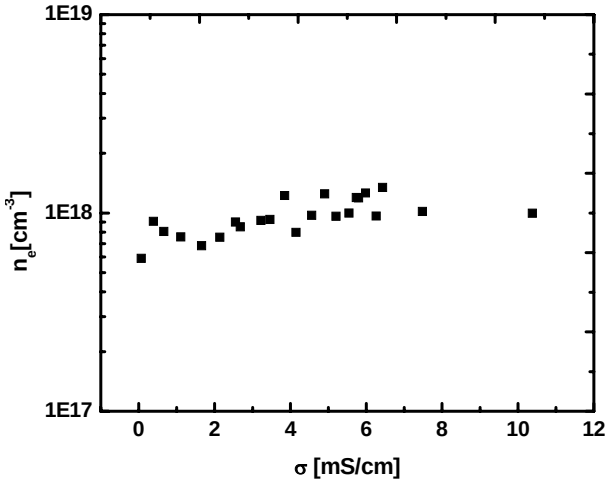

Fig. 2b. **The typical dependence of electron number density *vs.* conductivity for different Cu^{2+} solutions**

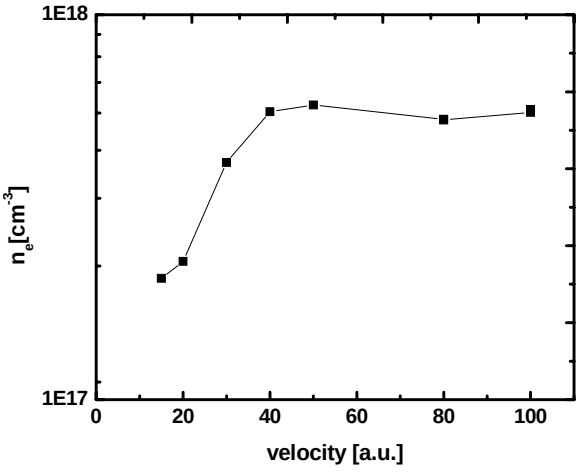

Fig. 3a. **The electron number density (n_e) *vs.* speed of the polypropylene nonwoven fabrics through the discharge for deionized water**

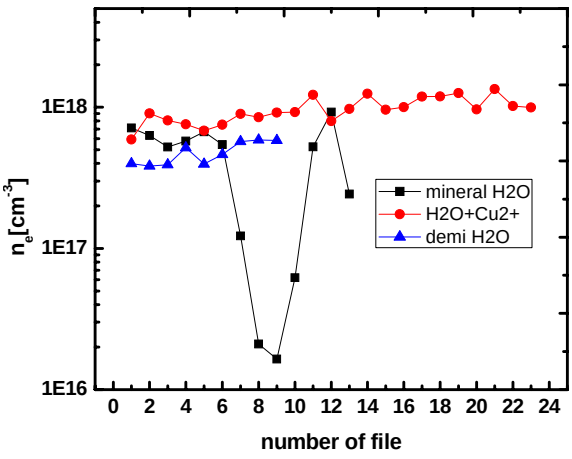

Fig. 3b. **Dispersion of n_e for different solutions during time interval of more than 1 hour is presented**

seems that the conductivity does not influence significantly the electron number density in the specified conductivity range.

In Fig. 3a, there is shown that the electron number density remains constant while the statistics presented in Fig. 3b demonstrate an interesting effect of CO_2 bubbles − the unexpected decrease of n_e in several cases. This phenomenon was also manifested on character of the discharge (suddenly, the intensity was higher, its colour became different). However, in this moment this is only a stochastic effect.

A practical application of diaphragm plasma treatment of PP is shown in Fig. 4a,b.

The textile was treated in water solution of Cu^{2+} in the same conditions as described above. The treatment was repeated after 1 minute on the same sample. Furthermore, we washed the sample in a detergent solution in Ultrasonic Bath for 15 minutes to see how much of copper attached to the textile material. The SEM photographs reveal a presence of copper microcrystals attached to the PP fabrics (Fig. 4a). More than 60 % of these crystals were still attached even after intense washing (Fig. 4b). This implies a strong chemical interaction between the crystals and PP. The chemical (copper) nature of crystal was confirmed by the EDX analysis of the sample. At this moment we are not able to confirm if the crystals are made from Cu only.

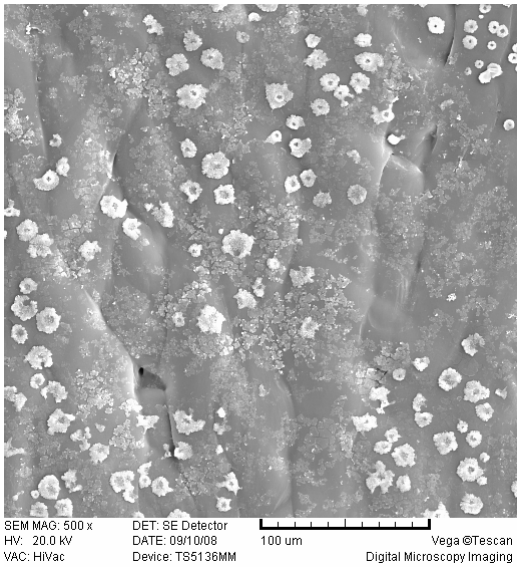

Fig. 4a. **SEM micrographs of textile surface treated twice in water solution of Cu^{2+} without washing**

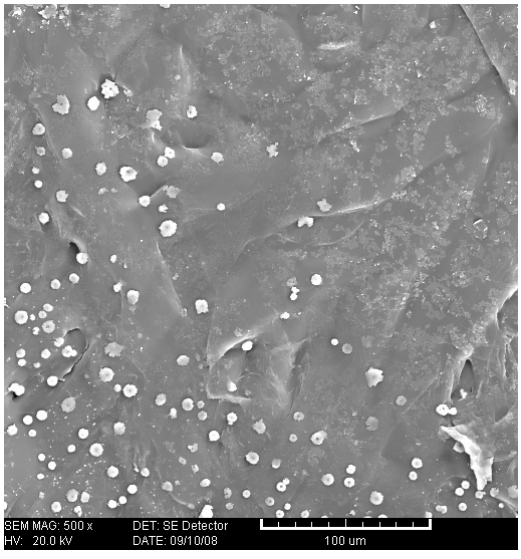

Fig. 4b. **SEM micrographs of textile surface. The textile was washed with detergent in Ultrasonic Bath for 15 minutes after double treatment**

Conclusion

The determination of n_e in case of selected quantities at optimized parameters show that their values do not influence significantly electron density and its fluctuation is almost covered with the confidence interval. It was found that the effect of CO_2 bubbles as well as the role of Cu^{2+} solution (or other metallic atoms) can bring interesting application. Further research is necessary in order to fully understand the influence of the double treatment and washing on the PP fiber and to compare these results with the case of single treatment applied to the PP fiber. By performing diaphragm plasma in the water solution of copper salt we were able to immobilize copper crystals on the PP surface.

This research has been supported by the Czech Science Foundation under the contract numbers KAN101630651 and 202/06/P337 and by the research intent MSM:0021622411 funding by the Ministry of Education of the Czech Republic.

REFERENCES

1. Brablec A., Slavicek P., Stahel P., Cizmar T., Trunec D., Simor M., Cernak M.: Czech. J. Phys. *52* Suppl. D491 (2002).
2. Simor M., Krump H., Hudec I., Rahel J., Brablec A., Cernak M.: Acta Physica Slovaca *54*, 43 (2004).
3. Chan C. M., Ko T. M., Hiraoka H.: Surf. Sci. Reports *24*, 1 (1996).
4. Okazaki S. : E.C. Chemical Co.,Ltd., JP 34425092 (1992).
5. Chou N. J. : US5, 019, 210 (1991).
6. Hayat U.: GB 9124467 (1993).
7. Clements J. S., Sato M., Davis R. H.: IEEE Trans. Ind. Appl. IA-23, 224 (1987).
8. Slobodskoi S. A. : Vopr. Technol. Ulavlivania i Pererab. Prod. Koksovania 71 (1978).
9. Sharma A. K., Locke B. R., Arce P., Finney W. C.: Hazardous Waste & Hazardous Materials *10*, 209 (1993).
10. Grimonpre D. R., Sharma A. K., Finney W. C., Locke B. R.: Chem. Eng. J. *82*, 189 (2001).
11. Lukes P.: *Ph.D. Thesis*, Prague 2001.
12. Sunka P., Clupek M., Lukes P., Simek M., Schmidt J., Cernak M.: Plasma Sources Sci. Technol. *8*, 258 (1999).

13. Sunka P., Babicky V., Clupek M., Kolacek K., Lukes P., Ripa M., Cernak M.: *In Proc. of 18th Symp. Plasma Physics and Technology, Prague, 1977*, 144 (1997).
14. Sunka P.: Phys. Plasmas *8*, 587 (2002).
15. Mikula M., Panak J., Dvonka V.: Plasma Sources Sci. Technol. *6*, 179 (1997).
16. Simor M., Cernak M., Krump H., Hudec J., Stefecka M.: *In Proc. of XXV Int. Conf. on Phenomena in Ionised Gases 4, Nagoya, 2001.* 63 (2001).
17. Griem H. R.: *Spectral line broadening by plasmas*. Academia Press, New York 1974.

G. Neagoe[a]*, A. Brablec[a], J. Ráhel[a,b], P. Slavíček[a], and M. Zahoran[b] *([a] Dep. of Physical Electronics, Faculty of Science, Masaryk University, Brno, Czech Republic, [b] Dep. of Experimental Physics, Comenius University, Bratislava, Slovak Republic):* **Study of Polypropylene Nonwoven Fabrics Treatment in Underwater Electrical Diaphragm Discharge**

During the last two decades functionalization of polymer surfaces has been recognized as a valuable tool to improve their adhesion properties. Underwater pulse diaphragm discharge is an effective tool in the production of hydrated electrons and hydroxyl radicals, which can be used for material surface modification (bondability, hydrophilicity, surface energy). For efficient material treatment it is necessary to identify operational key parameters controlling the discharge plasma characteristics and to establish some appropriate diagnostic methods and models for plasma characterization. The plasma parameters – electron number density, temperature of electrons, excitation temperature, have been measured by optical emission spectroscopy completed by the voltage, and current measurement. The sampling optical fiber was installed directly in the slit to minimize the water absorption of light emission. The electron number density will be estimated preferable from spectral line profile of H_α. Our contribution will summarize the results of our experiments.

Contrib. Plasma Phys. **44**, No. 5-6, 492 – 495 (2004) / **DOI** 10.1002/ctpp.200410069

Generation of Thin Surface Plasma Layers for Atmospheric-Pressure Surface Treatments

M. Černák [*1], **J. Ráheľ**[1], **D. Kováčik**[1], **M. Šimor**[2], **A. Brablec**[2], and **P. Slavíček**[2]

[1] Inst. of Physics, Faculty of Mat., Phys., and Informatics, Comenius University, Mlynská dolina F2, 842 48 Bratislava, Slovakia

[2] Department of Physical Electronics, Masaryk University, Kotlarská 2, 611 37 Brno, Czech Republic

Received 16 March 2004, accepted 16 March 2004
Published online 27 August 2004

Key words Plasma-surface, interactions, surface treatment.

PACS 52.50.Dg, 52.40.Hf, 81.65.-b

Thin layers of atmospheric-pressure non-equilibrium plasma can be generated by pulse surface corona discharges and surface barrier discharges developing on the treated surfaces or brought into a close contact with the treated surfaces. Plasma sources based on these discharge types have the potential of meeting the basic on-line production requirements in the industry and can be useful for a wide range of surface treatments and deposition processes including continuous treatment of textiles. Comparing with atmospheric pressure glow discharge sources, the potential advantages of these plasma sources include their simplicity, robustness, and capability to process in a wide range of working gases.

1 Introduction

The development of atmospheric pressure plasma sources to replace low-pressure plasma processing is a current trend in industrial plasma applications [1], reaching even the plasma etching in semiconductor manufacturing processes [2]. The advantages of operating at atmospheric pressure have led to the development of a variety of low-temperature plasma sources with quite different technical means of generating the plasma as, for example, microwave discharges [3, 4], corona discharges [1, 5], barrier discharges [6, 7], micro-hollow cathode discharges [8, 9], and plasma jets [10, 11]. Recently, the atmospheric-pressure glow discharges (APGDs) have been considered as the most promising non-equilibrium plasma source for surface treatments [1, 6, 12–16].

A common feature of most of these sources of atmospheric-pressure non-equilibrium plasmas is that they are producing the plasmas in volumes much larger than the volume in which active particles reacting with the treated surface are generated. As a consequence, a substantial part of the discharge power is uselessly dissipated in the plasma volume by, for example, recombination processes and gas heating. In particular it is true for APGDs, where without sufficient gas flow, the discharge tends break up into an array of thin filaments. We believe that for many surface treatment applications a thin (on the order of 0.1 mm) layers of plasma generated directly on the treated surface of brought into a close contact with the surface can provide substantial advantages in energy consumption, exposure time, and technical simplicity.

Thin layers of highly non-equilibrium plasmas, in which the plasma power density can reach the order of 100 W/cm^3, can be efficiently generated by various types of surface discharges developing in contact with the surfaces to be treated. Herein discussed pulse surface corona discharges and surface barrier discharges offer efficient ways to produce non-equilibrium plasmas for polymer surface treatment. This is illustrated by the successful surface treatments of polymer fibres and fabrics, which appear to be the most difficult forms of polymer materials from the viewpoint of plasma surface treatments [17].

* Corresponding author: e-mail: cernak@fmph.uniba.sk

2 Plasma sources studied and conclusions

2.1 Plasma source based on pulse surface corona discharges

Figure 1(a) shows the electrode arrangement of the plasma source designed for atmospheric-pressure plasma treatments of endless fibrous materials.

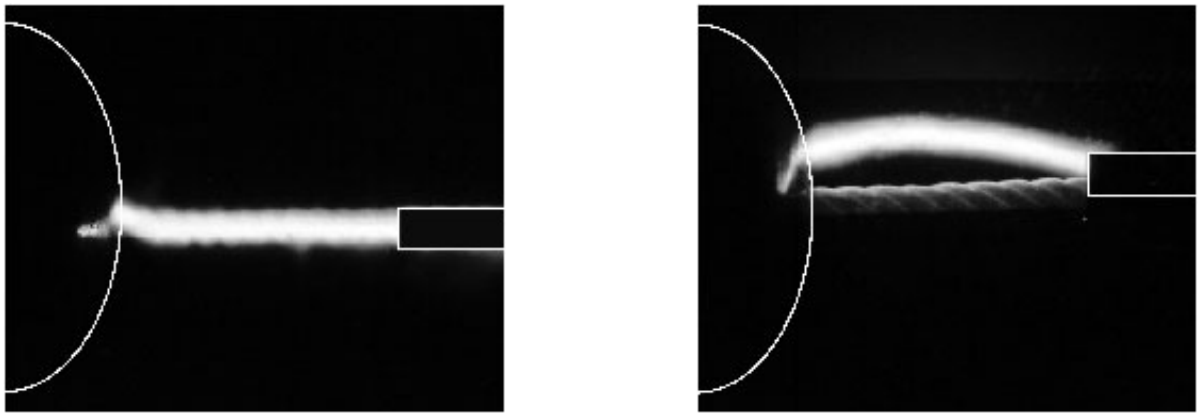

Fig. 1 Discharge generated on the surface of a polyester cord thread in (a) nitrogen (b) ambient air. The photos were taken during a single voltage pulse.

The electrode system consisted of two on-axis-arranged electrodes housed in a glass chamber. The grounded stainless-steel tubular anode was 1.5 mm in inner diameter. The cathode was a 15 mm-diam. hemispherically capped brass rod with a 2 mm-diam. hole in its axis. The distance between electrodes was adjusted to 1.5 cm. The treated fibrous material moved on the axis of the electrode system with a speed from 1 cm/s to 20 cm/s. The cathode was connected with a thyratron source of pulsed high voltage with a pulse frequency of 100 Hz, a peak voltage of 25 kV, pulse rise time of 75 ns, and pulse half-width of 400 ns. The discharge power was approximately 20 W. Full experimental details, including the gap voltage and discharge current pulse waveforms, can be found in Refs. 18-22.

As illustrated by Fig. 1(a), in certain experimental conditions a thin layer of the low-temperature plasma is generated in the close vicinity of the treated surface and surrounds it homogeneously. This results in high values of the power deposited on the treated surface, low power consumption, and high processing speeds. The reactor was successfully tested for surface activation of ultra-high molecular weight polyethylene multifilaments, polyester monofilaments, and polyester cord threads [18–21]. We believe that the discharge development can be envisaged as analogous to the pulsed positive streamer corona discharges used for flue gas cleaning [22, 23] and to multichannel surface discharge used, for example, in high-voltage switches [24]:

Avalanche multiplication in the strongly enhanced field leads to the formation of a large number of positive streamers propagating towards the cathode with speeds on the order of 10^7 cm/s. It is known that the positive streamers tend to propagate in the direction of higher seed electrons density ahead of them. In nitrogen, where the photoionization is weak, the most important source of the seed electrons appears to be photoemission from the treated polyester surface. Consequently, as seen in Fig. 1(a), in nitrogen the streamers tend to propagate in the close vicinity of the treated surface. This discharge behavior is in contrast to that observed in air (see Fig. 1(b)), where the much intense photoionization results in the streamers, which tend to propagate into the gas volume.

2.2 Plasma sources based on a surface dielectric barrier discharge and a coplanar diffuse surface barrier discharge

According to a commonly accepted nomenclature [25], there are three basic types of dielectric barrier discharges (DBDs): The most commonly used volume DBD, where the discharge mainly appears within a gas gap between parallel plates or concentric cylindrical electrodes; the surface DBD invented by Masuda et al. [26] (see Fig. 2(a)), where high - voltage electrodes in form of strips or wires are situated on the surface of a dielectric layer with an extended plane counter-electrode on its reverse surface; and the coplanar DBD (Fig. 2(b)) commonly

used in plasma displays, where the electrode arrangements consists of two electrode systems embedded inside a dielectric with a fixed electrode distance.

In typical operating conditions, the dielectric barrier discharges (DBDs) in its various forms consist from filamentary microdischarges and, consequently, are highly non-uniform. Moreover, new filamentary microdischarges ("streamers") strongly tend to be ignited at those places on the dielectric barrier where charges were deposited by preceding microdischarges and to use repeatedly the same incompletely deionised microdischarge channels. If the volume DBDs are used for a fabrics treatment, the streamers develop perpendicularly to the fabric fibers. As a consequence, the plasma is in a very limited contact with the fabric fiber surfaces, which results in a long exposure times necessary for the plasma activation and consequent low processing speeds, typically on the order of $\sim$1 m/min.

The surface DBDs applied to treat fabrics differ from the volume DBDs chiefly in that the plasma streamers are parallel with the fabric surface. In this way, the dense streamer plasma is in a much better contact with the fibers surfaces, which reduces the necessary exposure time significantly. Also, an important advantage is that the plasma is generated only in a thin layer that roughly equals to the volume of the fabric to be treated, resulting in reduced power consumption.

The surface DBDs has been successfully tested for surface activation of woven ultra-light-molecular-weight polypropylene fabrics [27], polyester and polypropylene nonwoven fabrics [28, 29], and polyester foils [30]. However, it has been found [31], that the surface DBDs systems are of limited value for industrial implementation because of a limited life-time (on the order of 10^2–10^3 hours) of the discharge electrodes that are in a direct contact with the discharge plasma.

To remedy this limitation a novel surface discharge type (the coplanar diffuse surface barrier discharge – CDSBD) has been developed [31, 32], where a macroscopically homogenous plasma layer is generated without any direct contact with electrodes, which protects the electrodes erosion (see Fig. 2(b)).

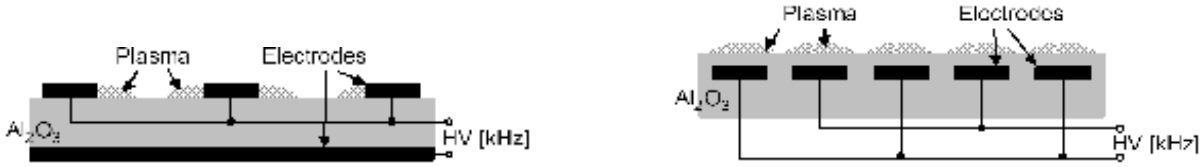

Fig. 2 Schematics of electrode arrangements of a) (left) surface dielectric barrier discharge and b) (rigth) coplanar diffuse surface barrier discharge

The CDSBD electrode arrangement used consisted of two systems of parallel striplike electrodes (1-mm wide, 50-μm thick, 0.5-mm strip-to-strip; molybdenum) embedded in 96 % alumina using a green tape technique. The thickness of the ceramic layer between the plasma and electrodes was 0.4 mm. A sinusoidal high-frequency high voltage (1 - 15 kHz, up to 10 kV peak) was applied between both electrode systems. Such a discharge electrode arrangement and energisation result in visually almost uniform diffuse plasmas of some 0.3-mm thickness generated in nitrogen, ambient air, and other technically important gases [32]. A high-speed camera study [33] has revealed that this is because the discharge consists of numerous H-shaped microdischarges developing with a high density and running on the alumina surface along the embedded strip electrodes. The higher the gap voltage, the faster the microdischarges move and the higher is their density. As a consequence, the homogeneity of the DCSBD plasma increases with the discharge power density. This discharge behaviour is in sharp contrast to the behaviour of other types of dielectric barrier discharges and APGDs, which makes possible to generate highly nonequilibrium DCSBD plasmas also at high plasma power densities.

The DCSBD generates thin (on the order of 0.1 mm) uniform plasma layer [32], which at surface power density up to 5 W/cm^2 gives the plasma power density of order of 100 W/cm^3. For the discharge in nitrogen a vibrational temperature of 1950 K and rotational temperature of 387 K (roughly equal to the gas temperature) were estimated from the second positive nitrogen band system and the band of OH [32]. To the best of our knowledge, this gives the highest power density of low-temperature highly nonequilibrium plasma among the plasma sources hitherto tested for textile surface treatment applications.

The simplicity of the electrode geometry allows the manufacturing of a flat plasma panel shown in Fig. 3. Such a DCSBD device is robust, safe at unintended contact, and its cooled version can operate close to room temperature even at high electrical input powers.

Fig. 3 Cooled 500 W plasma panel constructed on the base of coplanar diffuse surface barrier discharge. The picture illustrates mechanical and "electrical" robustness of the panel.

Acknowledgements This work was supported in by GACR Grant 202/03/0708 at the Masaryk University, and VEGA Grant 1/8316/01 and STAA Grant 013/2001 at the Comenius University.

References

[1] J.R. Roth, *Industrial Plasma Engineering*, *Vol. 2: Applications to Nonthermal Plasma Processing*, (Inst. of Phys. Publishing, Bristol and Philadelphia, 2001)
[2] Y. Kataoka, M. Kanoh, N. Makino, K. Suzuki, S. Saitoh, H. Miyajima, Y. Mori, Jpn. J. Appl. Phys. **39**, 294-298 (2000).
[3] M.J. Shenton, G.C. Stevens, Thermochemica Acta **332**, 151-160 (1999).
[4] M.J. Shenton, G.C. Stevens, N.P. Wright, X. Duan, J. Polymer Sci. **A 40**, 95-109 (2002).
[5] M. Sugawara, Surface and Coating Technology **142-144** , 290-292 (2001).
[6] H.-E. Wagner, R. Brandenburg, K.V. Kozlov, A. Sonnenfeld, P. Michel, J.F. Behnke, Vacuum **71**, 417-436 (2003).
[7] M. Koide, T. Horiuchi, T. Inushima, B.J. Lee, M. Tobayama, H. Koinuma, Thin Solid Films **316**, 65-67 (1998).
[8] A.A.H. Momamed, R. Block, K.H. Schoenbach, IEEE Trans. Plasma Sci. **30**, 182-183 (2002).
[9] C. Penache, S. Datta, S. Mukhopadhyay, A. Braunin-Demian, P. Joshi, O. Hohn, S. Schossler, T. Jahnke, H. Shmidt-Bocking, *Contrib. Papers of* 8^{th} *International Symposium on High Pressure Low Temperature Plasma Chemistry* (July 21 - 25, 2002, Pühajärve, Estonia) pp. 390-395.
[10] J.Y. Jeong, S.E. Babayan, V.J. Tu, J. Park, I. Henins, R.F. Hicks, G.S. Selwyn, Plasma Sources Sci. Technol. **7**, 282-285 (1998).
[11] A. Brablec, P. Slavíček, M. Klíma, V. Kapička, J.F. Behnke, M. Šícha, Czech. J. Phys. **52**, 561-566 (2002).
[12] L.J. Ward, W.C.E. Schonfield, J.P.S Badyal, A.J. Goodwin, P.J. Merlin, Chemistry of Materials **15** , 1466-1469 (2003).
[13] T. Nozaki, Y. Unno, K. Okazaki, Plasma Sources Sci. Technol. **11**, 431-438 (2002).
[14] S. Guimond, I. Radu, G. Czeremuszkin, D.J. Carlsson, M.R. Wertheimer, Plasmas and Polymers **7**, 71-88 (2002).
[15] Y. Akishev, M. Grushin, A. Napartovich, N. Trueshin, Plasmas and Polymers **7**, 261-289 (2002).
[16] R.A. Wolf, Paper, Film & Foil Converter (2003), http://pffc-online.com/ar/paper_atmospheric_plasma/
[17] A.J.A. Klomp, J.G.A. Terlingen, G.A.J. Takens, J. Appl. Polym. Sci. **75** , 480-494 (2000).
[18] M. Štefečka, J. Ráheľ, M. Černák, I. Hudec, M. Mikula, M. Mazúr, Journal of Materials Science Letters **18**, 2007-2009 (1999).
[19] M. Štefečka, J. Ráheľ, I. Hudec , P. Janypka, M. Černák, M. Mikula, M. Kando, Journal of Materials Science Letters **19**, 1869-1871 (2000).
[20] M. Černák, J. Ráheľ, I. Hudec, M. Štefečka, M. Kando, I. Chodák, Plasmas and Polymers **5**, 119-127 (2000).
[21] H. Krump, I. Hudec, M. Černák, P. Janypka, Elastomer **37**, 192-194 (2002).
[22] E.M. Van Velduizen, W.R. Rutgers, J. Phys. D-Appl. Phys. **35**, 2169-217 (2002).
[23] S. Masuda, Pure and Appl. Chem. **60**, 727-735 (1988).
[24] H.M. Von Bergman, in *Gas Discharge Closing Switches* (G. Schaefer, M. Kristiansen, A. Guether, eds., Plenum Press, N.Y.1990, pp.345-374).
[25] V.I. Gibalov, G.J. Pietsch, J. Phys. D: Appl. Phys. **33**, 2618-2636 (2000).
[26] S. Masuda, K. Akutsu, M. Kuroda, Y. Awatsu, Y. Shibuya, IEEE Trans. Ind. Appl. **24**, 223-231 (1988).
[27] J. Ráheľ, M. Černák, I. Hudec, A. Brablec, D. Trunec, Czech. J. Phys. **50** , Suppl. S3, 445-448 (2000).
[28] M. Šimor, J. Ráheľ, M. Černák, Y. Imahori, M. Štefečka, M. Kando, Surface and Coating Technology **172** , 1-6 (2003).
[29] J. Ráheľ, M. Šimor, M. Černák, M. Štefečka, Y. Imahori, M. Kando, Surface and Coating Technology **169-170**, 604-608 (2003).
[30] M. Štefečka, M. Kando, M. Černák, Acta Phys. Univ. Comenianae **XLIII**, 3-8 (2002).
[31] M. Šimor, J. Ráheľ, D. Kováčik, A. Zahoranová, M. Mazúr, M. Černák, Proc.of 12^{th} *Ann. Int. TANDEC Nonwovens Conference* (Univ. of Tennessee, Knxwille, November 19-21, 2002) Paper No. 6.2., http://tandec.utk.edu
[32] M. Šimor, J. Ráheľ, P. Vojtek, M. Černák, A. Brablec., Appl. Phys. Letters **81**, 2716-2718 (2002).
[33] ftp://ftp.muni.cz/mount/muni.cz/physics/texts/DCSD